

What is the relationship between Slow Feature Analysis and the Successor Representation?

Eddie Seabrook^{*1} and Laurenz Wiskott^{†1}

¹Institut für Neuroinformatik, Ruhr-Universität Bochum

September 26, 2024

Abstract

(This is a work in progress. Feedback is welcome) An analytical comparison is made between slow feature analysis (SFA) and the successor representation (SR). While SFA and the SR stem from distinct areas of machine learning, they share important properties, both in terms of their mathematics and the types of information they are sensitive to. This work studies their connection along these two axes. In particular, multiple variants of the SFA algorithm are explored analytically and then applied to the setting of an MDP, leading to a family of eigenvalue problems involving the SR and other related quantities. These resulting eigenvalue problems are then illustrated in the toy setting of a gridworld, where it is demonstrated that the place- and grid-like fields often associated to the SR can equally be generated using SFA.

Keywords: Time series analysis, correlation, slow feature analysis, Markov chains, reinforcement learning, successor representations, place fields, grid fields

Contents

1	Introduction	3
2	Successor Representation (SR)	3
2.1	Reinforcement Learning (RL)	3
2.2	Definition of SR	5
2.3	Eigenvalues and eigenvectors of SR	6
2.3.1	General case	6
2.3.2	Reversible Markov chains	6
2.3.3	Non-reversible Markov chains and additive reversibilization	7
2.4	Time indexing in the SR	8
3	Slow Feature Analysis (SFA)	9
3.1	Definition of SFA Problems	9
3.2	Optimal free responses in discrete time	11
3.3	Generalization to time-lags larger than 1	14
3.4	Generalization to multiple time-lags	14
3.5	Solving Type I SFA problems	15

^{*}Email: eddie.seabrook@ini.rub.de, ORCID-ID: 0000-0002-8985-1893

[†]Email: laurenz.wiskott@ini.rub.de, ORCID-ID: 0000-0001-6237-740X

3.5.1	SFA	16
3.5.2	CSFA	16
3.5.3	τ SFA	17
3.5.4	LFSFA	17
3.5.5	Corresponding regular eigenvalue problems	18
3.6	Solving Type II SFA Problems	20
3.7	Representation of the input signal	20
3.8	SFA in spatial environments	21
4	Results	22
4.1	Markovian one-hot trajectories	23
4.2	Convergence theorems	24
4.2.1	Type I SFA Problems	24
4.2.2	Type II SFA Problems	26
4.3	Experimentation	28
4.3.1	Setup	28
4.3.2	Simulation	28
5	Discussion	31
	Appendices	32
	Appendix A Linear Algebra	32
A.1	Eigenvalue problems	32
A.2	Square root and inverse square root of a positive definite matrix	33
A.3	Generalized eigenvalue problems	35
	Appendix B SR	37
	Appendix C SFA	41
C.1	Addition of noise	41
C.2	Symmetric normalization and whitening	42
	Appendix D Convergence Theorems	44
D.1	Type I SFA Problems	44
D.2	Type II SFA Problems	47

1 Introduction

Slow feature analysis (SFA) is an unsupervised learning method for performing dimensionality reduction on time series data (Wiskott and Sejnowski, 2002). The core idea underlying this method is to find representations of a time series that have a high degree of temporal coherence. Since its invention, SFA has received significant theoretical study (Blaschke et al., 2006; Creutzig and Sprekeler, 2008; Sprekeler, 2011; Sprekeler and Wiskott, 2008; Sprekeler et al., 2014, 2009; Wiskott, 2003), and has been used to model information processing in various domains of computational neuroscience (Berkes and Wiskott, 2005; Franzius et al., 2007, 2008; Legenstein et al., 2010; Schönfeld and Wiskott, 2015).

The successor representation (SR) is a core concept from reinforcement learning (RL) theory (Dayan, 1993). It describes a method for representing states in a Markov decision process (MDP) based on the predictions about which future states are likely to be observed, which makes it particularly useful in tackling sequential decision making problems. To date, the SR has achieved particularly widespread study, both within the RL community itself but also in the fields of computational neuroscience and cognitive science (for a review, see Carvalho et al. (2024)).

Despite coming from different areas of machine learning research, SFA and the SR overlap in two key ways. Firstly, both are relevant to the study of spatial representations in neuroscience, such as place- and grid-like maps that are observed in the hippocampal-entorhinal system (Franzius et al., 2007; Stachenfeld et al., 2014, 2017). Secondly, in all of these studies, grid-like maps are generated by finding the eigenvectors of a matrix that encodes the temporal statistics of an agent moving in a spatial environment. Thus, SFA and the SR agree in the type of signals they can produce as well as the mathematics with which they are formulated.

While some conceptual connections between SFA and the SR have already been pointed out in the literature (Stachenfeld et al., 2014, 2017), the relation has yet to be explored analytically or in significant depth. The current paper aims to fill this gap in the following way. Firstly, a comprehensive presentation of multiple variants of the SFA algorithm is given, each of which is studied in various toy settings in order to provide mathematical intuition for the different types of outputs that are possible. Secondly, each variant of the SFA problem is explored in the form of generalized and regular eigenvalue problems. Thirdly, the structure of each eigenvalue problem is studied in the particular case where SFA is applied to the setting of the SR, i.e. to state trajectories generated from an MDP. The resulting family of eigenvalue problems shows various connections to quantities associated to the underlying MDP, such as the transition matrix or SR matrix generated for a given policy. Thus, by considering SFA in this specific context, a direct connection to the SR is realised. Moreover, by giving a broad and detailed overview of multiple variants of the SFA algorithm, this paper additionally acts as a general reference work on SFA for researchers that are new to the topic.

The rest of the paper is structured as follows. In Section 2, the SR is introduced and summarized using various concepts from linear algebra and Markov chain theory. In Section 3, the SFA algorithm is introduced, both in its classical definition as well as a number of alternative variants. In Section 4, the main results of the paper are presented that connect SFA to the SR and in Section 5 these results are briefly discussed.

2 Successor Representation (SR)

2.1 Reinforcement Learning (RL)

Reinforcement learning (RL) is a core branch of machine learning that focuses on how agents learn behaviours by interacting with environments to maximize reward signals. The canonical paradigm of RL is a Markov decision process (MDP). This model class consists of a tuple $(\mathcal{S}, \mathcal{A}, p, r)$, where \mathcal{S} and \mathcal{A} are the state and action spaces that describe what situations an agent can encounter and what actions they can make, respectively. When an action $a \in \mathcal{A}$ is made in state $s \in \mathcal{S}$, the transition function $p(s'|s, a)$ determines the probability of being in state $s' \in \mathcal{S}$ at the next time point and the reward function $r(s, a)$ determines the scalar reward the agent receives. Together p and r define the dynamics of the MDP, and both can be

deterministic or stochastic, so long as they respect the Markov property, which requires that the new state s' and the reward received depend only on the current state s and action a . Furthermore, while in the most general case \mathcal{S} , \mathcal{A} , and t can be either finite or continuous, the current paper focuses on the simplest setting where all are finite.

The probability with which an agent chooses an action in a given state is given by the conditional distribution $\mu(a|s)$, which is known as the *policy*, and the general goal of RL is to learn policies that maximize the reward that the agent receives over time. In order to do this, an agent first needs to be able to assess how well a given policy optimizes the reward function, which is known as the *prediction problem*. Since behaviours are extended over time, it is more natural in RL to measure the cumulative reward received under a policy μ than the instantaneous reward. This cumulative notion of reward is typically referred to as the *return*, and can be expressed as

$$g_t = \sum_{k=0}^{\infty} \gamma^k r_{t+k} \quad (1)$$

where r_t denotes the reward received at each time point t and $\gamma \in (0, 1)$ is a *discount factor* that assigns larger importance to proximal over distal future rewards. Note that rewards in Equation (1) are indexed starting at the time point t . This reflects the convention used in this paper whereby an action a_t in state s_t yields a reward r_t at the same time point. An alternative convention is that the reward is received at the next time point, i.e. r_{t+1} . While both conventions commonly appear in the RL literature, the latter is somewhat more common. However, the former is used here for two reasons: 1) it is the convention used in many studies on the SR (Gershman, 2017, 2018; Piray and Daw, 2021; Russek et al., 2017; Stachenfeld et al., 2014, 2017), and 2) it simplifies various mathematical details in later sections of the paper.

In order for the return to be useful to an RL agent, two details need to be taken into account. Firstly, since MDPs often involve randomness, it is the expected value of g_t that gives the most informative measure of reward for a given policy μ . Secondly, the expected return naturally varies depending on which state the agent is in and what action it makes, meaning that it is natural condition on one or more of these variables. Conditioning on states leads to the following quantity

$$v(s_i) = \mathbb{E}_{\mu} [g_t | s_t = s_i] \quad (2)$$

$$= \mathbb{E}_{\mu} \left[\sum_{k=0}^{\infty} \gamma^k r_{t+k} \mid s_t = s_i \right] \quad (3)$$

which is known as the *state value function*, or simply *value function*.¹

A simple calculation shows that this function satisfies a self-consistency equation known as the *Bellman equation* (Sutton and Barto, 2018). This can be expressed most compactly using a vector \mathbf{v} containing the values of all states in \mathcal{S} . For this quantity, the Bellman equation is:

$$\mathbf{v} = \mathbf{r} + \gamma \mathbf{P} \mathbf{v} \quad (4)$$

The matrix \mathbf{P} is the result of combining the policy μ and the environment's transition model p by marginalizing over actions, and has entries equal to:

$$P_{ij} = \sum_a \mu(a|s_i) p(s_j|s_i, a) \quad (5)$$

Summing over the index j in Equation (5) gives $\sum_j P_{ij} = \sum_a \mu(a|s_i) \sum_j p(s_j|s_i, a) = \sum_a \mu(a|s_i) = 1$, meaning that the matrix \mathbf{P} has rows that sum to 1 and is therefore a right stochastic matrix or *transition matrix* (Seabrook and Wiskott, 2023). In words, \mathbf{P} describes the Markov chain induced across \mathcal{S} when the agent behaves according to μ . The vector \mathbf{r} involves the same type of marginalization, i.e. $r_i = \sum_a \mu(a|s_i) r(s_i, a)$, and its entries describe the instantaneous reward expected in each state s . In this paper, it is assumed that

¹Sometimes the value function is denoted with a subscript or superscript μ to emphasize that it is based on an expectation w.r.t. the policy. However, this is dropped in the current paper since only a single policy is considered in Section 4.

the Markov chain described by \mathbf{P} is ergodic. This assumption guarantees that the Markov chain converges to a unique stationary distribution, henceforth denoted $\boldsymbol{\pi}$, and is a common assumption in theoretical RL problems since it allows certain limits to be easily evaluated. In practice, ergodicity can be enforced by considering connected state spaces and allowing self-transitions (Seabrook and Wiskott, 2023).

If p and r are fully known, Equation (4) can either be solved exactly, which is explored in the following section, or iteratively using methods from *dynamic programming* (Sutton and Barto, 2018). However, in most practical situations, the MDP’s dynamics is either (i) modelled internally by the agent - referred to as *model-based learning*, or (ii) not modelled at all - referred to as *model-free learning*. In either of these cases, one must resort to approximating \mathbf{v} from sampled interactions with the environment, which come in the form of a time series $(s_0, a_0, r_0) \rightarrow (s_1, a_1, r_1) \rightarrow (s_2, a_2, r_2) \rightarrow \dots \rightarrow (s_t, a_t, r_t)$.

2.2 Definition of SR

Equation (4) is a self-consistency equation since \mathbf{v} appears on both the left- and right-hand sides. Bringing both terms onto the left-hand side gives

$$(\mathbb{1} - \gamma\mathbf{P})^{-1}\mathbf{v} = \mathbf{r} \tag{6}$$

which can then be rearranged to give

$$\mathbf{v} = (\mathbb{1} - \gamma\mathbf{P})^{-1}\mathbf{r} \tag{7}$$

$$:= \mathbf{M}\mathbf{r} \tag{8}$$

The matrix-vector product in Equation (8) decomposes \mathbf{v} into two distinct quantities that are related to μ : the instantaneous reward vector \mathbf{r} from Equation (4), and a matrix \mathbf{M} related to the transition statistics. Markov chain theory provides a few key insights about this latter quantity, two of which are (Seabrook and Wiskott, 2023):

Theorem 2.2.1. *The matrix \mathbf{M} is well-defined and can alternatively be expressed as*

$$\mathbf{M} = \sum_{k=0}^{\infty} \gamma^k \mathbf{P}^k \tag{9}$$

which is known as a Neumann series (proof: see Appendix B).

In Theorem 2.2.1, Equation (9) involves a sum over powers of the transition matrix \mathbf{P} . Each of these powers generalizes the notion of a transition matrix to multiple steps, meaning that \mathbf{P}^k describes the *k-step Markov chain* formed from the transitions that are realised by the policy μ at a time scale of k steps. The matrix \mathbf{M} therefore extends the concept of a Markov chain so that all time scales are considered, and discounted by γ .² The entries of this matrix, M_{ij} , then describe the cumulative, discounted probability of occupying a state s_j at some future time point given that s_i is occupied initially. In analogy to Equation (3), this can be expressed as:

$$M_{ij} = \mathbb{E}_{\mu} \left[\sum_{k=0}^{\infty} \gamma^k \mathbb{I}(s_{t+k} = s_j) \middle| s_t = s_i \right] \tag{10}$$

where $\mathbb{I}(s_t = s_j) = 1$ if $s_t = s_j$ and 0 otherwise. The i -th row of \mathbf{M} contains the probabilities in Equation (10) for a given initial state s_i and all possible successor states s_j , and therefore forms a representation of s_i based on this notion of cumulative, discounted probability. For this reason, the i -th row of \mathbf{M} is sometimes referred to as the *successor representation* (SR) s_i (Dayan, 1993), and similarly \mathbf{M} is referred to as the SR matrix.

In this paper, the SR is considered as a ground truth quantity associated to a Markov chain for some known model p and policy μ . However, it is worth noting in practical settings p and μ are typically not known a priori and meaning that the SR needs to be approximated based on samples in a similar way to the

²This is similar to the concept of the fundamental matrix for absorbing Markov chains, except that in this case only transient states are included and no discounting is applied (Seabrook and Wiskott, 2023).

value function \mathbf{v} , either using model-free or model-based methods (Russek et al., 2017). Unlike the value function, however, the SR has no explicit reward dependence, meaning that the samples used to approximate it are simply state sequences, i.e. $s(t_0) \rightarrow s(t_1) \rightarrow s(t_2) \rightarrow \dots \rightarrow s(t_T)$.

2.3 Eigenvalues and eigenvectors of SR

2.3.1 General case

This section introduces a relationship between the eigenvalues and eigenvectors of \mathbf{M} and \mathbf{P} that is relevant to the rest of the paper. For readers unfamiliar with eigenvalues and eigenvectors, or their respective generalized counterparts, a short introduction is provided in Appendices A.1-A.3. Moreover, a number of insights from the spectral theory of Markov chains are used, for which a comprehensive overview can be found in Seabrook and Wiskott (2023). The spectral properties of \mathbf{M} can be related to those of \mathbf{P} as follows (Seabrook and Wiskott, 2023):

Theorem 2.3.1. *If \mathbf{w} is an eigenvector of \mathbf{P} with eigenvalue $\lambda \in \mathbb{C}$, then it is also an eigenvector of \mathbf{M} with eigenvalue $\frac{1}{1-\gamma\lambda} \in \mathbb{C}$ (proof: see Appendix B).*

Theorem 2.3.1 implies that the eigenvalues and eigenvectors of \mathbf{M} can be obtained by first finding the same the quantities for \mathbf{P} . Since the latter case is well-understood both analytically and conceptually, Theorem 2.3.1 provides various mathematical insights for the matrix \mathbf{M} . This is particular the case for *reversible Markov chains*, which are introduced in the following section and play an important role throughout the current paper.

2.3.2 Reversible Markov chains

A reversible Markov chain is one for which the temporal dynamics in the stationary distribution $\boldsymbol{\pi}$ are equivalent to those of its time reversal, i.e. an associated Markov chain corresponding to the first one but evolving backwards in time. This symmetry w.r.t time corresponds to various symmetries of the transition matrices of such chains, namely the *flow matrix* $\boldsymbol{\Pi}\mathbf{P}$ is symmetric, as too is the similarity transformation on \mathbf{P} described by $\boldsymbol{\Pi}^{\frac{1}{2}}\mathbf{P}\boldsymbol{\Pi}^{-\frac{1}{2}}$. Moreover, it can be shown, as a result of the latter symmetry, that the transition matrices of reversible Markov chains share a number of properties with symmetric matrices. These results are typically established using the framework of spectral graph theory (for an in-depth exploration, see Seabrook and Wiskott (2023)).

For a reversible Markov chain, it is possible to show that the k -step transition statistics are also reversible, which allows the results described above to be extended to \mathbf{P}^k and \mathbf{M} , as outlined by the following theorem:

Theorem 2.3.2. *For a reversible Markov chain with stationary distribution $\boldsymbol{\pi}$, the matrices \mathbf{P}^k and \mathbf{M} satisfy the following properties:*

- $\boldsymbol{\Pi}\mathbf{P}^k$ and $\boldsymbol{\Pi}\mathbf{M}$ are symmetric.
- $\boldsymbol{\Pi}^{\frac{1}{2}}\mathbf{P}^k\boldsymbol{\Pi}^{-\frac{1}{2}}$ and $\boldsymbol{\Pi}^{\frac{1}{2}}\mathbf{M}\boldsymbol{\Pi}^{-\frac{1}{2}}$ are symmetric.
- \mathbf{P}^k and \mathbf{M} are diagonalizable with real eigenvalues and eigenvectors, and can be diagonalized by a common set of eigenvectors.
- The left and right eigenvectors of \mathbf{P}^k and \mathbf{M} can be chosen to be orthogonal w.r.t to the weighted inner products $\langle \cdot, \cdot \rangle_{\boldsymbol{\Pi}^{-1}}$ and $\langle \cdot, \cdot \rangle_{\boldsymbol{\Pi}}$, respectively.

where $\boldsymbol{\Pi} = \text{diag}(\boldsymbol{\Pi})$ and $k \geq 1$ (proof: see Appendix B).

The first and second points in Theorem 2.3.2 define transformations of \mathbf{P}^k and \mathbf{M} that are guaranteed to be symmetric if and only if the chain is reversible, and each of these transformations appear in Section 4. Note that $\boldsymbol{\Pi}\mathbf{P}^k$ is the flow matrix associated to the k -step Markov chain. Due to these symmetries, \mathbf{P}^k and \mathbf{M} share a number of properties with symmetric matrices, as outlined by the remaining points in

Theorem 2.3.2. The two most important insights in the context of the current paper are the following: i) since the eigenvectors are real-valued, they can easily be visualized as functions across the state space \mathcal{S} , and ii) since the eigenvalues are real-valued, they can be used to order the eigenvectors.

In Stachenfeld et al. (2014, 2017), the Markov chain underlying the SR is formulated as a random walk on an undirected graph, which is equivalent to assuming reversibility (Seabrook and Wiskott, 2023) and offers a number of insights about the eigenvectors of \mathbf{M} , such as those explored above. This assumption is valid in simplified settings such as a gridworld environment with a highly uniform policy (see for example the policy and environment introduced in Section 4.3.1). However, for a general environment and policy, Markov chains are typically non-reversible, in which case the application of spectral graph theory becomes much harder and often involves various types of symmetrization (Seabrook and Wiskott, 2023), with one example being the focus of the next section.

2.3.3 Non-reversible Markov chains and additive reversibilization

While reversible Markov chains are well-described by a number of theoretical results, non-reversible Markov chains are generally more complex and less understood. In particular, in the non-reversible case, there is no guarantee that the eigenvectors of \mathbf{P}^T are real-valued or that they can be ordered in the manner described above. One way to make the analysis of non-reversible Markov chains easier is to associate them to a related reversible Markov chain, which is often referred to as *reversibilization* (Seabrook and Wiskott, 2023). This involves combining the transition matrix of a Markov chain together with that of its time reversal, leading to a transition matrix that corresponds to a related reversible chain. For example, given a starting non-reversible Markov chain, the *additive reversibilization* is a Markov chain with the following transition matrix

$$\mathbf{P}_{\text{add}} := \frac{\mathbf{P} + \mathbf{\Pi}^{-1} \mathbf{P}^T \mathbf{\Pi}}{2} \quad (11)$$

where the term $\mathbf{\Pi}^{-1} \mathbf{P}^T \mathbf{\Pi}$ is the transition matrix associated to the time reversal of the starting chain, which is combined additively with \mathbf{P} , hence the name (Seabrook and Wiskott, 2023). Note that since the starting chain is ergodic, it has a unique stationary distribution with all non-zero entries, which therefore means that $\mathbf{\Pi}^{-1}$ is well-defined and unique (Seabrook and Wiskott, 2023).

Formally, the additive reversibilization is defined only for transition matrices. However, since the SR is based upon transition probabilities across different time scales (Equation (9)), it is also possible to consider the form that \mathbf{M} takes when these probabilities are additively mixed with their time reversed counterparts. Perhaps the simplest way to do this is to perform the reversibilization at a time scale of 1, i.e. $\mathbf{P} \rightarrow \mathbf{P}_{\text{add}}$, and then plug this matrix into Equation (9), which can be denoted $\mathbf{M}(\mathbf{P}_{\text{add}})$ and which satisfies the properties outlined in Theorem 2.3.2 since \mathbf{P}_{add} describes a reversible Markov chain.³ An alternative method that is more relevant to the current study, and which to the authors' knowledge has yet to be considered in the literature, is to apply the transformation in Equation (11) directly to \mathbf{M} . This gives:

$$\mathbf{M}_{\text{add}} := \frac{\mathbf{M} + \mathbf{\Pi}^{-1} \mathbf{M}^T \mathbf{\Pi}}{2} \quad (12)$$

$$\stackrel{(9)}{=} \frac{\sum_{k=0}^{\infty} \gamma^k \mathbf{P}^k + \mathbf{\Pi}^{-1} (\sum_{k=0}^{\infty} \gamma^k \mathbf{P}^k)^T \mathbf{\Pi}}{2} \quad (13)$$

$$= \sum_{k=0}^{\infty} \gamma^k \left(\frac{\mathbf{P}^k + \mathbf{\Pi}^{-1} (\mathbf{P}^k)^T \mathbf{\Pi}}{2} \right) \quad (14)$$

$$\stackrel{(11)}{=} \sum_{k=0}^{\infty} \gamma^k (\mathbf{P}^k)_{\text{add}} \quad (15)$$

where $(\mathbf{P}^k)_{\text{add}}$ is a transition matrix describing the additive reversibilization of the k -step Markov chain. Therefore, in comparison to $\mathbf{M}(\mathbf{P}_{\text{add}})$ which performs reversibilization only at time scale of 1, \mathbf{M}_{add} computes

³This notion of a reversibilized SR is the one considered in the model of Keck et al. (2024) for a parameter value of $\alpha = \frac{1}{2}$.

the reversibilization at each time scale individually. Moreover, it is possible to show that for a general Markov chain, i.e. not necessarily reversible, $(\mathbf{P}^k)_{\text{add}}$ and \mathbf{M}_{add} share many of the properties outlined in Theorem 2.3.2:

Theorem 2.3.3. *For a Markov chain with stationary distribution $\boldsymbol{\pi}$, the matrices $(\mathbf{P}^k)_{\text{add}}$ and \mathbf{M}_{add} satisfy the following properties:*

- $\boldsymbol{\Pi}(\mathbf{P}^k)_{\text{add}}$ and $\boldsymbol{\Pi}\mathbf{M}_{\text{add}}$ are symmetric.
- $\boldsymbol{\Pi}^{\frac{1}{2}}(\mathbf{P}^k)_{\text{add}}\boldsymbol{\Pi}^{-\frac{1}{2}}$ and $\boldsymbol{\Pi}^{\frac{1}{2}}\mathbf{M}_{\text{add}}\boldsymbol{\Pi}^{-\frac{1}{2}}$ are symmetric.
- $(\mathbf{P}^k)_{\text{add}}$ and \mathbf{M}_{add} are diagonalizable with real eigenvalues and eigenvectors.
- The left and right eigenvectors of $(\mathbf{P}^k)_{\text{add}}$ and \mathbf{M}_{add} can be chosen to be orthogonal w.r.t to the weighted inner products $\langle \cdot, \cdot \rangle_{\boldsymbol{\Pi}^{-1}}$ and $\langle \cdot, \cdot \rangle_{\boldsymbol{\Pi}}$, respectively.

where $\boldsymbol{\Pi} = \text{diag}(\boldsymbol{\Pi})$ and $k \geq 1$ (proof: see Appendix B).

Two details are worth pointing out regarding how Theorem 2.3.3 differs from Theorem 2.3.2. Firstly, in Theorem 2.3.2 both the SR matrix \mathbf{M} and each power of the transition matrix \mathbf{P}^k correspond to the same underlying Markov chain. By contrast, there is no guarantee that $(\mathbf{P}^k)_{\text{add}}$ is the k -step analogue of $(\mathbf{P})_{\text{add}}$, since generally $(\mathbf{P}^k)_{\text{add}} \neq (\mathbf{P}_{\text{add}})^k$, and similarly \mathbf{M}_{add} is generally not a sum over powers of \mathbf{P}_{add} . Secondly, one corollary of the previous point is that while \mathbf{M} and all powers of \mathbf{P} share a common set of eigenvectors in Theorem 2.3.3, the same is generally not the case for the matrices in Theorem 2.3.3. One special case in which Theorem 2.3.3 and Theorem 2.3.2 perfectly align is for a reversible Markov chain, since in this case the additive reversibilization is redundant and all matrices in the two theorems are the same.

Theorem 2.3.3 is particularly relevant to the results of Section 4, which involve all the matrices described in this theorem.

2.4 Time indexing in the SR

There are two details worth pointing out about the index k in the definition of the SR. Firstly, the starting value is $k = 0$. In Equation (10), this corresponds to the probability of being in state s_j at time t given that one is in state s_i at time t , i.e. a probability of 1 for $i = j$ and 0 otherwise. Equivalently, this contributes an identity matrix $\mathbf{P}^0 = \mathbb{1}$ to the sum in Equation (9). This first term in the SR arises due to the convention of assigning rewards at time t (see Section 2.1). If the alternative convention is used whereby rewards are assigned at time $t + 1$, then it is possible to show that the resulting SR is equivalent to that in Equations (9) and (10) except that k starts at 1 (see for example the formalism of Carvalho et al. (2024)). Note that none of the key properties established for \mathbf{M} or \mathbf{M}_{add} in the previous section are impacted by this detail. Secondly, in Equations (9) and (10) the index k increases without bound, meaning that the SR describes transitions between states across arbitrarily large time scales. This stems from the fact that the value function defined in Equation (3) similarly involves rewards that extend arbitrarily far into the future. However, both the value function and SR can alternatively be defined with a finite temporal horizon k_{max} (Carvalho et al., 2024), which in some contexts is a more computationally convenient formalism to use. Like for the previous point, none of the core results of the previous section are impacted by this choice of convention. For a finite horizon, the main difference is that in order to evaluate the eigenvalues in Theorem 2.3.1 a finite geometric series is used. One practical difference this can lead to is that eigenvalues of \mathbf{M} are not guaranteed to be ordered in exactly the same way as those of \mathbf{P} , however this is a finite size effect that becomes negligible for larger values of k_{max} . Note that the only point at which a finite horizon is used in the current paper is in the convergence results of Section 4.2, since this is the most natural choice in the context of SFA. Moreover, in the experiments of Section 4.3, which illustrate these results, a sufficiently large horizon is used such that the finite size effect just described is not observed.

3 Slow Feature Analysis (SFA)

3.1 Definition of SFA Problems

Slow feature analysis (SFA) is an unsupervised dimensionality reduction technique for time series data. Given a multivariate time series $\mathbf{x}(t) = [x_1(t), x_2(t), \dots, x_N(t)] \in \mathbb{R}^N$, it aims to find a set of scalar input-output functions such that the outputs generated vary slowly in time. Moreover, SFA stipulates that these outputs should capture meaningful features of variation without redundancy, and this is usually achieved by requiring that they have zero mean, unit variance, and are uncorrelated. The standard definition of SFA, referred to in this paper as Type I SFA, is described formally by the following:

Type I SFA problem: *Given a function space \mathcal{F} and an N -dimensional input signal $\mathbf{x}(t) \in \mathbb{R}^N$, find a set of J real-valued input-output functions $g_j(\mathbf{x})$ generating the output signals $y_j(t) := g_j(\mathbf{x}(t))$ such that for $j = 1, 2, \dots, J$*

$$\Delta(y_j) = \langle \dot{y}_j(t)^2 \rangle_t \quad \text{is minimal} \quad (16)$$

under the constraints

$$\langle y_j(t) \rangle_t = 0 \quad (\text{zero mean}) \quad (17)$$

$$\langle y_j(t)^2 \rangle_t = 1 \quad (\text{unit variance}) \quad (18)$$

$$\forall i < j \quad \langle y_i(t)y_j(t) \rangle_t = 0 \quad (\text{decorrelation and order}) \quad (19)$$

with $\langle \cdot \rangle_t$ and $\dot{y}_j(t)$ representing temporal averaging and the time derivative of $y_j(t)$, respectively.

If the function space \mathcal{F} is linear, i.e. $g_j(\mathbf{x}) = \mathbf{w}_j^T \mathbf{x}$, then the resulting problem is typically referred to as *linear SFA*. However, a key strength of SFA is that the function space \mathcal{F} can be chosen flexibly, meaning that unlike other classical dimensionality reduction methods it is not constrained to linear transformations. Non-linear function spaces are typically achieved in SFA by first applying a k -th degree polynomial expansion to the input time series, i.e. $\mathbf{x}(t) \rightarrow \mathbf{h}(t) = \mathcal{P}_k(\mathbf{x}(t))$, and then considering linear input-output functions on the expanded input, i.e. $g_j(\mathbf{h}) = \mathbf{w}_j^T \mathbf{h}$ (Wiskott and Sejnowski, 2002). Under this procedure, linear SFA corresponds either to an expansion of degree $k = 1$ or to no expansion at all. Although the expansion step is an important component of SFA that is widely used in applications, it is not relevant to the results in Section 4. Therefore, unless otherwise stated, this paper focuses on the setting of no expansion, meaning that linear input-output functions are applied to the input time series.

The quantity in Equation (16) is sometimes referred to as the Δ -value of the output signal $y_j(t)$, and it defines a measure of slowness of this signal. In practical applications, time series data is discretized over time and is of finite length, i.e. $t = 1, 2, \dots, T$. Therefore, in order to be able to compute the Δ -value of an output signal, it is necessary to define a discrete analogue of the time derivative $\dot{y}_j(t)$. The most intuitive, and also the most commonly utilized, method for doing this is to use the differences between neighbouring values, i.e.

$$\dot{y}_j(t) \approx y_j(t+1) - y_j(t) \quad (20)$$

It is worth noting that for a finite data set with T time points this can only be computed for $t = 1, 2, \dots, T-1$. Inserting Equation (20) into Equation (16) then yields (Blaschke et al., 2006):

$$\Delta(y_j) = \langle (y_j(t+1) - y_j(t))^2 \rangle_t \quad (21)$$

$$= \langle y_j(t+1)^2 \rangle_t + \langle y_j(t)^2 \rangle_t - 2 \underbrace{\langle y_j(t)y_j(t+1) \rangle_t}_{=C_1(y_j)} \quad (22)$$

$$\stackrel{(18)}{=} 1 + 1 - 2C_1(y_j) \quad (23)$$

$$= 2(1 - C_1(y_j)) \quad (24)$$

Two details are worth pointing out about the equations above. Firstly, in Equation (23) the first and second terms are evaluated to 1 using the unit variance constraint of SFA. Formally, since t runs from $t = 0$ to $t = T - 1$ for the time differences, first and second terms miss the first and last data point, respectively, meaning that they are not numerically equal to 1. However, since SFA is typically applied to very long time series', this edge effect is in practice negligible. Secondly, the quantity $C_1(y_j)$ is a measure of the average similarity between $y_j(t)$ and $y_j(t + 1)$ over time. Provided that the zero mean and unit variance constraints have already been satisfied, it is the correlation between $y_j(t)$ and $y_j(t + 1)$, and is denoted the *time-lagged correlation* of $y_j(t)$ with time-lag 1 in this paper. Equation (22) expresses the intuitive fact that a given signal being slow is equivalent to it having similar values over time, and therefore having a large value of $C_1(y_j)$ (Blaschke et al., 2006). Hence, minimizing $\Delta(y_j)$ is equivalent to maximizing $C_1(y_j)$, and to make the comparison between these two perspectives easier the latter is henceforth referred to as CSFA in this paper.

It is also possible to formulate SFA without the zero mean constraint, which in this paper is referred to as Type II SFA. While this variant of SFA has received less study in the literature (but see for example Franzius et al. (2007); Sprekeler and Wiskott (2008); Sprekeler et al. (2009)), it plays an important role in the results of Section 4. The corresponding optimization problem can be expressed in a form analogous to Type I SFA:

Type II SFA problem: *Given a function space \mathcal{F} and an N -dimensional input signal $\mathbf{x}(t) \in \mathbb{R}^N$, find a set of J real-valued input-output functions $g_j(\mathbf{x})$ generating the output signals $y_j(t) := g_j(\mathbf{x}(t))$ such that for $j = 1, 2, \dots, J$*

$$\Delta(y_j) = \langle \dot{y}_j(t)^2 \rangle_t \quad \text{is minimal} \quad (25)$$

under the constraints

$$\langle y_j(t)^2 \rangle_t = 1 \quad (\text{unit 2nd moment}) \quad (26)$$

$$\forall i < j \quad \langle y_i(t)y_j(t) \rangle_t = 0 \quad (\text{zero 2nd cross-moment and order}) \quad (27)$$

with $\langle \cdot \rangle_t$ and $\dot{y}_j(t)$ representing temporal averaging and the time derivative of $y_j(t)$, respectively.

Many of the details outlined so far for Type I SFA apply also for Type II SFA. For example, non-linear function spaces are most naturally achieved using polynomial expansions, and consideration in this paper is restricted to the simpler linear case. Moreover, the Δ -value of Type II SFA can be reformulated following the same steps as in Equations (21)–(24), leading to a quantity $C_1(y_j)$ that is instead maximized, which for consistency is referred to as Type II CSFA in this paper. One difference between Type I and Type II SFA problems is that they involve slightly different statistical quantities. This is most evident in the constraints, where in Type II problems $\langle y(j)^2 \rangle_t$ is the *2nd moment* of $y_j(t)$ and $\langle y_i(t)y_j(t) \rangle_t$ is the *2nd cross-moment* of $y_i(t)$ and $y_j(t)$. Moreover, in Type II CSFA the quantity $C_1(y_j)$ is not formally the correlation between $y_j(t)$ and $y_j(t + 1)$, and is more accurately referred to as the *time-lagged 2nd moment* of $y_j(t)$. Note that each of these statistical quantities reduces to its corresponding Type I counterpart if $y_j(t)$ has zero mean, and in that sense they are the most natural generalizations of the Type I quantities. Moreover, they play similar roles to their Type I counterparts, with $\langle y(j)^2 \rangle_t$ fixing the scale of variation, $\langle y_i(t)y_j(t) \rangle_t$ reducing redundancy between distinct features, and $C_1(y_j)$ measuring the similarity of each feature over time.

Formally, there is no guarantee that the solutions to Type I and Type II SFA problems are the same. However, provided that the function space \mathcal{F} can represent a constant signal given the input $\mathbf{x}(t)$,⁴ then the Type I and Type II solutions can be easily related. To see this, consider the following constant signal:

$$y_1(t) = \pm[1, 1, \dots, 1] \quad (28)$$

⁴Note that due to the way in which function spaces are defined, this is equivalent to assuming that \mathcal{F} can represent *any* constant signal.

Since this signal does not change over time, it has a minimal Δ -value of 0 and a maximal correlation of $C_1 = 1$, and is therefore the slowest or most correlated signal possible. Since it has a mean value of 1 and no variation, it is prohibited in Type I problems, however it is allowed in Type II problems since it has unit 2nd moment. Therefore, under the assumption that $y_1(t)$ can be represented by the function space \mathcal{F} , $y_1(t)$ is the first output for Type II problems, hence the index $j = 1$. Furthermore, if $y_2(t)$ is the second solution to this problem then applying the zero 2nd cross-moment constraint to $y_1(t)$ and $y_2(t)$ gives

$$\langle y_1(t)y_2(t) \rangle_t = \pm \langle y_2(t) \rangle_t = 0 \quad (29)$$

meaning that this constraint effectively forces $y_2(t)$ to have zero mean, and by extension unit variance. Therefore, $y_2(t)$ is the slowest signal satisfying all Type I constraints and thus corresponds to $j = 1$ for Type I problems. Using similar argumentation, it is possible to show that for any $j > 1$ the j -th solution for a Type II problem is equivalent to the $(j - 1)$ -th solution of the corresponding Type I problem. Thus, under the assumption stated, the solutions to a Type II problem are the same as those of the corresponding Type I problem except for the signal $y_1(t)$ and a shift in the indexing of outputs. Although there is no guarantee that the constant function $y_1(t)$ can be represented for any input $\mathbf{x}(t)$ and function space \mathcal{F} , it can be guaranteed through a preprocessing step in which an extra constant component is added to the input time series $\mathbf{x}(t)$, since this ensures that a constant output can be generated by simply picking this component and leaving all others out. Note that polynomial expansions typically include such a constant term, meaning that Type I and II solutions are related in this way for most practical applications of SFA.

Although Type I and II problems are both relevant to the results in Section 4, the rest of this section focuses primarily on the former, unless stated otherwise.

3.2 Optimal free responses in discrete time

In most cases, it is not possible to find analytical solutions to the problems presented in the previous section. However, in Wiskott (2003) it was demonstrated that analytical solutions do exist to a simplified variant of the Type I SFA problem in which *free responses* are considered, i.e. the input time series $\mathbf{x}(t)$ and input-output function $g(\mathbf{x})$ are ignored and the goal is to find *any* signals $y_j(t)$ that optimize the objective in Equation (16) subject to the constraints in Equations (17)–(19). Formally, this problem is described as follows:

Type I free response SFA problem: Find a set of J real-valued signals $y_j(t)$ such that for $j = 1, 2, \dots, J$

$$\Delta(y_j) = \langle \dot{y}_j(t)^2 \rangle_t \text{ is minimal} \quad (30)$$

under the constraints

$$\langle y_j(t) \rangle_t = 0 \quad (\text{zero mean}) \quad (31)$$

$$\langle y_j(t)^2 \rangle_t = 1 \quad (\text{unit variance}) \quad (32)$$

$$\forall i < j \quad \langle y_i(t)y_j(t) \rangle_t = 0 \quad (\text{decorrelation and order}) \quad (33)$$

with $\langle \cdot \rangle_t$ and $\dot{y}_j(t)$ representing temporal averaging and the time derivative of $y_j(t)$, respectively.

This problem is a useful abstraction to Type I SFA since it provides intuition regarding what the solutions typically work towards. This is insightful for two reasons. Firstly, it provides better expectations regarding what the outputs to SFA might be in a given application domain. Secondly, it provides intuition on how the Δ -value relates to the form of each signal, which is useful from the perspective of parameter tuning.

In Wiskott (2003), methods from variational calculus were used to find optimal solutions to the problem described above in the case of continuous time. In the case of free boundary conditions, the solutions are

$$y_j(t) = \sqrt{2} \cos\left(j\pi \frac{t - t_A}{t_B - t_A}\right) \quad \text{for } t \in [t_A, t_B] \quad \text{and } j = 1, 2, \dots, J \quad (34)$$

meaning that each solution is equal to a sinusoidal standing wave defined over this time interval with frequency $f_j = \frac{j\pi}{2\pi(t_B - t_A)} = \frac{j}{2(t_B - t_A)}$. Moreover, due to the properties of sinusoidal functions, each solution is guaranteed to have zero mean and to be decorrelated with all others, and the scaling factor of $\sqrt{2}$ enforces unit variance.

Like the majority of studies on SFA, this paper assumes that time is discrete. While the solutions described by Equation (34) do not strictly apply in this setting, they can be partially extended by letting $t_A = 1, t_B = T$ and sampling at integer time points. Performing this discretization is insightful since it provides a set of approximate solutions to the discrete time version of the free response problem, however when doing this there are a number of technical details worth taking into account. Firstly, for a fixed sampling rate of f_s , it is only possible to accurately sample continuous signals with an underlying frequency less than or equal to $f_{\max} = \frac{f_s}{2}$, and for $f > f_{\max}$ any sample is equivalent to another obtained for some frequency $f < f_{\max}$.⁵ Therefore, since the free response problem requires decorrelated signals, this upper bound needs to be respected when sampling the solutions described by Equation (34). Discretizing at integer time points is equivalent to a sampling rate of 1Hz, meaning that $f_{\max} = 0.5\text{Hz}$, and since $f_j = \frac{j}{2(T-1)}$ this frequency is reached at $j = T - 1$. The discretized signal obtained at this value of j oscillates between ± 1 , i.e. $y_{T-1}(t) = [1, -1, 1, -1, \dots]$, and in order to preserve a unit variance of 1 it is necessary to remove the scaling factor of $\sqrt{2}$ in Equation (34). Secondly, although j typically starts at 1 in SFA problems, inserting $j = 0$ into Equation (34) and removing the factor of $\sqrt{2}$ produces a constant signal with values equal to 1. This is precisely the positive variant of Equation (28), and therefore including this value of j offers a useful generalization to the Type II setting.⁶ Lastly, for $0 < j < T - 1$ the scaling factor of $\sqrt{2}$ remains, and for these signals the Type I SFA constraints are only approximately satisfied. This is because the constraints involve averages, i.e. $\langle \cdot \rangle_t$, which are not guaranteed to be exactly preserved when sampling the signals in Equation (34). However, this is a finite size effect and therefore becomes less significant as T is increased. Moreover, a similar finite size effect applies to the Δ -values, which are also based on time averages, meaning that the values obtained for the discretized signals may deviate numerically from those of the continuous signals described by Equation (34), which were computed in Wiskott (2003).

Provided all details outlined in the previous paragraph are taken into account, the discrete time analogues of the solutions described in Equation (34) are given by

$$y_j(t) = c_j \cos\left(j\pi \frac{t-1}{T-1}\right) \quad \text{for } t = 1, 2, \dots, T \quad \text{and } j = 0, 1, 2, \dots, T-1 \quad (35)$$

where

$$c_j = \begin{cases} 1 & \text{if } j = 0 \text{ or } T-1 \\ \sqrt{2} & \text{otherwise} \end{cases} \quad (36)$$

A number of the signals described in Equations (35) and (36) are depicted in Figure 1 for $T = 45$. In Figures 1a and 1f, the aforementioned cases of $j = 0$ and $j = T - 1 = 44$ are depicted, respectively. In the former case, the signal does not change at all and therefore has $\Delta = 0$, whereas in the latter case the difference between successive time points is always 2 which means that $\Delta = 4$. Moreover, since these are the slowest and fastest possible signals of length $T = 45$, they provide lower and upper bounds for the Δ -value, i.e. $\Delta \in [0, 4]$. Conversely, successive values of the signal in Figure 1a are perfectly correlated over time, i.e. $C_1 = 1$, whereas those of the signal in Figure 1f are perfectly anti-correlated over time, i.e. $C_1 = -1$. Furthermore, the interval to which Δ belongs implies a corresponding interval of $C_1 \in [-1, 1]$ (see Equation (24)), which is consistent with the notion of how correlation coefficients are bounded. It is worth noting that since $y_0(t)$ is only a possible solution if the zero mean constraint is removed, the intervals $\Delta \in [0, 4]$ and $C_1 \in [-1, 1]$ strictly apply to Type II SFA, while for Type I SFA the values $\Delta = 0$ and $C_1 = 1$ are not possible, in which case $\Delta \in (0, 4]$ and $C_1 \in [-1, 1)$.

In Figures 1b–1d, the signals corresponding to $j = 1, 2, 3$ are depicted, and the cosine form described in Equation (35) is clearly visible. Since all of these signals do not change much between neighbouring time

⁵In signal processing, this phenomenon is known as *aliasing* and is a consequence of the *Nyquist-Shannon sampling theorem* (Oppenheim et al., 2016).

⁶It is also worth noting that by including the constant signal, the set of signals collectively forms a *Fourier basis*.

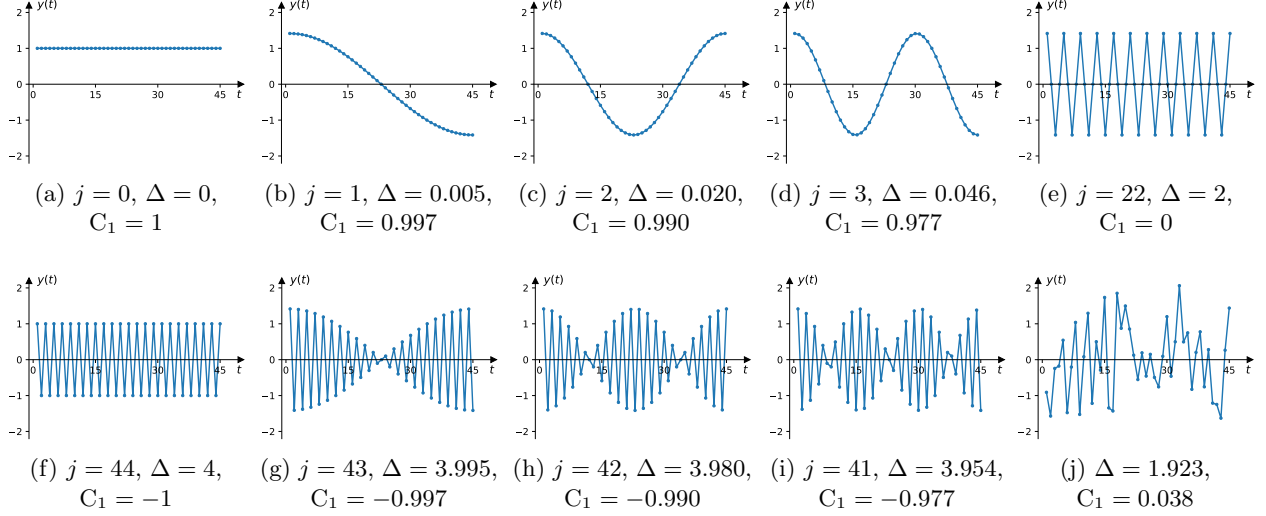


Figure 1: An illustration of the discrete time free responses described by Equations (35) and (36) for $T = 45$. (a-d) and (f-i) show the signals corresponding to the four smallest and largest values of j , respectively, while (e) shows the signal for the middlemost value of j . For comparison, in (j) an output is shown resembling a realistic output of SFA with value of Δ and C_1 that is far away from the extreme cases considered in (a-d) and (f-i).

points, the Δ -values are close to 0 and increase with the frequency, while the values of C_1 are close to 1 and decrease with the frequency. In Figures 1g–1i, the cases corresponding to $j = T - 2, T - 3, T - 4 = 43, 42, 41$ are depicted. Like the signal in Figure 1f, these signals all change a lot on average between successive time points, and therefore have $\Delta \approx 4$ and $C_1 \approx -1$, again with the former (latter) increasing (decreasing) with the frequency. Visually, the signals in Figures 1g–1i take the form of beat patterns that would emerge when performing amplitude modulation (AM) of the signal in Figure 1f using those in Figures 1b–1d. This pairing between signals is further evident in the fact that the values of C_1 for the signals in Figures 1g–1i are of equal magnitude and opposite sign to those of the signals in Figures 1b–1d, or equivalently the Δ -values are equally far from the lower/upper bounds of 0 and 4.

Equidistant from $j = 0$ and $j = T - 1$ is $j = \frac{T-1}{2} = 22$, for which the corresponding signal is shown in Figure 1e. This signal takes the form of a fixed oscillation $y(t) = [\sqrt{2}, 0, -\sqrt{2}, 0, \sqrt{2}, \dots]$, and is therefore analogous to the one in Figure 1f, but instead having a frequency half as large and the scaling factor $\sqrt{2}$ included. Moreover, this signal has $\Delta = 2$ which is exactly half as large as the Δ -value of the signal in Figure 1f.⁷

Considering the signals in Figures 1a–1i, all display a high degree of regularity. Thus, for any of these signals, it is easy to predict future values given knowledge of a value at some time t , meaning that all of them, both slow and fast, are highly *predictable* (Creutzig and Sprekeler, 2008)⁸. In fact, for the basis described by Equations (35) and (36) this property holds for all values of j by virtue of the periodicity of the underlying cosine functions. However, this property is a pathological feature of the free response problem. In real applications of SFA, it is only the signals with $\Delta \approx 0, 4$ that are highly predictable, and the majority of other signals resemble noise (Creutzig and Sprekeler, 2008; Escalante-B. and Wiskott, 2020). Thus, signals with Δ -values far away from 0 and 4 are unlikely to have a profile like the signal in Figure 1e, and are instead more likely to be highly irregular like the signal illustrated in Figure 1j, which is an i.i.d. sample of Gaussian noise with zero mean and unit variance.

⁷It is worth noting that the signal for $j = \frac{T-1}{2}$ has this pattern and a Δ -value of exactly 2 only if T is odd. Since this signal offers useful insight on the middle of the interval $\Delta \in [0, 4]$, an odd value of $T = 45$ is considered here.

⁸Note that if features are selected based on predictability, i.e. the slowest and fastest signals, then the corresponding method is related to predictive coding and information bottlenecks (Creutzig and Sprekeler, 2008).

3.3 Generalization to time-lags larger than 1

The quantities $\Delta(y_j)$ and $C_1(y_j)$ introduced in Section 3.1 are both computed using successive data points in the time series $\mathbf{x}(t)$. For the Δ -value, this is necessary in order to maintain an analogy to the continuous-time derivative. By contrast, temporal correlations can be computed between data points that are separated by time lags larger than 1. In particular, provided that $y_j(t)$ satisfies the zero mean and unit variance constraints of Type I SFA, then the time-lagged correlation of $y_j(t)$ for a general time-lag $\tau \geq 1$ is given by

$$C_\tau(y_j) = \langle y_j(t)y_j(t + \tau) \rangle_t \tag{37}$$

which reduces to $C_1(y_j)$ for $\tau = 1$, and therefore generalizes this quantity.

Replacing the CSFA objective with the maximization of $C_\tau(y_j)$ is one way to generalize this problem to larger time scales. In the literature, this has initially been explored as a method for performing *independent component analysis* (ICA), in particular when statistical independence is defined in terms of temporal decorrelation (Belouchrani et al., 1997; Blaschke et al., 2006; Molgedey and Schuster, 1994; Ziehe and Müller, 1998). More recently, this method has become a popular tool for analyzing molecular dynamics trajectories, and is often referred to as *time-lagged independent component analysis* (tICA) (Klus et al., 2018; Moffett and Shukla, 2017; Naritomi and Fuchigami, 2011; Pérez-Hernández et al., 2013; Schultze and Grubmüller, 2021). However, in order to emphasize that this method is a generalization of CSFA to larger time-lags (Blaschke et al., 2006), and to make the terminology of the current paper more consistent, it is referred to henceforth as τ SFA. Like SFA and CSFA, this method has both Type I and II variants depending on whether the zero mean constraint is included or omitted.

Some intuition regarding the relationship of $C_\tau(y_j)$ and $C_1(y_j)$ can be gained by applying the former to the signals in Figure 1 and comparing to the insights found in Section 3.2. The most important factor that determines whether $C_\tau(y_j)$ orders these signals in the same way as the $\tau = 1$ case is the parity of τ . For even τ , slow signals are ordered in the same way, but fast signals are assigned large positive correlation, while for odd τ the ordering is in full agreement with the $\tau = 1$ case. For example, for a time-lag of $\tau = 2$, the values of the constant signal in Figure 1a are perfectly correlated over time, meaning that $C_2 = 1$, and the other slow signals in Figures 1b–1d have highly correlated values for this time lag, meaning that $C_2 \approx 1$. Therefore, for $\tau = 2$ all slow signals have large correlations either equal or close to 1, in agreement with the $\tau = 1$ case. By contrast, the signal in Figure 1f oscillates between ± 1 , meaning that the values 2 steps apart are equal, and therefore $C_2 = 1$. Likewise, for the other fast signals in Figures 1g–1i, the values 2 steps apart are similar over time, and therefore $C_2 \approx 1$. Thus, for $\tau = 2$ the fast signals are correlated in the same way as the slow signals, in contrast to the $\tau = 1$ case.⁹ Now contrast this to a time-lag of $\tau = 3$. In this case, the slow signals in Figures 1a–1d have high values of C_3 either equal or close to 1, in agreement with both the $\tau = 1, 2$ cases, which can be demonstrated using the same argument as above. However, for the fast signals the values that are spaced by 3 steps are very different, meaning that they have low values of C_3 either equal or close to -1 , which agrees with the $\tau = 1$ case but disagrees with the $\tau = 2$ case. To summarize, many of the intuitive properties regarding how $C_1(y_j)$ measures the variation of a signal over time carry over to $C_\tau(y_j)$, however for even values of τ it is important to be careful when dealing with quickly oscillating signals.

3.4 Generalization to multiple time-lags

A number of studies have extended τ SFA by considering correlations across multiple time-lags simultaneously (Blaschke et al., 2006; Wang and Zhao, 2020; Ziehe and Müller, 1998). These methods all aim at maximizing a quantity that sums over correlations at different time-lags, i.e.

$$F_\gamma(y_j) = \sum_{\tau=0}^{\tau_{\max}} \kappa_\tau C_\tau(y_j) \tag{38}$$

⁹Note in particular that due to the structure of the cosine waves, the value of C_2 for each signal in Figures 1a–1d is exactly same as the value of its fast counterpart in Figures 1f–1i

where κ_τ are a set of weights specifying the contribution at each time-lag τ . While Wang and Zhao (2020); Ziehe and Müller (1998) consider all time-lags equally, i.e. $\kappa_\tau = 1 \forall \tau$, Blaschke et al. (2006) use a set of exponentially decaying weights, i.e. $\kappa_\tau := \exp(-\beta\tau)$ with β controlling the speed of decay. The latter formulation is focused on in this paper as it is more relevant to the results in Section 4. Assuming a parameter $\gamma \in (0, 1)$, analogous to the one in RL, exponentially decaying weights can be written as $\kappa_\tau = \gamma^\tau$, meaning that

$$F_\gamma(y_j) = \sum_{\tau=0}^{\tau_{\max}} \gamma^\tau C_\tau(y_j) \quad (39)$$

is the exact quantity to be maximized. Since the $\tau = 1$ term in Equation (39) corresponds to CSFA, this is perhaps a natural choice for the starting value of τ . However, like in Ziehe and Müller (1998), this paper uses a starting value of $\tau = 0$, and there are two reasons for this choice. Firstly, starting at $\tau = 0$ leads to more insightful results in Section 4. Secondly, assuming the unit variance constraint has been satisfied, then including an additional $\tau = 0$ term in practice only adds $\gamma^0 \langle y_j(t)y_j(t) \rangle_t = \langle y_j(t)^2 \rangle_t = 1$ to the sum in Equation (39), meaning that the ordering of signals is invariant to this detail. The maximum value τ_{\max} is left as a free parameter, however it is important to note that is in practice bound from above by the length of the input time series.

The variant of SFA involving the maximization of $F_\gamma(y_j)$ has, like τ SFA, mostly been studied as a technique for performing ICA based on temporal decorrelation (Blaschke et al., 2006; Wang and Zhao, 2020; Ziehe and Müller, 1998). In Blaschke et al. (2006), it was referred to as *linear filtering*, and this terminology can be understood through the following rearrangement of Equation (39):

$$F_\gamma(y_j) = \sum_{\tau=0}^{\tau_{\max}} \gamma^\tau C_\tau(y_j) \quad (40)$$

$$= \sum_{\tau=0}^{\tau_{\max}} \gamma^\tau \langle y_j(t)y_j(t+\tau) \rangle_t \quad (41)$$

$$= \left\langle y_j(t) \left(\sum_{\tau=0}^{\tau_{\max}} \gamma^\tau y_j(t+\tau) \right) \right\rangle_t \quad (42)$$

Equation (42) says that computing $F_\gamma(y_j)$ is equivalent to first applying an exponentially decaying filter to $y_j(t)$ and then computing the correlation of $y_j(t)$ with the resulting signal.¹⁰ For this reason, $F_\gamma(y_j)$ is referred to henceforth as the *linearly filtered correlation* of $y_j(t)$, and the variant of SFA that seeks to maximize this quantity is referred to as *linear filtering slow feature analysis* (LFSFA), in order to emphasize the relation to SFA. Moreover, like all problems introduced so far, LFSFA has both Type I and Type II variants depending on whether the zero mean constraint is included or omitted.

Note that the linearly filtered correlation is not applied to the free response signals in Figure 1 since this provides less insight in comparison to $\Delta(y_j)$ and $C_\tau(y_j)$.

3.5 Solving Type I SFA problems

This section describes how each variant of Type I SFA presented in the previous section can be solved in the form of a generalized eigenvalue problem. It is worth noting that while the linear setting of each of these problems is considered in this paper, the extension to non-linear transformations involves the same mathematical framework but with the input $\mathbf{x}(t)$ exchanged for a polynomially expanded signal $\mathbf{h}(t)$ (Sprekeler et al., 2014).

¹⁰Note that in Földiák (1991) an analogous quantity is used to model memory traces as part of a learning rule for extracting slowly varying features.

3.5.1 SFA

If a centering process is applied to the raw signal $\mathbf{x}(t)$, i.e. $\mathbf{c}(t) = \mathbf{x}(t) - \langle \mathbf{x}(t) \rangle_t$, then the Type I SFA problem reduces to the following generalized eigenvalue problem (Berkas and Wiskott, 2005; Creutzig and Sprekeler, 2008)

$$\dot{\Sigma} \mathbf{W} = \Sigma \mathbf{W} \Lambda' \quad (43)$$

where $\Sigma = \langle \mathbf{c}(t) \mathbf{c}(t)^T \rangle_t$ and $\dot{\Sigma} = \langle \dot{\mathbf{c}}(t) \dot{\mathbf{c}}(t)^T \rangle_t$ are the *covariance matrices* of the input signal $\mathbf{x}(t)$ and its time derivative $\dot{\mathbf{x}}(t)$, respectively, with the former arising from the constraints in Equations (18) and (19) and the latter from the definition of slowness in Equation (16). The matrix $\mathbf{W} \in \mathbb{R}^{N \times J}$ contains J generalized eigenvectors of $(\dot{\Sigma}, \Sigma)$ which are precisely the optimal weight vectors \mathbf{w}_j , and which satisfy the following relation:

$$\mathbf{W}^T \Sigma \mathbf{W} = \mathbb{1} \quad (44)$$

Since Σ is a covariance matrix, it is guaranteed to be positive semi-definite (Potters and Bouchaud, 2020), and in the case where it is positive definite Equation (44) says that the weight vectors are orthonormal w.r.t the associated inner product $(\cdot, \cdot)_{\Sigma}$ (for a definition of positive definite and positive semi-definite matrices, see Section A.1). The matrix $\Lambda' \in \mathbb{R}^{J \times J}$ is a diagonal matrix containing the corresponding generalized eigenvalues on the diagonals, which are equal to the Δ -values and are therefore bound by $\Lambda'_{jj} \in (0, 4]$. Therefore, SFA consists in finding the generalized eigenvectors of $(\dot{\Sigma}, \Sigma)$ that have the smallest generalized eigenvalues.

3.5.2 CSFA

In Section 3.1, the objectives of SFA and CSFA are related by Equation (24). By applying a similar set of steps as in Equations (21)–(24), it is possible to deduce an analogous relationship between $\dot{\Sigma}$ and a matrix based on time-lagged statistics of the input (Blaschke et al., 2006; Creutzig and Sprekeler, 2008). In particular:

$$\dot{\Sigma} = \langle \dot{\mathbf{c}}(t) \dot{\mathbf{c}}(t)^T \rangle_t \quad (45)$$

$$= \langle (\mathbf{c}(t+1) - \mathbf{c}(t))(\mathbf{c}(t+1) - \mathbf{c}(t))^T \rangle_t \quad (46)$$

$$= \langle \mathbf{c}(t+1) \mathbf{c}(t+1)^T \rangle_t + \langle \mathbf{c}(t) \mathbf{c}(t)^T \rangle_t - \langle \mathbf{c}(t) \mathbf{c}(t+1)^T \rangle_t - \langle \mathbf{c}(t+1) \mathbf{c}(t)^T \rangle_t \quad (47)$$

$$= \langle \mathbf{c}(t+1) \mathbf{c}(t+1)^T \rangle_t + \langle \mathbf{c}(t) \mathbf{c}(t)^T \rangle_t - 2 \underbrace{\left(\frac{\langle \mathbf{c}(t) \mathbf{c}(t+1)^T \rangle_t + \langle \mathbf{c}(t+1) \mathbf{c}(t)^T \rangle_t}{2} \right)}_{=\Omega_1} \quad (48)$$

$$= 2(\Sigma - \Omega_1) \quad (49)$$

The matrix Ω_1 can be thought of as a matrix analogue of $C_1(y_j)$, and before moving on it is worth pointing out a number of details about this quantity. Firstly, since $\langle \mathbf{c}(t+1) \mathbf{c}(t)^T \rangle_t = (\langle \mathbf{c}(t) \mathbf{c}(t+1)^T \rangle_t)^T$, the matrix Ω_1 has the form $\frac{1}{2}(\mathbf{A} + \mathbf{A}^T)$ for $\mathbf{A} = \langle \mathbf{c}(t) \mathbf{c}(t+1)^T \rangle_t$ and is therefore symmetric. Secondly, \mathbf{A} contains second moments between the entries of $\mathbf{c}(t)$ and $\mathbf{c}(t+1)$, or equivalently covariances between the entries of $\mathbf{x}(t)$ and $\mathbf{x}(t+1)$, and can therefore be interpreted as a *time-lagged covariance matrix*. By extension, Ω_1 can be interpreted as a *symmetrized time-lagged covariance matrix*, or *STC matrix* for short. Thirdly, while $(\mathbf{A})_{ij} = \langle c_i(t) c_j(t+1)^T \rangle_t$ describes covariances between x_i and x_j in the forward direction, i.e. $t \rightarrow t+1$, the corresponding entry of \mathbf{A}^T can be expressed as $(\mathbf{A}^T)_{ij} = \langle c_i(t+1) c_j(t)^T \rangle_t = \langle c_i(t) c_j(t-1)^T \rangle_t$ and therefore describes covariances between x_i and x_j in the backward direction, i.e. $t \rightarrow t-1$. Thus, the symmetrization in Ω_1 effectively averages the forward and backward covariances and is therefore analogous to the additive reversibilization described in Section 2.3. This insight is relevant to the results in Section 4.

The generalized eigenvalue problem described in Equation (43) can be transformed into one based on Ω_1 , which describes the solutions to the Type I CSFA problem. In particular, inserting Equation (49) into Equation (43) gives

$$2(\Sigma - \Omega_1) \mathbf{W} = \Sigma \mathbf{W} \Lambda' \quad (50)$$

which can be easily rearranged to

$$\mathbf{\Omega}_1 \mathbf{W} = \mathbf{\Sigma} \mathbf{W} (\mathbf{1} - \frac{1}{2} \mathbf{\Lambda}') \quad (51)$$

$$= \mathbf{\Sigma} \mathbf{W} \mathbf{\Lambda} \quad (52)$$

It is worth noting that Equation (43) and Equation (52) have the same generalized eigenvectors, which is in agreement with the insight from Sections 3.1 and 3.2 that the solutions of SFA and CSFA are the same. The main difference between the equations is the eigenvalue arrays, that are related by $\mathbf{\Lambda} = (\mathbf{1} - \frac{1}{2} \mathbf{\Lambda}')$, meaning that for CSFA the generalized eigenvectors with largest generalized eigenvalues are optimal. Moreover, each eigenvalue associated to the CSFA problem can be expressed as

$$\Lambda_{jj} = 1 - \frac{1}{2} \Lambda'_{jj} \quad (53)$$

$$= 1 - \frac{1}{2} \Delta(y_j) \quad (54)$$

$$\stackrel{(24)}{=} 1 - \frac{2(1 - C_1(y_j))}{2} \quad (55)$$

$$= 1 - 1 + C_1(y_j) \quad (56)$$

$$= C_1(y_j) \quad (57)$$

meaning that $\Lambda_{jj} \in [-1, 1)$. To summarize, the generalized eigenvalue problems described by Equations (43) and (52) capture the notion that SFA and CSFA differ only in terms of whether slowness is measured with $\Delta(y_j)$ or $C_1(y_j)$, respectively.

3.5.3 τ SFA

Since τ SFA is a generalization of CSFA to larger time-lags, its corresponding generalized eigenvalue problem shares much in common with the one presented in the previous section. In particular, the solutions to the τ SFA problem can be formulated as (Blaschke et al., 2006)

$$\mathbf{\Omega}_\tau \mathbf{W} = \mathbf{\Sigma} \mathbf{W} \mathbf{\Lambda} \quad (58)$$

where

$$\mathbf{\Omega}_\tau = \frac{1}{2} (\langle \mathbf{c}(t) \mathbf{c}(t + \tau)^T \rangle_t + \langle \mathbf{c}(t + \tau) \mathbf{c}(t)^T \rangle_t) \quad (59)$$

is the STC matrix with time-lag τ , which corresponds to the objective of τ SFA and generalizes $\mathbf{\Omega}_1$ to $\tau \geq 1$. Therefore, Equation (58) generalizes Equation (52) to $\tau \geq 1$, in agreement with the relation of τ SFA to CSFA. Moreover, it is possible to show that $\Lambda_{jj} = C_\tau(y_j)$,¹¹ meaning that the generalized eigenvectors with largest generalized eigenvalues are optimal, like in CSFA. It is worth noting that the symbols $\mathbf{\Lambda}$ and \mathbf{W} in Equation (58) are used simply as place holders for eigenvalues and eigenvectors, are generally not the same as the quantities labelled in this way in Equation (52). This notation is maintained henceforth throughout the paper.

In order to make the following sections of the paper more concise, focus is placed on the more general method of τ SFA, with CSFA being discussed as a special case whenever necessary.

3.5.4 LFSFA

Since the LFSFA objective involves correlations at multiple time-lags, with all other aspects of the problem equivalent to the others presented so far, the solutions to this algorithm resemble those of τ SFA provided that

¹¹In particular, this requires the method of Lagrange multipliers as in Creutzig and Sprekeler (2008) but with $\mathbf{\Sigma}$ exchanged for $\mathbf{\Omega}_\tau$.

multiple time scales are included with temporal discounting. In particular, generalized eigenvalue problem corresponding to LFSFA is (Blaschke et al., 2006)

$$\Psi_\gamma \mathbf{W} = \Sigma \mathbf{W} \Lambda \quad (60)$$

where

$$\Psi_\gamma = \sum_{\tau=0}^{\tau_{\max}} \gamma^\tau \Omega_\tau \quad (61)$$

$$= \sum_{\tau=0}^{\tau_{\max}} \frac{\gamma^\tau}{2} (\langle \mathbf{c}(t) \mathbf{c}(t+\tau)^T \rangle_t + \langle \mathbf{c}(t+\tau) \mathbf{c}(t)^T \rangle_t) \quad (62)$$

is referred to as the *LF matrix*. In analogy to the previous sections, it is possible to show that $\Lambda_{jj} = F_\gamma(y_j)$, meaning that for LFSFA the generalized eigenvectors with largest generalized eigenvalues are optimal. Moreover, the $\tau = 0$ term contributes the following term to the LF matrix:

$$\frac{\gamma^0}{2} (\langle \mathbf{c}(t) \mathbf{c}(t)^T \rangle_t + \langle \mathbf{c}(t) \mathbf{c}(t)^T \rangle_t) = \frac{1}{2} (2\Sigma) \quad (63)$$

$$= \Sigma \quad (64)$$

Thus, in comparison to using a starting value of $\tau = 1$, all generalized eigenvalues Λ_{jj} , or equivalently all linearly filtered correlations $F_\gamma(y_j)$, are increased by a value of 1, which is consistent with the analysis of $F_\gamma(y_j)$ given in Section 3.4.

3.5.5 Corresponding regular eigenvalue problems

The generalized eigenvalue problems of the previous sections all take the form

$$\mathbf{A} \mathbf{W} = \Sigma \mathbf{W} \Lambda \quad (65)$$

where \mathbf{A} is symmetric and Σ is the data covariance matrix which is guaranteed to be positive semi-definite (Potters and Bouchaud, 2020). If additionally Σ has no eigenvalues of zero, then it is positive definite, meaning that each of these generalized eigenvalue problems can be converted to a regular eigenvalue problem using either symmetric or left normalization (see Appendices A.1 and A.3). This property is important analytically, since regular eigenvalue problems are typically easier to solve, but also practically, since most approaches to SFA involves preprocessing transformations that implicitly enforce this type of normalization as a way to satisfy the constraints. The generalized eigenvalue problems explored in the previous sections, together with the corresponding regular eigenvalue problems that result from applying symmetric and left normalization, are shown in the second column of Table 1, where $\widetilde{\mathbf{W}} = (\Sigma^{\frac{1}{2}})^T \mathbf{W}$. Note that the prime symbol used to denote generalized eigenvalues for SFA in Section 3.5.1 is dropped in order to simplify notation.

Three details are worth pointing out about the application of these normalization techniques to the generalized eigenvalue problems considered in this section. Firstly, both symmetric and left normalization are only applicable if Σ is positive definite, since they involve $\Sigma^{-\frac{1}{2}}$ and Σ^{-1} , respectively. One way they can be generalized to the case where Σ is positive semi-definite is by perturbing this matrix along its diagonals and then normalizing the resulting generalized eigenvalue problem (see Appendix A.3).¹² Such perturbations can be induced in Σ by adding Gaussian noise to the starting time series $\mathbf{x}(t)$ (see Appendix C.1), which is sometimes used as a preprocessing step in applications of SFA (Konen, 2009). For the results presented in Section 4, noise is added only if necessary, in which case the resulting perturbations are explicitly formulated.

¹²An alternative method is to compute the Moore-Penrose pseudoinverse using singular value decomposition (SVD), as in the original SFA publication Wiskott and Sejnowski (2002). This method effectively constrains the system to the subspace spanned by the eigenvectors of Σ with $\lambda > 0$.

			General input	Markovian one-hot trajectory, $T \rightarrow \infty$
SFA	No normalization	Type I	$\dot{\Sigma} \mathbf{W} = \Sigma \mathbf{W} \Lambda$	$(2\mathcal{L}_{\text{dir}} + \pi \pi^T) \mathbf{W} = (\Pi - \pi \pi^T) \mathbf{W} \Lambda$
		Type II	$\hat{\Sigma} \mathbf{W} = \hat{\Sigma} \mathbf{W} \Lambda$	$2\mathcal{L}_{\text{dir}} \mathbf{W} = \Pi \mathbf{W} \Lambda$
	Symmetric normalization	Type I	$\Sigma^{-\frac{1}{2}} \dot{\Sigma} (\Sigma^{-\frac{1}{2}})^T \tilde{\mathbf{W}} = \tilde{\mathbf{W}} \Lambda$	$(\Pi - \pi \pi^T + \sigma^2 \mathbb{1})^{-\frac{1}{2}} (2\mathcal{L}_{\text{dir}} + \pi \pi^T) (\Pi - \pi \pi^T + \sigma^2 \mathbb{1})^{-\frac{1}{2}} \tilde{\mathbf{W}} = \tilde{\mathbf{W}} \Lambda$
		Type II	$\hat{\Sigma}^{-\frac{1}{2}} \hat{\Sigma} (\hat{\Sigma}^{-\frac{1}{2}})^T \tilde{\mathbf{W}} = \tilde{\mathbf{W}} \Lambda$	$2\mathcal{L}_{\text{dir}} \tilde{\mathbf{W}} = \tilde{\mathbf{W}} \Lambda$
	Left normalization	Type I	$\Sigma^{-1} \dot{\Sigma} \mathbf{W} = \mathbf{W} \Lambda$	$(\Pi - \pi \pi^T + \sigma^2 \mathbb{1})^{-1} (2\mathcal{L}_{\text{dir}} + \pi \pi^T) \mathbf{W} = \mathbf{W} \Lambda$
		Type II	$\hat{\Sigma}^{-1} \hat{\Sigma} \mathbf{W} = \mathbf{W} \Lambda$	$2\mathcal{L}_{\text{dir}}^{\text{RW}} \mathbf{W} = \mathbf{W} \Lambda$
τ SFA	No normalization	Type I	$\Omega_\tau \mathbf{W} = \Sigma \mathbf{W} \Lambda$	$(\Pi (\mathbf{P}^\tau)_{\text{add}} - \pi \pi^T) \mathbf{W} = (\Pi - \pi \pi^T) \mathbf{W} \Lambda$
		Type II	$\hat{\Omega}_\tau \mathbf{W} = \hat{\Sigma} \mathbf{W} \Lambda$	$\Pi (\mathbf{P}^\tau)_{\text{add}} \mathbf{W} = \Pi \mathbf{W} \Lambda$
	Symmetric normalization	Type I	$\Sigma^{-\frac{1}{2}} \Omega_\tau (\Sigma^{-\frac{1}{2}})^T \tilde{\mathbf{W}} = \tilde{\mathbf{W}} \Lambda$	$(\Pi - \pi \pi^T + \sigma^2 \mathbb{1})^{-\frac{1}{2}} (\Pi (\mathbf{P}^\tau)_{\text{add}} - \pi \pi^T) (\Pi - \pi \pi^T + \sigma^2 \mathbb{1})^{-\frac{1}{2}} \tilde{\mathbf{W}} = \tilde{\mathbf{W}} \Lambda$
		Type II	$\hat{\Sigma}^{-\frac{1}{2}} \hat{\Omega}_\tau (\hat{\Sigma}^{-\frac{1}{2}})^T \tilde{\mathbf{W}} = \tilde{\mathbf{W}} \Lambda$	$\Pi^{\frac{1}{2}} (\mathbf{P}^\tau)_{\text{add}} \Pi^{-\frac{1}{2}} \tilde{\mathbf{W}} = \tilde{\mathbf{W}} \Lambda$
	Left normalization	Type I	$\Sigma^{-1} \Omega_\tau \mathbf{W} = \mathbf{W} \Lambda$	$(\Pi - \pi \pi^T + \sigma^2 \mathbb{1})^{-1} (\Pi (\mathbf{P}^\tau)_{\text{add}} - \pi \pi^T) \mathbf{W} = \mathbf{W} \Lambda$
		Type II	$\hat{\Sigma}^{-1} \hat{\Omega}_\tau \mathbf{W} = \mathbf{W} \Lambda$	$(\mathbf{P}^\tau)_{\text{add}} \mathbf{W} = \mathbf{W} \Lambda$
LFSFA	No normalization	Type I	$\Psi_\gamma \mathbf{W} = \Sigma \mathbf{W} \Lambda$	$(\Pi \mathbf{M}_{\text{add}} - \pi \pi^T) \mathbf{W} = (\Pi - \pi \pi^T) \mathbf{W} \Lambda$
		Type II	$\hat{\Psi}_\gamma \mathbf{W} = \hat{\Sigma} \mathbf{W} \Lambda$	$\Pi \mathbf{M}_{\text{add}} \mathbf{W} = \Pi \mathbf{W} \Lambda$
	Symmetric normalization	Type I	$\Sigma^{-\frac{1}{2}} \Psi_\gamma (\Sigma^{-\frac{1}{2}})^T \tilde{\mathbf{W}} = \tilde{\mathbf{W}} \Lambda$	$(\Pi - \pi \pi^T + \sigma^2 \mathbb{1})^{-\frac{1}{2}} (\Pi \mathbf{M}_{\text{add}} - \pi \pi^T) (\Pi - \pi \pi^T + \sigma^2 \mathbb{1})^{-\frac{1}{2}} \tilde{\mathbf{W}} = \tilde{\mathbf{W}} \Lambda$
		Type II	$\hat{\Sigma}^{-\frac{1}{2}} \hat{\Psi}_\gamma (\hat{\Sigma}^{-\frac{1}{2}})^T \tilde{\mathbf{W}} = \tilde{\mathbf{W}} \Lambda$	$\Pi^{\frac{1}{2}} \mathbf{M}_{\text{add}} \Pi^{-\frac{1}{2}} \tilde{\mathbf{W}} = \tilde{\mathbf{W}} \Lambda$
	Left normalization	Type I	$\Sigma^{-1} \Psi_\gamma \mathbf{W} = \mathbf{W} \Lambda$	$(\Pi - \pi \pi^T + \sigma^2 \mathbb{1})^{-1} (\Pi \mathbf{M}_{\text{add}} - \pi \pi^T) \mathbf{W} = \mathbf{W} \Lambda$
		Type II	$\hat{\Sigma}^{-1} \hat{\Psi}_\gamma \mathbf{W} = \mathbf{W} \Lambda$	$\mathbf{M}_{\text{add}} \mathbf{W} = \mathbf{W} \Lambda$

Table 1: The generalized and regular eigenvalue problems corresponding to the variants of SFA considered in this paper. In the first column, the problems are shown for a general input $\mathbf{x}(t)$, as introduced in Section 3.5, with the distinct types of objective (i.e. SFA, τ SFA, and LFSFA) illustrated in blue and the difference between Type I and Type II illustrated in red. In the second column, the input is assumed to be a Markovian one-hot trajectory and the limit $T \rightarrow \infty$ of each problem is shown, as introduced in Section 4, and a similar color scheme is used as in the first column. For example, each of the basic graph theoretic quantities involved in these limits (i.e. Laplacian, transition matrix, SR matrix) is highlighted in blue and the quantities highlighted in red are the ones which differ between Type I and Type II problems.

Secondly, while left normalization has been utilized in at least one study on SFA (Creutzig and Sprekeler, 2008), symmetric normalization is more common since it corresponds to the use of whitening in the data preprocessing phase (see Appendix C.2), which is common for implementations of all the variants of SFA considered in this section (Blaschke et al., 2006; Wang and Zhao, 2020; Wiskott and Sejnowski, 2002; Ziehe and Müller, 1998). Thirdly, while the eigenvectors $\widehat{\mathbf{W}}$ are orthogonal w.r.t. to the Euclidean inner product, those in \mathbf{W} are orthogonal w.r.t. to the weighted inner product $(\cdot, \cdot)_{\Sigma}$ (see Section 3.5.1 and Appendix A.3). In practice, most eigenvalue solvers choose vectors with Euclidean norm 1 by default, in which case the eigenvectors in \mathbf{W} need rescaled by $\mathbf{w}_i \rightarrow \frac{\mathbf{w}_i}{|\mathbf{w}_i|_{\Sigma}}$, such that $|\mathbf{w}_i|_{\Sigma} = 1$ which ensures that the unit variance constraint is met.

3.6 Solving Type II SFA Problems

For Type II problems, the solutions can similarly be described in terms of a generalized eigenvalue problem, with the only difference being that the zero mean constraint is no longer applied. For each of the Type I problems considered in the previous section, this constraint is enforced through the centering transformation $\mathbf{x}(t) \rightarrow \mathbf{c}(t)$ (Berkes and Wiskott, 2005; Creutzig and Sprekeler, 2008). Therefore, the solutions to the corresponding Type II problems can be found by omitting this transformation and leaving all other analytical details the same. In other words, the solutions of the last section are modified by replacing the vector $\mathbf{c}(t)$ with $\mathbf{x}(t)$, which leads to a set of generalized eigenvalue problems involving new matrices. In order to emphasize the correspondence of these new matrices with those of the last section, they are denoted using the same symbol but with an additional hat. For example, replacing $\mathbf{c}(t)$ for $\mathbf{x}(t)$ in Σ and $\widehat{\Sigma}$ gives

$$\widehat{\Sigma} = \langle \mathbf{x}(t)\mathbf{x}(t)^T \rangle_t \quad (66)$$

$$\widehat{\dot{\Sigma}} = \langle \dot{\mathbf{x}}(t)\dot{\mathbf{x}}(t)^T \rangle_t \quad (67)$$

which are the *second moment matrices* of $\mathbf{x}(t)$ and $\dot{\mathbf{x}}(t)$, respectively. Doing the same for Ω_{τ} and Ψ_{γ} gives

$$\widehat{\Omega}_{\tau} = \frac{1}{2} (\langle \mathbf{x}(t)\mathbf{x}(t+\tau)^T \rangle_t + \langle \mathbf{x}(t+\tau)\mathbf{x}(t)^T \rangle_t) \quad (68)$$

$$\widehat{\Psi}_{\gamma} = \sum_{\tau=0}^{\tau_{\max}} \frac{\gamma^{\tau}}{2} (\langle \mathbf{x}(t)\mathbf{x}(t+\tau)^T \rangle_t + \langle \mathbf{x}(t+\tau)\mathbf{x}(t)^T \rangle_t) \quad (69)$$

which for simplicity are not given new names. Like in the previous section, $\widehat{\Sigma}$, $\widehat{\Omega}_{\tau}$, and $\widehat{\Psi}_{\gamma}$ arise from the objectives of Type II SFA, τ SFA, and LFSFA, respectively, while $\widehat{\dot{\Sigma}}$ arises from the constraints of these problems. Moreover, the generalized eigenvalue problems associated to these problems now involve the matrix pencils $(\widehat{\Sigma}, \widehat{\dot{\Sigma}})$, $(\widehat{\Omega}_{\tau}, \widehat{\Sigma})$, and $(\widehat{\Psi}_{\gamma}, \widehat{\Sigma})$, respectively, and in the first case it is the generalized eigenvectors with smallest generalized eigenvalues that are optimal, while in the latter case it is those with largest generalized eigenvalues, again in analogy to the previous section. Moreover, the first output is guaranteed to be a constant signal in each case, which corresponds to a generalized eigenvalue of 0 and 1 in Type II SFA and CSFA, respectively. Thus, the eigenvalue intervals for these problems are $[0, 4]$ and $[-1, 1]$, respectively. Most details regarding normalization of these problems to regular eigenvalue problems generalize from the Type I case. The only major difference is that the connection between symmetric normalization and whitening does not apply to Type II problems, since whitening is formally defined only for data that has zero mean (see Appendix C.2). Each Type II generalized eigenvalue problem, together with the corresponding regular eigenvalue problems that result from symmetric/left normalization, are shown in the second column of Table 1.

3.7 Representation of the input signal

One context in which it is insightful to study SFA is where the input signal $\mathbf{x}(t) \in \mathbb{R}^N$ is generated by a lower dimensional set of source signals or latent variables, i.e. $\mathbf{u}(t) = [u_1(t), u_2(t), \dots, u_n(t)] \in \mathbb{R}^n$ with $n \ll N$,

through some non-linear transformation, i.e. $\mathbf{x}(t) = \mathbf{F}(\mathbf{u}(t))$. In this setting, which is conceptually related to the problem of non-linear blind source separation (Sprekeler et al., 2014), it is possible to show that the optimal SFA solutions are independent of the transformation \mathbf{F} and can be formulated purely in terms of the source signal $\mathbf{u}(t)$ (Franzius et al., 2007; Sprekeler and Wiskott, 2008; Sprekeler et al., 2014, 2009). In order for this argument to hold, two assumptions are necessary. Firstly, the transformation \mathbf{F} must be injective, or in other words there must be a one-to-one mapping between input data points in \mathbb{R}^N and points in the space of sources in \mathbb{R}^n . Note that this effectively implies that the input data is embedded on an n -dimensional surface in \mathbb{R}^N that is parametrized by \mathbf{u} . Secondly, the function space \mathcal{F} must be unrestricted. Together with the first assumption, this implies that any function of the input $\tilde{g}_j(\mathbf{x}(t))$ can equivalently be described as a function of the source signal, i.e.

$$\tilde{g}_j(\mathbf{x}(t)) = \tilde{g}_j(\mathbf{x}(\mathbf{u}(t))) = g_j(\mathbf{u}(t)) \quad \text{where} \quad \tilde{g}_j, g_j \in \mathcal{F} \quad (70)$$

In words, Equation (70) says that while the optimal function depends upon the choice of coordinate system, the optimal outputs do not. Thus, under both assumptions, the SFA problem can be equivalently be formulated in terms of the sources $\mathbf{u}(t)$. The key utility of this result is that by assumption $\mathbf{u}(t)$ has much lower dimensionality than $\mathbf{x}(t)$. Because of this, the application of variational calculus to the SFA problem becomes tractable and produces a partial differential equation (PDE) in terms of $\mathbf{u}(t)$ and $\dot{\mathbf{u}}(t)$ that describe the optimal SFA solutions (Franzius et al., 2007; Sprekeler and Wiskott, 2008; Sprekeler et al., 2014, 2009). It is worth noting that since it is more natural to omit the zero mean constraint in the variational calculus formalism, these studies formally correspond to Type II SFA. However, since an unrestricted function space is assumed, the solutions are equivalent to those of Type I SFA up to the constant signal and the indexing of outputs (see Section 3.1). It is also worth noting that although the optimal outputs do not depend on the coordinate system used, the SFA constraints are satisfied w.r.t. to time and not necessarily w.r.t the source variables \mathbf{u} . For example, in Type I SFA it is guaranteed that $\langle y_j(t) \rangle_t = 0$ but not necessarily that $\langle y_j(\mathbf{u}) \rangle_{\mathbf{u}} = 0$.

Clearly, an unrestricted function space is in practice not realizable, which means that the argument given above formally applies to an abstracted version of the SFA problem. However, it is possible to achieve something close to an unrestricted function space using a highly expressive variant of SFA such as a hierarchical SFA (hSFA) network, in which case the PDE described above applies to a good degree of approximation (Franzius et al., 2007).

A further simplification studied in (Franzius et al., 2007; Sprekeler and Wiskott, 2008; Sprekeler et al., 2014, 2009) is the case where each of the source signals $u_1(t)$, $u_2(t)$, ..., $u_n(t)$ are statistically independent. Under this assumption, the optimal SFA functions factorize into products of functions defined over each individual source $u_\alpha(t)$, i.e.

$$g_j(\mathbf{u}(t)) = \prod_{\alpha} g_{j\alpha}(u_\alpha(t)) \quad (71)$$

where $g_{j\alpha}$ can be thought of as a harmonic function of the source $u_\alpha(t)$ with a frequency that increases with the index j (for an in-depth discussion, see Sprekeler and Wiskott (2008); Sprekeler et al. (2014)). Moreover, if Type II SFA is considered, as in Sprekeler and Wiskott (2008); Sprekeler et al. (2014), then the $j = 1$ harmonic of each source is guaranteed to be a constant. Therefore, setting $j = 1$ for all but one source $u_\alpha(t)$ in Equation (71) shows that the corresponding single source harmonics, i.e. $g_{j\alpha} \forall j$, are also solutions to the full problem.

3.8 SFA in spatial environments

A particularly relevant application of the theory from the previous section is the case where $\mathbf{x}(t)$ is generated from sensors monitoring an agent moving around in a spatial environment. In this setting, a plausible set of source signals $\mathbf{u}(t)$ are the variables that spatially describe the agent's state in the environment. For example, in the model of Franzius et al. (2007), an agent explores a virtual open-field environment with dimensions $L_x \times L_y$ and with a visual data stream as input that is determined by the agent's position and head direction,

i.e. $\mathbf{u} = [x, y, \varphi]$. For this model, the mapping between $\mathbf{x}(t)$ and $\mathbf{u}(t)$ is injective¹³ and an hSFA network is used which offers a degree of flexibility that approaches the abstract setting of an unrestricted function space \mathcal{F} . Thus, to a good degree of approximation the optimal SFA solutions in this context are described by a PDE involving the sources $\mathbf{u}(t)$ and the corresponding time derivatives or velocities $\dot{\mathbf{u}}(t) = [v_x, v_y, \omega]$. In Franzius et al. (2007), this PDE is further simplified by assuming that the positions and orientations are homogeneously distributed over time and that the velocities are decorrelated, which the authors referred to as the *simple movement paradigm*. Since this movement paradigm satisfies the condition of statistical independence discussed in the last section, the optimal SFA solutions factorize into products of functions over x , y , and φ , and are given by:

$$g_{jln}(x, y, \varphi) = \begin{cases} \sqrt{8} \cos\left(j\pi \frac{x}{L_x}\right) \cos\left(l\pi \frac{y}{L_y}\right) \sin\left(\frac{n+1}{2}\varphi\right) & \text{for } n \text{ odd} \\ \sqrt{8} \cos\left(j\pi \frac{x}{L_x}\right) \cos\left(l\pi \frac{y}{L_y}\right) \sin\left(\frac{n}{2}\varphi\right) & \text{for } n \text{ even} \end{cases} \quad (72)$$

Using an analogous derivation, it is possible to study the optimal solutions for this movement paradigm but where the source signals only involve location, i.e. $\mathbf{u} = [x, y]$, which is more relevant to the experiments performed in Section 4. In this case, the optimal SFA solutions are given by:

$$g_{jl}(x, y) = \sqrt{4} \cos\left(j\pi \frac{x}{L_x}\right) \cos\left(l\pi \frac{y}{L_y}\right) \quad (73)$$

$$= \underbrace{\sqrt{2} \cos\left(j\pi \frac{x}{L_x}\right)}_{=g_j(x)} \underbrace{\sqrt{2} \cos\left(l\pi \frac{y}{L_y}\right)}_{=g_l(y)} \quad (74)$$

$$= g_j(x)g_l(y) \quad (75)$$

Equations (73)–(75) describe a set of 2D standing waves defined over a rectangular open field environment that decompose into a product of two 1D standing waves $g_j(x)$ and $g_l(y)$ defined over the horizontal and vertical axes of the environment, respectively. In Franzius et al. (2007), Type II SFA was considered which means that $g_j(x)$ and $g_l(y)$ are also solutions to the full problem, as explained in the previous section. Moreover, it is worth noting that $g_j(x)$ and $g_l(y)$ are equivalent to the continuous free responses in Equation (34), provided that the relative time $\frac{t-t_A}{t_B-t_A}$ is replaced by a relative position $\frac{x}{L_x}$ or $\frac{y}{L_y}$, respectively. The grid of plots in Figure 2 illustrates the solutions described by Equations (73)–(75) for $j, l = 0, 1, 2, 3$ and $\frac{L_x}{L_y} = 1.5$. The first row and column in this grid depict $g_j(x)$ and $g_l(y)$ as line plots and the remaining plots depict the corresponding products $g_{j,l}(x, y)$ as a heat maps over the open field.

Plotting SFA outputs in terms of underlying source variables, i.e. $y_j(\mathbf{u})$, can be particularly insightful when source variables are spatial. This is true not only for the optimal outputs predicted by theory, such as in Figure 2, but also for real outputs of an SFA computation. In the latter case, once a set of SFA weight vectors have been found, it is necessary to perform a post-processing phase in which the space of source signals is explored and the corresponding outputs $y_j(\mathbf{u}) = g_j(\mathbf{u})$ are computed (see Franzius et al. (2007)). Moreover, while the theory of the current and previous sections applies only to SFA, it is possible to visualize the outputs of CSFA, τ SFA and LFSFA in an equivalent manner when the underlying environment is spatial, which is done in Section 4.

4 Results

This section presents the main results of this paper, that identify analytical and conceptual relationships between the SR and all variants of SFA introduced in Section 3. Section 4.1 introduces the type of time

¹³In particular, the environment studied is sufficiently rich such that each input image \mathbf{x} corresponds to a unique position and head direction, and the environment does not change over time which means that each position and head direction corresponds to unique image \mathbf{x} .

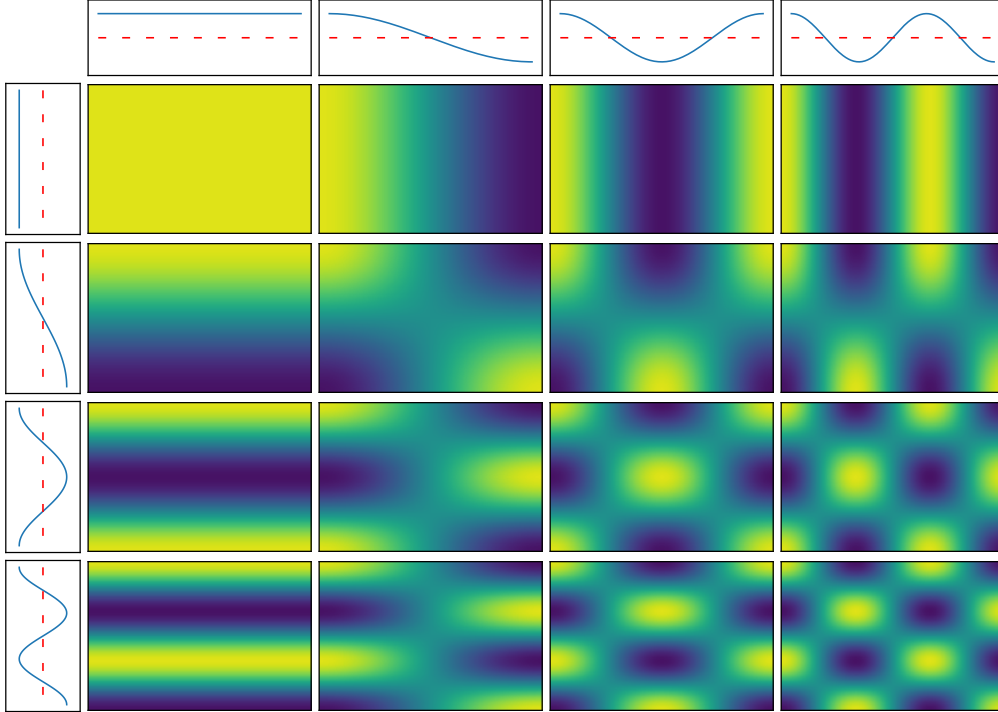


Figure 2: An illustration of the solutions described by Equations (73)–(75) for a rectangular open field with $\frac{L_x}{L_y} = 1.5$ and for $j, l = 1, 2, 3$ ordered from left to right and top to bottom, respectively.

series for which these relationships are best explored, and Section 4.2 then formalizes the relationships in the form of a set of convergence theorems that describe the particular form that the SFA problems take in the limit $T \rightarrow \infty$ for this type of time series. Then, Section 4.3 explores these theorems empirically by studying each variant of SFA for a particular type of environment and policy.

It is worth noting that although the results presented in this section are motivated by connections between SFA and the SR, they in principle apply to any use of SFA as a state representation method for finite MDPs. In particular, provided that $\mathbf{x}(t)$ satisfies the conditions outlined in Section 4.1, then the outputs of all SFA variants considered in the current study are described by the theorems of Section 4.2.

4.1 Markovian one-hot trajectories

Since SFA and the SR are defined in different contexts of machine learning, making a formal comparison between the two requires adapting one to the setting of the other. One fact that makes such an adaptation straightforward is that both are based upon the notion of a time series. In the case of SFA, this is trivially true since it is a time series method, while for the SR it stems from the fact RL is the study of temporal decision making processes. One key difference between the two is that in SFA the input time series can in principle be any sequence of observations. By contrast, the classical definition of the SR is a matrix/vector quantity and assumes a finite state space MDP as a data generating process (see Section 2.2), which restricts the resulting time series in two crucial ways. Firstly, a time series $\mathbf{x}(t)$ generated from an MDP is Markovian. This applies both to sequences of state-action pairs that are used to approximate the value function \mathbf{v} as well as sequences of states that are used to approximate the SR matrix \mathbf{M} . Secondly, in either of the cases just mentioned, each time point in $\mathbf{x}(t)$ corresponds uniquely to a choice of action and/or state. In the case of the SR, this implies a one-to-one mapping between each time point in $\mathbf{x}(t)$ and some state $s_t \in \mathcal{S}$, meaning that the time series describes a *trajectory* through the state space. In finite state space MDPs, is typical to

represent state occupation using a one-hot encoding¹⁴, i.e.

$$x_i(t) = \begin{cases} 1 & \text{if } s_i \text{ is occupied} \\ 0 & \text{otherwise} \end{cases} \quad (76)$$

Together, these two properties embody one way in which the time series' underlying the SR, henceforth referred to as *Markovian one-hot trajectories*, are less general than those considered by SFA.

The above insights suggest that one possible way to adapt SFA to the setting of the SR is to constrain the input of SFA by assuming that it is a Markovian one-hot trajectory resulting from an RL agent exploring its environment using some policy μ . The general pipeline corresponding to this is illustrated in Figure 3, where the model and policy are initially defined, before rolling out the policy to obtain the input time series $\mathbf{x}(t)$, and then applying one of the variants of SFA presented in Section 3. Note that in the last step one starts with a generalized eigenvalue problem involving some matrix pencil (\mathbf{A}, \mathbf{B}) , where either $\mathbf{A} \in \{\hat{\Sigma}, \hat{\Omega}_\tau, \hat{\Psi}_\gamma\}$ and $\mathbf{B} = \hat{\Sigma}$ or $\mathbf{A} \in \{\hat{\Sigma}, \hat{\Omega}_\tau, \hat{\Psi}_\gamma\}$ and $\mathbf{B} = \hat{\Sigma}$, which is normalized using either symmetric or left normalization to provide a regular eigenvalue problem.

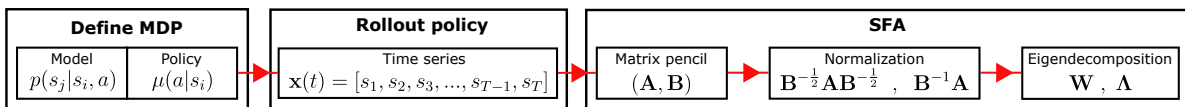


Figure 3: A data pipeline for applying SFA, τ SFA, or LFSFA to Markovian one-hot trajectories sampled from an MDP.

When applying SFA to Markovian one-hot trajectories, there are two relevant details that relate to the theory presented thus far. Firstly, for a one-hot encoding it is always possible to produce a constant output. For example, if $\mathbf{w} = \mathbf{1}$ is a constant vector of ones, then the output at each time point is always 1, i.e. $y(t) = \mathbf{1}^T \mathbf{x}(t) = 1$. Therefore, performing SFA without the zero mean constraint simply adds the additional constant output and changes the indexing of outputs by 1 (see Section 3.1). Secondly, since the value of the input $\mathbf{x}(t)$ are determined by the state occupied, one can think of the state space \mathcal{S} as a set of sources for signal. Moreover, the conditions outlined in Section 3.8 that allow the SFA problem to be formulated in terms of these sources are satisfied: i) the relation between $\mathbf{x}(t)$ and \mathcal{S} is one-to-one, ii) a one-hot encoding spans the input space \mathbb{R}^N , meaning that even without any expansions the corresponding function space is unrestricted. This implies that for such applications of SFA, each output can be visualized, like in Figure 2, as a function over the source variables, i.e. $y_j(s) \forall s \in \mathcal{S}$.

4.2 Convergence theorems

This section explores the specific form that the SFA problems of Section 3 take in the case of a Markovian one-hot trajectory, by studying the matrices involved in these problems in the limit $T \rightarrow \infty$. Sections 4.2.1 and 4.2.2 focus on Type I and Type II problems, respectively. It is worth noting that in keeping with the rest of the paper, the Markov chain underlying the input data is assumed to be ergodic, which plays an important role in the proofs of the results that are presented.

4.2.1 Type I SFA Problems

Type I problems are equivalent to eigenvalue problems involving the matrices Σ , $\hat{\Sigma}$, Ω_τ , and Ψ_γ (see Table 1). While for a general time series $\mathbf{x}(t)$ there is no rule about what the exact entries of these matrices are, for a Markovian one-hot trajectory they converge as $T \rightarrow \infty$ to values associated to the underlying Markov chain, as outlined by the following two results:

¹⁴Some extensions of the SR beyond this encoding and to continuous state spaces have been formulated using tools from deep learning (see Carvalho et al. (2024) for a review)

Theorem 4.2.1. For a Markovian one-hot trajectory $\mathbf{x}(t)$, the matrix Σ associated to the Type I constraints obeys the following limit:

$$\lim_{T \rightarrow \infty} \Sigma = \mathbf{\Pi} - \boldsymbol{\pi}\boldsymbol{\pi}^T \quad (77)$$

where $\boldsymbol{\pi}$ is the unique stationary distribution of the underlying Markov chain and $\mathbf{\Pi} = \text{diag}(\boldsymbol{\pi})$. Moreover, the limiting matrix $\mathbf{\Pi} - \boldsymbol{\pi}\boldsymbol{\pi}^T$ is guaranteed to have a single eigenvalue of 0 (proof: see Appendix D.1).

Theorem 4.2.2. For a Markovian one-hot trajectory $\mathbf{x}(t)$, the matrices $\dot{\Sigma}$, Ω_τ , and Ψ_γ associated to the Type I objectives obey the following limits:

$$\lim_{T \rightarrow \infty} \dot{\Sigma} = \mathbf{L}_{\text{dir}} + \boldsymbol{\pi}\boldsymbol{\pi}^T \quad (78)$$

$$\lim_{T \rightarrow \infty} \Omega_\tau = \mathbf{\Pi}(\mathbf{P}^\tau)_{\text{add}} - \boldsymbol{\pi}\boldsymbol{\pi}^T \quad (79)$$

$$\lim_{T \rightarrow \infty} \Psi_\gamma = \mathbf{\Pi}\mathbf{M}_{\text{add}} - \alpha\boldsymbol{\pi}\boldsymbol{\pi}^T \quad (80)$$

where \mathbf{L}_{dir} is the combinatorial directed Laplacian matrix associated to the underlying Markov chain, \mathbf{P} is the transition matrix, \mathbf{M} is the SR matrix with discount factor γ , and $\alpha = \frac{1-\gamma^{\tau_{\text{max}}+1}}{1-\gamma} \in [1, \frac{1}{1-\gamma})$ is a scalar constant (proof: see Appendix D.1).

The main insight from Theorems 4.2.1 and 4.2.2 is that for this type of input the Type I generalized eigenvalue problems converge as $T \rightarrow \infty$ to:

$$(\mathbf{L}_{\text{dir}} + \boldsymbol{\pi}\boldsymbol{\pi}^T)\mathbf{W} = (\mathbf{\Pi} - \boldsymbol{\pi}\boldsymbol{\pi}^T)\mathbf{W}\boldsymbol{\Lambda} \quad (\text{SFA}) \quad (81)$$

$$(\mathbf{\Pi}(\mathbf{P}^\tau)_{\text{add}} - \boldsymbol{\pi}\boldsymbol{\pi}^T)\mathbf{W} = (\mathbf{\Pi} - \boldsymbol{\pi}\boldsymbol{\pi}^T)\mathbf{W}\boldsymbol{\Lambda} \quad (\tau\text{SFA}) \quad (82)$$

$$(\mathbf{\Pi}\mathbf{M}_{\text{add}} - \alpha\boldsymbol{\pi}\boldsymbol{\pi}^T)\mathbf{W} = (\mathbf{\Pi} - \boldsymbol{\pi}\boldsymbol{\pi}^T)\mathbf{W}\boldsymbol{\Lambda} \quad (\text{LFSFA}) \quad (83)$$

Equation (81) relates the SFA problem to a graph Laplacian matrix \mathbf{L}_{dir} associated to the underlying Markov chain (Chung, 2005). Equation (82) relates the τ SFA problem to $\mathbf{\Pi}(\mathbf{P}^\tau)_{\text{add}}$, which is the flow matrix associated to the additive reversibilization of the underlying τ -step Markov chain (see Section 2.3). Thus, the time scale used in τ SFA extracts information relating to the τ -step transition statistics of the underlying process. For $\tau = 1$, Equation (82) relates the CSFA problem to $\mathbf{\Pi}\mathbf{P}_{\text{add}}$. Comparing this to Equation (81) indicates that swapping time derivatives for time-lagged correlations corresponds to swapping \mathbf{L}_{dir} for $\mathbf{\Pi}\mathbf{P}_{\text{add}}$, which is intuitive since in both settings the generalized eigenvectors remain the same and only the generalized eigenvalues change (see Section 3.5.2 and Seabrook and Wiskott (2023)). Equation (83) relates the LFSFA problem to $\mathbf{\Pi}\mathbf{M}_{\text{add}}$, which essentially generalizes Equation (82) across different time scales and applies temporal discounting. It is worth noting that the relation of SFA to graph Laplacians is consistent both previous and ongoing work (Schüler and Wiskott, 2024; Sprekeler, 2011), but that the relations of τ SFA and LFSFA to transition matrices and successor representations, respectively, are novel insights.

An important general feature of Equations (81)–(83) is that all matrices on the left-hand side involve symmetrization, which arises from the definitions of $\dot{\Sigma}$, Ω_τ , and Ψ_γ . In Equation (81), \mathbf{L}_{dir} is formulated in terms of a directed graph and the symmetrization is needed in order for it to be symmetric (see Section D.1). In Equations (82) and (83), the symmetrization is related to the notion of additive reversibilization, which is consistent with the observation that Ω_1 involves an additive mixture of the forwards and backwards correlations (see the discussion in Section 3.5.2), as do Ω_τ and Ψ_γ . Practically, the role of symmetrization in Equations (81)–(83) is crucial since it guarantees that all matrices on the left-hand side can be diagonalized and have real eigenvalues and eigenvectors (in the case of $\mathbf{\Pi}\mathbf{P}_{\text{add}}$ and $\mathbf{\Pi}\mathbf{M}_{\text{add}}$ these properties are proven in Theorem 2.3.3). It is worth noting that some studies on SFA introduce additional assumptions that circumvent the need for symmetrization, since this makes various analytical details more straightforward. For example, Sprekeler (2011) consider only Laplacians defined on undirected graphs and Blaschke et al. (2006); Creutzig and Sprekeler (2008) both assume that the temporal statistics of the input data are time

reversible. Conceptually, this is equivalent to the assumption made in some SR studies whereby the underlying Markov chain is formulated as a random walk on an undirected graph (Stachenfeld et al., 2014, 2017). The absence of such assumptions in the convergence results of this paper reflects the fact that SFA generally receives an input $\mathbf{x}(t)$ generated from a non-reversible process, and produces features that are related to a symmetrized/reversibilized version of this process. To the author’s knowledge, the only other study in which this has been explored is the ongoing work of Schüler and Wiskott (2024), which also relates SFA to \mathbf{L}_{dir} .

As explained in Section 3, solving the generalized eigenvalue problems corresponding to SFA, τ SFA, and LFSFA typically involves transforming them to regular eigenvalue problems using symmetric or left normalization. This similarly applies to the limits of these problems introduced above. Normalizing Equations (81)–(83) directly is not possible since $\mathbf{\Pi} - \boldsymbol{\pi}\boldsymbol{\pi}^T$ has an eigenvalue of 0 (see Section A.3 and Section 3.5.5). However, if $\mathbf{x}(t)$ is perturbed with Gaussian noise of variance σ^2 , these generalized eigenvalue problems become (see Section C.1):

$$(\mathbf{L}_{\text{dir}} + \boldsymbol{\pi}\boldsymbol{\pi}^T)\mathbf{W} = (\mathbf{\Pi} - \boldsymbol{\pi}\boldsymbol{\pi}^T + \sigma^2\mathbb{1})\mathbf{W}\boldsymbol{\Lambda} \quad (\text{SFA}) \quad (84)$$

$$(\mathbf{\Pi}(\mathbf{P}^\tau)_{\text{add}} - \boldsymbol{\pi}\boldsymbol{\pi}^T)\mathbf{W} = (\mathbf{\Pi} - \boldsymbol{\pi}\boldsymbol{\pi}^T + \sigma^2\mathbb{1})\mathbf{W}\boldsymbol{\Lambda} \quad (\tau\text{SFA}) \quad (85)$$

$$(\mathbf{\Pi}\mathbf{M}_{\text{add}} - \alpha\boldsymbol{\pi}\boldsymbol{\pi}^T)\mathbf{W} = (\mathbf{\Pi} - \boldsymbol{\pi}\boldsymbol{\pi}^T + \sigma^2\mathbb{1})\mathbf{W}\boldsymbol{\Lambda} \quad (\text{LFSFA}) \quad (86)$$

Provided that enough noise is added such that $(\mathbf{\Pi} - \boldsymbol{\pi}\boldsymbol{\pi}^T + \sigma^2\mathbb{1})$ can be inverted to a suitable degree of precision, each of the generalized eigenvalue problems above can be converted to a regular eigenvalue problem using either symmetric or left normalization. Equations (84)–(86), together with resulting regular eigenvalue problems are shown in the third column of Table 1, where the general structure of the table remains the same as for the first column except that $\mathbf{x}(t)$ is assumed to be a Markovian one-hot trajectory and the limit $T \rightarrow \infty$ is taken. The only difference lies in the choice of inverse root matrix in the case of symmetric normalization. In the first column, $\boldsymbol{\Sigma}^{-\frac{1}{2}}$ is defined only up to some rotation matrix \mathbf{Q} , since general applications of SFA do not require a specific choice of inverse root matrix. By contrast, in the second column it is assumed that $\mathbf{Q} = \mathbb{1}$ since this is the only suitable choice for a Markovian one-hot trajectory. In particular, $\mathbf{Q} = \mathbb{1}$ is the only choice that maintains the orientation of data points and therefore preserving the correspondence between each state $s_i \in \mathcal{S}$ and each entry of $\mathbf{x}(t)$. This choice leads to a symmetric inverse root matrix, i.e.

$$((\mathbf{\Pi} - \boldsymbol{\pi}\boldsymbol{\pi}^T + \sigma^2\mathbb{1})^{-\frac{1}{2}})^T = (\mathbf{\Pi} - \boldsymbol{\pi}\boldsymbol{\pi}^T + \sigma^2\mathbb{1})^{-\frac{1}{2}} \quad (87)$$

which is why the transposes are dropped in the rows corresponding to symmetric normalization of the third column in Table 1. Note that since Type I problems are considered in this section, doing symmetric normalization with $\mathbf{Q} = \mathbb{1}$ corresponds to ZCA-whitening (see Appendix C.2).

4.2.2 Type II SFA Problems

For a Markovian one-hot trajectory, the matrices $\widehat{\boldsymbol{\Sigma}}$, $\widehat{\boldsymbol{\Omega}}_\tau$ and $\widehat{\boldsymbol{\Psi}}_\gamma$ associated to the Type II problems are described in the limit $T \rightarrow \infty$ by the following pair of results that are analogous to those of the previous section:

Theorem 4.2.3. *For a Markovian one-hot trajectory $\mathbf{x}(t)$, the matrix $\widehat{\boldsymbol{\Sigma}}$ associated to the Type II constraints obeys the following limit:*

$$\lim_{T \rightarrow \infty} \widehat{\boldsymbol{\Sigma}} = \mathbf{\Pi} \quad (88)$$

where $\boldsymbol{\pi}$ is the unique stationary distribution of the underlying Markov chain and $\mathbf{\Pi} = \text{diag}(\boldsymbol{\pi})$. Moreover, the limiting matrix $\mathbf{\Pi}$ is guaranteed to have no eigenvalues of 0 (proof: see Appendix D.2).

Theorem 4.2.4. *For a Markovian one-hot trajectory $\mathbf{x}(t)$, the matrices $\widehat{\boldsymbol{\Sigma}}$, $\widehat{\boldsymbol{\Omega}}_\tau$, and $\widehat{\boldsymbol{\Psi}}_\gamma$ associated to the*

Type II objectives obey the following limits:

$$\lim_{T \rightarrow \infty} \widehat{\Sigma} = \mathbf{L}_{\text{dir}} \quad (89)$$

$$\lim_{T \rightarrow \infty} \widehat{\Omega}_\tau = \mathbf{\Pi}(\mathbf{P}^\tau)_{\text{add}} \quad (90)$$

$$\lim_{T \rightarrow \infty} \widehat{\Psi}_\gamma = \mathbf{\Pi} \mathbf{M}_{\text{add}} \quad (91)$$

where \mathbf{L}_{dir} is the combinatorial directed Laplacian matrix associated to the underlying Markov chain, \mathbf{P} is the transition matrix, and \mathbf{M} is the SR matrix with discount factor γ (proof: see Appendix D.2).

The main insight from Theorem 4.2.3 and Theorem 4.2.4 is that for this type of input, the Type II generalized eigenvalue problems converge as $T \rightarrow \infty$ to

$$\mathbf{L}_{\text{dir}} \mathbf{W} = \mathbf{\Pi} \mathbf{W} \mathbf{\Lambda} \quad (\text{SFA}) \quad (92)$$

$$\mathbf{\Pi}(\mathbf{P}^\tau)_{\text{add}} \mathbf{W} = \mathbf{\Pi} \mathbf{W} \mathbf{\Lambda} \quad (\tau\text{SFA}) \quad (93)$$

$$\mathbf{\Pi} \mathbf{M}_{\text{add}} \mathbf{W} = \mathbf{\Pi} \mathbf{W} \mathbf{\Lambda} \quad (\text{LFSFA}) \quad (94)$$

Thus, like in the previous section, SFA is related to \mathbf{L}_{dir} , τSFA to $\mathbf{\Pi}(\mathbf{P}^\tau)_{\text{add}}$, and LFSFA to $\mathbf{\Pi} \mathbf{M}_{\text{add}}$. The only difference in comparison to Type I problems is that the outer products $\boldsymbol{\pi} \boldsymbol{\pi}^T$ are no longer present on either side of the equations, which is due to the fact that the centering step is omitted (see Appendix D.2). This distinction offers a number of simplifications. Firstly, the generalized eigenvalue problems described by Equations (92)–(94) can be normalized directly without the need for adding noise since $\mathbf{\Pi}$ has no eigenvalues of 0. Secondly, since $\mathbf{\Pi}$ is a diagonal matrix, the normalization matrices take on a particularly simple form. For example, the inverse $\mathbf{\Pi}^{-1}$ is diagonal and contains the reciprocals of the stationary probabilities, i.e. $\frac{1}{\pi_i}$. Similarly, for $\mathbf{Q} = \mathbb{1}$ the inverse root matrix $\mathbf{\Pi}^{-\frac{1}{2}}$ is also diagonal and contains the reciprocal square roots of the stationary probabilities, i.e. $\frac{1}{\sqrt{\pi_i}}$. Thirdly, the regular eigenvalue problems that result from normalizing Equations (92)–(94) involve matrices that are well understood analytically. For example, symmetric and left normalization of the SFA problem described by Equation (92) leads to

$$\mathcal{L}_{\text{dir}} \widetilde{\mathbf{W}} = \widetilde{\mathbf{W}} \mathbf{\Lambda} \quad (95)$$

and

$$\mathbf{L}_{\text{dir}}^{\text{RW}} \mathbf{W} = \mathbf{W} \mathbf{\Lambda} \quad (96)$$

, respectively, where $\mathcal{L}_{\text{dir}} = \mathbf{\Pi}^{-\frac{1}{2}} \mathbf{L}_{\text{dir}} \mathbf{\Pi}^{-\frac{1}{2}}$ and $\mathbf{L}_{\text{dir}}^{\text{RW}} = \mathbf{\Pi}^{-1} \mathbf{L}_{\text{dir}}$ are known as the *symmetric normalized* and *random walk normalized* directed Laplacian matrices, respectively (Wiskott and Schönfeld, 2019). Moreover, symmetric and left normalization of the τSFA problem described by Equation (93) leads to

$$\mathbf{\Pi}^{\frac{1}{2}} (\mathbf{P}^\tau)_{\text{add}} \mathbf{\Pi}^{-\frac{1}{2}} \widetilde{\mathbf{W}} = \widetilde{\mathbf{W}} \mathbf{\Lambda} \quad (97)$$

and

$$(\mathbf{P}^\tau)_{\text{add}} \mathbf{W} = \mathbf{W} \mathbf{\Lambda} \quad (98)$$

, respectively, and for the LFSFA problem described by Equation (94) to

$$\mathbf{\Pi}^{\frac{1}{2}} \mathbf{M}_{\text{add}} \mathbf{\Pi}^{-\frac{1}{2}} \widetilde{\mathbf{W}} = \widetilde{\mathbf{W}} \mathbf{\Lambda} \quad (99)$$

and

$$\mathbf{M}_{\text{add}} \mathbf{W} = \mathbf{W} \mathbf{\Lambda} \quad (100)$$

, respectively. Note that the eigenvalues and eigenvectors of $\mathbf{\Pi}^{\frac{1}{2}} (\mathbf{P}^\tau)_{\text{add}} \mathbf{\Pi}^{-\frac{1}{2}}$, $(\mathbf{P}^\tau)_{\text{add}}$, $\mathbf{\Pi}^{\frac{1}{2}} \mathbf{M}_{\text{add}} \mathbf{\Pi}^{-\frac{1}{2}}$, and \mathbf{M}_{add} are all explored in Theorem 2.3.3. All generalized and regular eigenvalue problems discussed in this section are shown in the third column of Table 1.

4.3 Experimentation

This section illustrates the results of the previous section by following the pipeline outlined in Figure 3 for a specific environment and policy. Since the main novel insight of these results concerns the relationship of τ SFA and LFSFA to transition matrices and SRs, respectively, focus is placed on these two versions of SFA. Moreover, the Type II left normalized versions of these problems are considered since the relationship to transition matrices and SRs is clearest for these cases (see Table 1), and also since they do not require the addition of noise. In Section 4.3.1 the choice of environment and policy is discussed, and in Section 4.3.2 the matrices involved in these problems as well as the corresponding outputs are computed for a time series $\mathbf{x}(t)$ resulting from this policy and environment.

4.3.1 Setup

The environment considered in this paper is a *gridworld*, which is a canonical choice of toy model in RL research. In a gridworld, the state space \mathcal{S} is a finite 2D lattice of states, often having some degree of spatial regularity, and from each state the agent can make actions that typically induce deterministic transitions to neighbouring states. This paper considers the most simple example of a gridworld, namely a rectangular open field with no barriers or obstacles, and with fixed boundaries (i.e. no cyclic topology). States are arranged in a square geometry, with the action set fixed across all states and involving the four cardinal directions and the possibility of remaining in the same state, i.e. $\mathcal{A} = (\leftarrow, \rightarrow, \uparrow, \downarrow, \circ)$. When a forbidden action is made, such as moving right at a state on the rightmost edge, this results in a transition in the opposite direction, i.e. left. This rule is referred to as a *reflective boundary condition* in this paper.

The policy considered in this paper is one in which actions are selected with equal probability in each state, which is referred to henceforth as a *uniform policy* and which corresponds to $p(\leftarrow, \rightarrow, \uparrow, \downarrow, \circ) = \frac{1}{5} = 0.2$, for the environment just described. The combination of this policy together with the environment produces a Markov chain with transition statistics that are highly uniform, depending only on whether the starting state is located in the bulk, on an edge, or in a corner. This is referred to as a *uniform random walk* in the current paper.

Despite being highly simplified, the choice of environment and policy is fitting to this paper for three reasons. Firstly, the results of the previous section only require that the Markov chain is ergodic, which is satisfied for any uniform random walk provided that self-transitions are allowed (Seabrook and Wiskott, 2023). Secondly, SR models of place- and grid-like maps often consider uniform random walks as a baseline case of interest (Stachenfeld et al., 2014, 2017). Thirdly, a rectangular open field together with a uniform policy is the closest discrete analogue of the visual environment and simple movement paradigm considered in Franzius et al. (2007), meaning that useful comparisons can be made to the theoretical and experimental results of this study.

4.3.2 Simulation

The simulations of this section involve a rectangular open field gridworld with dimensions $L_x \times L_y = 15 \times 10$, which an agent explores using a uniform policy. This policy is rolled out for $T = 10^6$ steps, producing a Markovian one-hot trajectory $\mathbf{x}(t)$ where each vector has 150 entries corresponding to each possible state that can be occupied. The Type II left normalized variants of τ SFA and LFSFA are then applied this time series.

It is worth noting that the uniform random walk is guaranteed to be reversible since there are no cycles in the state space that involve a net flow of probability (Seabrook and Wiskott, 2023). Thus, for the resulting time series $\mathbf{x}(t)$ the additive reversibilization can w.l.o.g. be dropped in all limits of Table 1. For the Type II left normalized variants of τ SFA and LFSFA this yields

$$P^T W = W \Lambda \tag{101}$$

and

$$M W = W \Lambda \tag{102}$$

, respectively. Note that a single eigenbasis can be chosen for all τ in Equation (101) (Seabrook and Wiskott, 2023) and that Theorem 2.3.1 states that this basis is also a solution to Equation (102).

The performance of τ SFA and LFSFA in the setting described can first be analyzed at the level of the matrices involved. One way to visualize the matrices is to plot the rows or columns as fields over the state space. In this paper, the latter option is used since it offers a closer comparison with studies of the SR that focus on the column structure (Gershman, 2018; Stachenfeld et al., 2014, 2017). The τ SFA problem is illustrated in Figure 4(a-f), where a single column of $\widehat{\Sigma}^{-1}\widehat{\Omega}_\tau$ is shown for $\tau = 0, 1, 2, 3, 4, 5$, corresponding to a state s in the right-hand side of the open field. For $\tau = 1$, the shape of the field shows equal values for the state and its neighbours, and zero for all other states. This can be understood from the fact that $\widehat{\Sigma}^{-1}\widehat{\Omega}_1$ is close to \mathbf{P} in the large data limit (see Equation (101)), and so the corresponding column of this matrix represents the set of transition probabilities that lead into state s , which are equal to 0.2 for the state itself and the nearest neighbours but 0 for all others. For $\tau > 1$, $\widehat{\Sigma}^{-1}\widehat{\Omega}_\tau$ is close to \mathbf{P}^τ which contains the τ -step transition statistics. As τ increases, each column of \mathbf{P}^τ becomes increasingly diffuse since the number of states from which it is possible to access a given state s increases. This is demonstrated in Figure 4(c-f), where the corresponding columns of $\widehat{\Sigma}^{-1}\widehat{\Omega}_\tau$ have a spatial resolution that decreases as τ increases. For $\tau = 0$, the field is non-zero only for the state itself, which agrees with the fact that $\mathbf{P}^0 = \mathbf{1}$. The LFSFA problem is illustrated in Figure 4(g-l), where a single column of $\widehat{\Sigma}^{-1}\widehat{\Psi}_\gamma$ is shown for multiple values of γ , corresponding to the same state as in Figure 4(a-f). As γ increases, the fields show a decreasing spatial resolution, which reflects how smaller (larger) values of γ assign less (more) weight to the larger values of τ . For example, for $\gamma = 0.5, 0.6$ the fields consist mostly in the $\tau = 0, 1$ components illustrated in Figure 4(a,b), whereas for $\gamma = 0.9, 0.99$ the fields are widely diffuse and take into account correlations at large time scales, such as those illustrated in Figure 4(c-f). Note that for large γ values the fields look more smooth than the fields corresponding to a single large value of τ , which by comparison appear more granular. This stems from the fact that the LF matrix, as well as the SR matrix, applies an exponential decay over time, which effectively averages the information present in the different time scales of the underlying Markov chain.

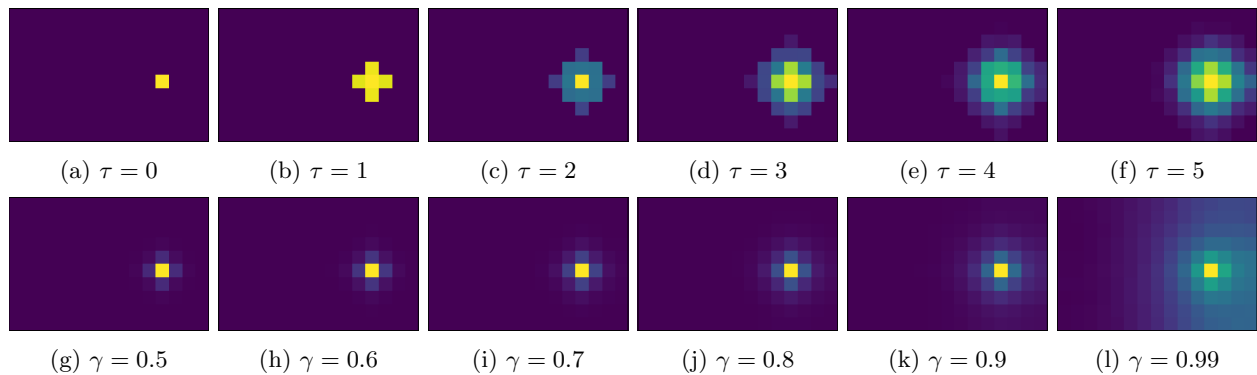


Figure 4: The column of $\widehat{\Sigma}^{-1}\widehat{\Omega}_\tau$ and $\widehat{\Sigma}^{-1}\widehat{\Psi}_\gamma$ corresponding to a single state s , for $\tau = 0, 1, 2, 3, 4, 5$ and $\gamma = 0.5, 0.6, 0.7, 0.8, 0.9, 0.99$.

Since Equations (101) and (102) can be solved with a common set of eigenvectors, this section focuses on a single set of solutions for $\tau = 1$, i.e. CSFA, and studies how the correlation values, or equivalently the eigenvalues, of these solutions differ between each problem. The CSFA solutions are computed by performing an eigendecomposition on $\widehat{\Sigma}^{-1}\widehat{\Omega}_1 \in \mathbb{R}^{150 \times 150}$, which produces 150 solutions in total. In Figure 5, a selection of the outputs are visualized as functions over the state space \mathcal{S} . The index j beneath each plot reflects how the selected outputs are ordered for this problem, i.e. the first and last row contain the 6 most highly correlated and anti-correlated outputs, respectively, while the middle row contains 6 intermediate outputs that are roughly equally spaced in this ordering. The correlation/eigenvalue C_1 corresponding to each output is shown in the second row of Table 2.

The CSFA outputs in Figure 5 can be interpreted using Equation (101) which describes the limit of this

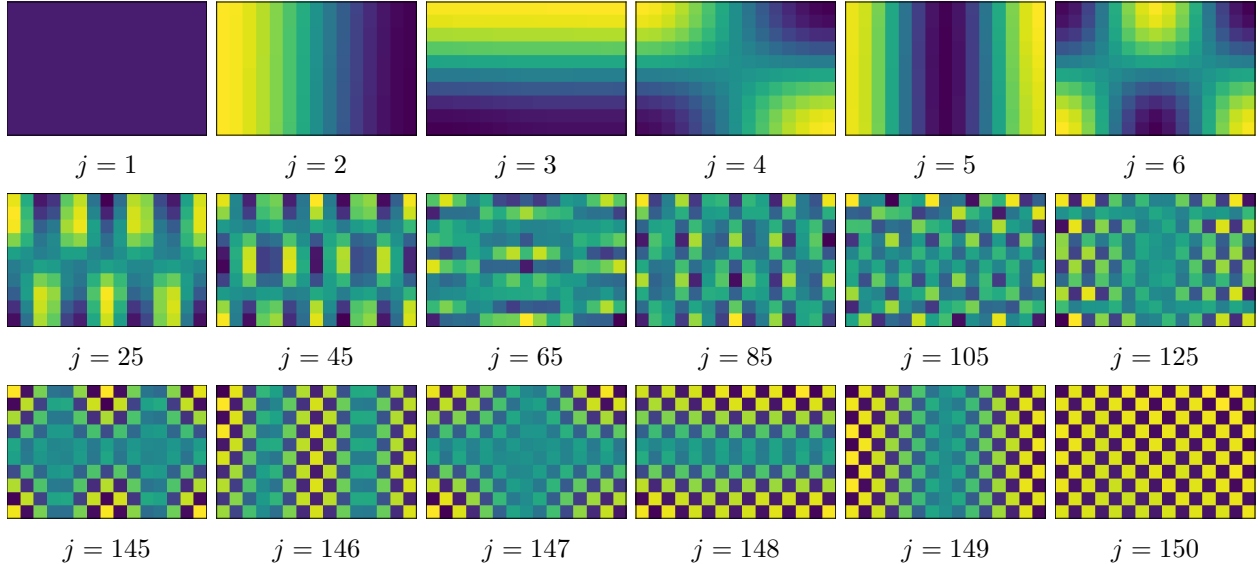


Figure 5: A selection of 18 outputs of the Type II left normalized CSFA problem, computed with the eigenvectors of $\hat{\Sigma}^{-1}\hat{\Omega}_1$, with the index of each output indicated below each plot.

j	1	2	3	4	5	6	25	45	65	85	105	125	145	146	147	148	149	150
C_1	1	0.99	0.98	0.97	0.96	0.94	0.67	0.42	0.26	0.15	0	-0.26	-0.54	-0.56	-0.57	-0.58	-0.59	-0.6
C_2	1	0.98	0.95	0.93	0.92	0.88	0.44	0.17	0.06	0.02	0	0.07	0.29	0.31	0.32	0.33	0.35	0.36
C_3	1	0.97	0.93	0.9	0.89	0.82	0.3	0.07	0.02	0	0	-0.02	-0.15	-0.18	-0.18	-0.19	-0.21	-0.22
$F_{0.8}$	5	4.81	4.57	4.4	4.32	3.99	2.14	1.5	1.25	1.14	1.0	0.83	0.7	0.69	0.69	0.68	0.68	0.68
$F_{0.9}$	10	9.16	8.21	7.64	7.36	6.35	2.51	1.59	1.29	1.16	0.99	0.81	0.67	0.66	0.66	0.66	0.65	0.65

Table 2: The values of C_1 , C_2 , C_3 , $F_{0.8}$, and $F_{0.9}$ for all outputs visualized in Figure 5.

problem in the large data limit. In particular, as $T \rightarrow \infty$ the matrix $\hat{\Sigma}^{-1}\hat{\Omega}_1$ converges to the underlying transition matrix \mathbf{P} . Such matrices are guaranteed to have a constant right eigenvector with eigenvalue $\lambda = 1$ (Seabrook and Wiskott, 2023), which corresponds to the constant output that is guaranteed whenever the zero mean constraint is omitted from SFA. This output is the first one illustrated in Figure 5. Moreover, since the underlying Markov chain is reversible, the other eigenvectors of \mathbf{P} are described by spectral graph theory, with the eigenvalues describing the smoothness of each eigenvector across the state space \mathcal{S} (Seabrook and Wiskott, 2023). In particular, eigenvectors with large positive eigenvalues have similar values for nearby states, while those with large negative eigenvalues alternate a lot between nearby states, which can be clearly seen in first and last rows of Figure 5, respectively.

Alternatively, the plots of Figure 5 can be interpreted using various theoretical insights from Section 3. In particular, they have the form of discretized 2D cosine functions, and therefore resemble discrete analogues of the analytical solutions found in Franzius et al. (2007) and explored in Section 3.8. Moreover, in analogy to those solutions, each output illustrated in Figure 5 factorizes into a product of 1D cosine functions defined over the x and y axes of the gridworld, with each 1D function having a correspondence to the discrete free responses explored in Section 3.2. One difference between the two cases is that while the analytical solutions

found in Franzius et al. (2007) all have positive correlations, the outputs in the second row of Figure 5, as well as some in the middle row, have a negative correlation (see Table 2). These negatively correlated solutions occur as a result of the environment being discretized, in analogy to the discretized free responses explored in Section 3.2.

It is worth noting that the exact form of the CSFA outputs, as well as the associated correlation values, depends in part on various implementation details of the underlying model. For example, while the simulations of this paper use a reflective boundary condition, other choices of boundary condition produce similar outputs to those in Figure 5 but with additional edge effects. A reflective boundary condition is used in this paper since it offers the closest correspondence to the solutions studied in Section 3.2 and Section 3.8. Moreover, self-transitions are allowed in the random walk since this is one way to ensure ergodicity, which is required for the results of Section 4.2 to hold. One side effect this has is that the correlation values of all outputs except $j = 1$ are slightly larger than their counterparts in the free response setting. For example, the output for $j = 150$ resembles a product of signals that correspond to the strictly alternating free response in Figure 1f. While the latter is perfectly anti-correlated, i.e. $C_1 = -1$, the former is only moderately anti-correlated since the random walker can remain in the same state and see the same values in this output from one time point to the next. One way to reduce this disagreement while maintaining ergodicity is to decrease the probability of self-transitions to some value $\epsilon \ll 1$.

For each output $y_j(t) = \mathbf{w}_j^T \mathbf{x}(t)$ found for the CSFA problem, the values of C_τ and F_γ can be computed using the following *generalized Rayleigh quotients* (Ghojogh et al., 2023):

$$C_\tau = \frac{\mathbf{w}_j^T \widehat{\mathbf{\Omega}}_\tau \mathbf{w}_j}{\mathbf{w}_j^T \widehat{\mathbf{\Sigma}} \mathbf{w}_j} \quad (103)$$

$$F_\gamma = \frac{\mathbf{w}_j^T \widehat{\mathbf{\Psi}}_\gamma \mathbf{w}_j}{\mathbf{w}_j^T \widehat{\mathbf{\Sigma}} \mathbf{w}_j} \quad (104)$$

The third and fourth rows of Table 2 show the values of C_2 and C_3 for each of the outputs in Figure 5, respectively. Note that outputs with positive C_1 have positive C_2 and C_3 , while outputs with negative C_1 have positive C_2 and negative C_3 . In agreement with the free responses presented in Section 3.2, this reflects the fact that even values of τ tend to order outputs in a different way to $\tau = 1$ while odd values tend to maintain the same ordering. Moreover, Equation (101) implies that C_2 and C_3 are approximately the eigenvalues of \mathbf{P}^2 and \mathbf{P}^3 , respectively, which are known to be λ^2 and λ^3 for each eigenvalue of \mathbf{P} (Seabrook and Wiskott, 2023). Analogously, in Figure 5 the values of C_2 and C_3 are approximately equal to C_1^2 and C_1^3 for each output.¹⁵ The fifth and sixth row of Table 2 show the values of $F_{0.8}$ and $F_{0.9}$ for each of the signals in Figure 5, respectively. The values of F_γ have a magnitude that is inversely related to γ , in analogy to how the eigenvalues of \mathbf{M} relate to γ , and they are ordered in the same way as C_1 , in analogy to how the eigenvalues of \mathbf{M} are ordered in the same way as those of \mathbf{P} for a sufficiently large horizon (see Theorem 2.3.1 and Section 2.4). One detail worth emphasizing about time lags larger than 1 is that the associated matrix $\widehat{\mathbf{\Omega}}_\tau$ is related to the τ -step transition statistics of the underlying random walk, which become more noisy as τ increases. Therefore, performing τ SFA with $\tau > 1$ produces outputs that are subject to more noise than for the $\tau = 1$ case. In the example studied above, the clearest indicator of this effect is that the uniform patterns in the first and third rows of Figure 5 typically become increasingly distorted as τ increases. A similar effect happens when the parameter γ in LFSFA is set very close to 1, since this assigns more weight to larger values of τ .

5 Discussion

This paper presents a conceptual bridge between SFA and the SR, by first exploring a set of variants of the SFA algorithm each of which corresponding to a generalized or regular eigenvalue problem. Each eigenvalue

¹⁵Note that in order for the correlations to be related in this way, it is necessary that the underlying chain is reversible so that all additive reversibilizations can be dropped, which was assumed in Equation (101)

problem is studied in the specific case of a Markovian one-hot trajectory, which is the typical type of time series used to make sample-based approximations of SR matrices. The outputs of each SFA variant in this context is considered in the large data limit, leading to a number of convergence results. These convergence results are then demonstrated for a gridworld, which is a typical toy setting in which the SR is studied.

Perhaps the main conceptual insight of the results is the close correspondence between the matrices, eigenvalues, and eigenvectors involved in each variant of SFA and their counterparts associated to the underlying Markov chain. For example, SFA is related to \mathbf{L}_{dir} , τ SFA to $(\mathbf{P}^T)_{\text{add}}$, and LFSFA to \mathbf{M}_{add} , and in each case the delta/correlation values and outputs correspond to the eigenvalues and eigenvectors of these matrices, respectively. These observations point towards spectral graph theory as a unified formalism for understanding both SFA and the SR.

A more practical insight is that SFA and the SR can be used as complementary methods for state representation of an MDP. On one hand, SRs are perhaps a more natural choice for doing this than SFA since they: i) are defined in terms of an MDP, ii) can be learnt in different ways depending on the type of RL task being studied (Russek et al., 2017), and iii) can alternatively be defined for state action pairs (Ducarouge and Sigaud, 2017). On the other hand, while the SR in its classical definition is restricted to finite MDPs, SFA can essentially be performed on any time series and can flexibly deal with different choices of function spaces. Therefore, SFA is comparatively more adaptable to general RL tasks than the SR.

The second point above underscores one of the main limitation of the current paper, namely, that the input to SFA is restricted to a Markovian one-hot trajectory. While this choice enables the main results of the paper to be established, it also limits the scope of the connection established between SFA and the SR. However, it is worth noting that some generalizations of the SR beyond finite MDPs have been made, which are typically referred to as *successor features* (Carvalho et al., 2024). Therefore, one potential future development of this work would be to explore how, if at all, the application of SFA to a general time series $\mathbf{x}(t)$ is related to these methods.

Appendices

Appendix A Linear Algebra

A.1 Eigenvalue problems

Given a real square matrix $\mathbf{A} \in \mathbb{R}^{N \times N}$, an eigenvector is any vector $\mathbf{w} \in \mathbb{R}^N$ that when multiplied by \mathbf{A} produces a new vector that is simply a scaled version \mathbf{w} (Banerjee and Roy, 2014). If such a vector is a column vector, this can be expressed as

$$\mathbf{A}\mathbf{w} = \lambda\mathbf{w} \tag{105}$$

and \mathbf{w} is known as a *right eigenvector* of \mathbf{A} . If instead the vector is a row vector, then the corresponding equation is

$$\mathbf{w}^T \mathbf{A} = \lambda\mathbf{w}^T \tag{106}$$

and \mathbf{w} is known as a *left eigenvector* of \mathbf{A} . In Equations (105) and (106), the scaling factor λ is known as the *eigenvalue* associated to the eigenvector, and the problem of finding solutions to these equations is referred to as an *eigenvalue problem*. If there exist a set of N linearly independent right eigenvectors of \mathbf{A} , Equation (105) can be written for all these vectors simultaneously as

$$\mathbf{A}\mathbf{W} = \mathbf{W}\mathbf{\Lambda} \tag{107}$$

where $\mathbf{W} \in \mathbb{R}^{N \times N}$ contains the vectors as columns and $\mathbf{\Lambda} \in \mathbb{R}^{N \times N}$ is a diagonal matrix containing the corresponding eigenvalues. Since the columns of \mathbf{W} are linearly independent, its inverse \mathbf{W}^{-1} is well-defined and by multiplying Equation (107) in various ways with this matrix leads to insight on the relationship between \mathbf{A} and \mathbf{W} . Firstly, multiplying Equation (107) from the left by \mathbf{W}^{-1} gives

$$\mathbf{W}^{-1}\mathbf{A}\mathbf{W} = \mathbf{\Lambda} \tag{108}$$

which says that the matrix \mathbf{A} is a diagonal transformation when expressed in the basis \mathbf{W} . Secondly, multiplying Equation (108) from the right by \mathbf{W}^{-1} gives

$$\mathbf{W}^{-1}\mathbf{A} = \mathbf{\Lambda}\mathbf{W}^{-1} \quad (109)$$

which says that the rows of \mathbf{W}^{-1} are a basis of left eigenvectors of \mathbf{A} . Lastly, multiplying Equation (107) from the right by \mathbf{W}^{-1} gives

$$\mathbf{A} = \mathbf{W}\mathbf{\Lambda}\mathbf{W}^{-1} \quad (110)$$

Equation (110) expresses the matrix \mathbf{A} purely in terms of its eigenvalue and eigenvector matrices, and for this reason is often referred to as the *eigendecomposition* of \mathbf{A} (Banerjee and Roy, 2014).

Not all matrices are diagonalizable. However, *the spectral theorem* states that this property holds for all symmetric real matrices and describes a number of properties belonging to the eigenvalues and eigenvectors. In particular, if \mathbf{A} is a real symmetric matrix, then the eigenvalues are real and the eigenvectors can be chosen to be both real and orthonormal (Banerjee and Roy, 2014). If the eigenvectors are chosen in this way, i.e. $\mathbf{W} \in \mathbb{R}^{N \times N}$ and $\mathbf{W}^{-1} = \mathbf{W}^T$, then Equation (110) simplifies to

$$\mathbf{A} = \mathbf{W}\mathbf{\Lambda}\mathbf{W}^T \quad (111)$$

Moreover, if the eigenvectors are chosen such that $\mathbf{W}^{-1} = \mathbf{W}^T$ then the rows of \mathbf{W}^{-1} are equal to the columns of \mathbf{W} , meaning that the left and right eigenvectors are the same (Seabrook and Wiskott, 2023).

If a symmetric matrix has only positive eigenvalues, then it is called *positive-definite* (Banerjee and Roy, 2014). This means that all diagonal entries of $\mathbf{\Lambda}$ are positive, and the inverse of \mathbf{A} is

$$\mathbf{A}^{-1} = (\mathbf{W}\mathbf{\Lambda}\mathbf{W}^T)^{-1} \quad (112)$$

$$= \mathbf{W}\mathbf{\Lambda}^{-1}\mathbf{W}^T \quad (113)$$

where $\mathbf{\Lambda}^{-1}$ contains the inverses of the diagonals of $\mathbf{\Lambda}$. Comparing Equation (113) to Equation (111), one sees that \mathbf{A}^{-1} has the same eigenvectors as \mathbf{A} and its eigenvalues are simply the reciprocals of the eigenvalues of \mathbf{A} , and that therefore \mathbf{A}^{-1} is also positive definite.

If the eigenvalues of \mathbf{A} are instead non-negative (so that $\lambda = 0$ is allowed), the matrix is called *positive semi-definite* and \mathbf{A}^{-1} is not well-defined.

A.2 Square root and inverse square root of a positive definite matrix

Let $\mathbf{B} \in \mathbb{R}^{N \times N}$ be a symmetric positive definite matrix. If \mathbf{U} is an orthonormal set of eigenvectors for this matrix and \mathbf{D} is a diagonal matrix containing the corresponding real and positive eigenvalues, then $\mathbf{B} = \mathbf{U}\mathbf{D}\mathbf{U}^T$ as in Equation (110). The square root of \mathbf{B} can be defined as some matrix $\mathbf{B}^{\frac{1}{2}}$ that satisfies the following equation:

$$\mathbf{B} = \mathbf{C}\mathbf{C} = \mathbf{C}^2 \quad (114)$$

Solutions to this equation can be constructed using the eigenvector and eigenvalue matrices \mathbf{U} and \mathbf{D} , respectively (Banerjee and Roy, 2014). In particular, consider the matrix $\mathbf{B}^{\frac{1}{2}} = \mathbf{U}\mathbf{D}^{\frac{1}{2}}\mathbf{U}^T$ where $\mathbf{D}^{\frac{1}{2}}$ contains the square roots of the eigenvalues of \mathbf{B} . This matrix clearly satisfies Equation (114):

$$\mathbf{B}^{\frac{1}{2}}\mathbf{B}^{\frac{1}{2}} = \mathbf{U}\mathbf{D}^{\frac{1}{2}}\underbrace{\mathbf{U}^T\mathbf{U}}_{=\mathbf{1}}\mathbf{D}^{\frac{1}{2}}\mathbf{U}^T \quad (115)$$

$$= \mathbf{U}\underbrace{\mathbf{D}^{\frac{1}{2}}\mathbf{D}^{\frac{1}{2}}}_{=\mathbf{D}}\mathbf{U}^T \quad (116)$$

$$= \mathbf{U}\mathbf{D}\mathbf{U}^T \quad (117)$$

$$= \mathbf{B} \quad (118)$$

Two similarities of \mathbf{B} and $\mathbf{B}^{\frac{1}{2}}$ are worth mentioning. Firstly, they are simultaneously diagonalizable by the basis \mathbf{U} , and the eigenvalues of $\mathbf{B}^{\frac{1}{2}}$ are the square roots of the eigenvalues of \mathbf{B} . Secondly, like \mathbf{B} , the matrix $\mathbf{B}^{\frac{1}{2}}$ is symmetric:

$$(\mathbf{B}^{\frac{1}{2}})^T = (\mathbf{U}\mathbf{D}^{\frac{1}{2}}\mathbf{U}^T)^T \quad (119)$$

$$= \mathbf{U}\mathbf{D}^{\frac{1}{2}}\mathbf{U}^T \quad (120)$$

$$= \mathbf{B}^{\frac{1}{2}} \quad (121)$$

One difference is that, unlike \mathbf{B} , the matrix $\mathbf{B}^{\frac{1}{2}}$ is not necessarily positive definite. To see this, note that each eigenvalue of \mathbf{B} has both a positive and negative square root, meaning that there are in fact 2^n choices for the matrix $\mathbf{D}^{\frac{1}{2}}$ where n is the number of distinct eigenvalues. The unique choice for which $\mathbf{B}^{\frac{1}{2}}$ is positive definite is when only the positive roots are chosen, in which case $\mathbf{B}^{\frac{1}{2}}$ is referred to as the *positive square root* of \mathbf{B} . Henceforth and in the main text it is assumed that the square root of a diagonal matrix always uses the positive roots only.

Since \mathbf{B} is positive definite, it has an inverse $\mathbf{B}^{-1} = \mathbf{U}\mathbf{D}^{-1}\mathbf{U}^T$ that is also positive definite. Therefore, like \mathbf{B} , the matrix \mathbf{B}^{-1} has a positive square root $(\mathbf{B}^{-1})^{\frac{1}{2}} = \mathbf{U}\mathbf{D}^{-\frac{1}{2}}\mathbf{U}^T$ that satisfies the property of Equation (114) but for \mathbf{B}^{-1} :

$$(\mathbf{B}^{-1})^{\frac{1}{2}}(\mathbf{B}^{-1})^{\frac{1}{2}} = \mathbf{U}\mathbf{D}^{-\frac{1}{2}}\underbrace{\mathbf{U}^T\mathbf{U}}_{=1}\mathbf{D}^{-\frac{1}{2}}\mathbf{U}^T \quad (122)$$

$$= \mathbf{U}\underbrace{\mathbf{D}^{-\frac{1}{2}}\mathbf{D}^{-\frac{1}{2}}}_{\mathbf{D}^{-1}}\mathbf{U}^T \quad (123)$$

$$= \mathbf{U}\mathbf{D}^{-1}\mathbf{U}^T \quad (124)$$

$$= \mathbf{B}^{-1} \quad (125)$$

Note that $(\mathbf{B}^{-1})^{\frac{1}{2}}$ is also the inverse of $\mathbf{B}^{\frac{1}{2}}$ and can therefore be thought of as the inverse square root of \mathbf{B} . For this reason $\mathbf{B}^{-\frac{1}{2}}$ is used as a shorthand to denote this matrix. Moreover, using an equivalent argument to Equations (119)–(121) it can be shown that $\mathbf{B}^{-\frac{1}{2}}$ is symmetric, and like with $\mathbf{B}^{\frac{1}{2}}$ it is assumed that $\mathbf{D}^{-\frac{1}{2}}$ contains only the positive inverse square roots so that $\mathbf{B}^{-\frac{1}{2}}$ is positive definite.

An alternative way to define the square root of \mathbf{B} is some matrix \mathbf{C} that satisfies (Banerjee and Roy, 2014):

$$\mathbf{B} = \mathbf{C}\mathbf{C}^T \quad (126)$$

Equation (126) generalizes Equation (114), since for the special case where \mathbf{C} is symmetric the two equations are the same. Therefore, one possible solution to Equation (126) is the positive square root introduced above. However, multiplying the positive square root from the right by some orthogonal matrix \mathbf{Q}^T produces a matrix $\mathbf{B}^{\frac{1}{2}} = \mathbf{U}\mathbf{D}^{\frac{1}{2}}\mathbf{U}^T\mathbf{Q}^T$ that also satisfies Equation (126):

$$\mathbf{B}^{\frac{1}{2}}(\mathbf{B}^{\frac{1}{2}})^T = (\mathbf{U}\mathbf{D}^{\frac{1}{2}}\mathbf{U}^T\mathbf{Q}^T)(\mathbf{U}\mathbf{D}^{\frac{1}{2}}\mathbf{U}^T\mathbf{Q}^T)^T \quad (127)$$

$$= \mathbf{U}\mathbf{D}^{\frac{1}{2}}\mathbf{U}^T\underbrace{\mathbf{Q}^T\mathbf{Q}}_{=1}\mathbf{U}\mathbf{D}^{\frac{1}{2}}\mathbf{U}^T \quad (128)$$

$$= \mathbf{U}\mathbf{D}^{\frac{1}{2}}\mathbf{U}^T\mathbf{U}\mathbf{D}^{\frac{1}{2}}\mathbf{U}^T \quad (129)$$

$$= \mathbf{B} \quad (130)$$

where the last step in Equation (130) can be made using the same argument as in Equations (115)–(118). Thus, this definition of $\mathbf{B}^{\frac{1}{2}}$ defines a family of solutions to Equation (126) that are parameterized by \mathbf{Q} , with $\mathbf{Q} = \mathbf{1}$ corresponding to the positive square root.

For any choice of \mathbf{Q} , the corresponding inverse square root can be found by inverting $\mathbf{B}^{\frac{1}{2}}$

$$\mathbf{B}^{-\frac{1}{2}} = (\mathbf{B}^{\frac{1}{2}})^{-1} \quad (131)$$

$$= (\mathbf{U}\mathbf{D}^{\frac{1}{2}}\mathbf{U}^T\mathbf{Q}^T)^{-1} \quad (132)$$

$$= \mathbf{Q}\mathbf{U}\mathbf{D}^{-\frac{1}{2}}\mathbf{U}^T \quad (133)$$

which also simplifies to the positive square root for $\mathbf{Q} = \mathbb{1}$. As before, the matrix $\mathbf{B}^{-\frac{1}{2}}$ can be thought of as a square root of \mathbf{B}^{-1} , and indeed this matrix satisfies the analogue of Equation (130) for \mathbf{B}^{-1} , but with the difference that the order of transposing is swapped:

$$(\mathbf{B}^{-\frac{1}{2}})^T \mathbf{B}^{-\frac{1}{2}} = (\mathbf{Q}\mathbf{U}\mathbf{D}^{-\frac{1}{2}}\mathbf{U}^T)^T (\mathbf{Q}\mathbf{U}\mathbf{D}^{-\frac{1}{2}}\mathbf{U}^T)^T \quad (134)$$

$$= \mathbf{U}\mathbf{D}^{-\frac{1}{2}}\mathbf{U}^T \underbrace{\mathbf{Q}^T\mathbf{Q}}_{=\mathbb{1}}\mathbf{U}\mathbf{D}^{-\frac{1}{2}}\mathbf{U}^T \quad (135)$$

$$= \mathbf{U}\mathbf{D}^{-\frac{1}{2}}\mathbf{U}^T\mathbf{U}\mathbf{D}^{-\frac{1}{2}}\mathbf{U}^T \quad (136)$$

$$= \mathbf{B}^{-1} \quad (137)$$

where the last step in Equation (137) can be made using the same argument as in Equations (122)–(125).

In this paper, the square root and inverse square root of a positive definite matrix \mathbf{B} is interpreted in the more general sense involving \mathbf{Q} , while maintaining the assumption that $\mathbf{D}^{\frac{1}{2}}$ contains only the positive square roots of the eigenvalues of \mathbf{B} . It is worth noting that for this definition there is no guarantee that $\mathbf{B}^{\pm\frac{1}{2}}$ is symmetric for $\mathbf{Q} \neq \mathbb{1}$.

A.3 Generalized eigenvalue problems

The eigenvalue problem described in Equation (105) can be extended by considering an ordered pair of matrices (\mathbf{A}, \mathbf{B}) , often referred to as a *matrix pencil* (Ikramov, 1993), and a vector \mathbf{w} such that

$$\mathbf{A}\mathbf{w} = \lambda\mathbf{B}\mathbf{w} \quad (138)$$

or

$$\mathbf{w}^T \mathbf{A} = \lambda \mathbf{w}^T \mathbf{B} \quad (139)$$

Clearly, for $\mathbf{B} = \mathbb{1}$ these problems reduce to the ones described in Equations (105) and (106), respectively. For this reason, they are known as *generalized eigenvalue problems*, with the vector \mathbf{w} being a *generalized right/left eigenvector* of (\mathbf{A}, \mathbf{B}) and λ being the corresponding *generalized eigenvalue* (Banerjee and Roy, 2014). Moreover, if (\mathbf{A}, \mathbf{B}) have N linearly independent right generalized eigenvectors, Equation (138) can be expressed as

$$\mathbf{A}\mathbf{W} = \mathbf{B}\mathbf{W}\Lambda \quad (140)$$

which is the generalized analogue of Equation (107).

Generalized eigenvalue problems are often encountered in applications of linear algebra. A common method for solving such problems is to transform them into regular eigenvalue problems, since these are typically easier to solve. One special case that has received a lot of attention in the literature, and also the one most relevant to this paper, is where \mathbf{A} is symmetric and \mathbf{B} is positive definite. Converting this problem to a regular eigenvalue problem has the benefit that a number of insights regarding symmetric matrices can be utilized. One way to make this conversion uses the fact that if \mathbf{B} is positive definite then it has a square root and inverse square root given by $\mathbf{B}^{\frac{1}{2}} = \mathbf{U}\mathbf{D}^{\frac{1}{2}}\mathbf{U}^T\mathbf{Q}^T$ and $\mathbf{B}^{-\frac{1}{2}} = \mathbf{Q}\mathbf{U}\mathbf{D}^{-\frac{1}{2}}\mathbf{U}^T$, respectively (see Appendix A.2). Using these matrices, together with the fact that $\mathbb{1} = \mathbf{B}^{\frac{1}{2}}\mathbf{B}^{-\frac{1}{2}} = (\mathbf{B}^{\frac{1}{2}}\mathbf{B}^{-\frac{1}{2}})^T = (\mathbf{B}^{-\frac{1}{2}})^T(\mathbf{B}^{\frac{1}{2}})^T$, it is

possible to convert Equation (140) into a regular eigenvalue problem as follows (Banerjee and Roy, 2014):

$$\mathbf{A} \underbrace{(\mathbf{B}^{-\frac{1}{2}})^T (\mathbf{B}^{\frac{1}{2}})^T}_{=1} \mathbf{W} = \mathbf{B} \mathbf{W} \mathbf{\Lambda} \quad (\text{insertion of identity}) \quad (141)$$

$$\iff \mathbf{B}^{-\frac{1}{2}} \mathbf{A} (\mathbf{B}^{-\frac{1}{2}})^T (\mathbf{B}^{\frac{1}{2}})^T \mathbf{W} = \mathbf{B}^{-\frac{1}{2}} \mathbf{B} \mathbf{W} \mathbf{\Lambda} \quad (\text{multiplication from left by } \mathbf{B}^{-\frac{1}{2}}) \quad (142)$$

$$= (\mathbf{B}^{\frac{1}{2}})^T \mathbf{W} \mathbf{\Lambda} \quad (\text{because } \mathbf{B} = \mathbf{B}^{\frac{1}{2}} (\mathbf{B}^{\frac{1}{2}})^T) \quad (143)$$

$$\iff \mathbf{B}^{-\frac{1}{2}} \mathbf{A} (\mathbf{B}^{-\frac{1}{2}})^T \widetilde{\mathbf{W}} = \widetilde{\mathbf{W}} \mathbf{\Lambda} \quad (\widetilde{\mathbf{W}} = (\mathbf{B}^{\frac{1}{2}})^T \mathbf{W}) \quad (144)$$

Equation (144) describes a regular eigenvalue problem of the matrix $\mathbf{B}^{-\frac{1}{2}} \mathbf{A} (\mathbf{B}^{-\frac{1}{2}})^T$, which is guaranteed to be symmetric since $(\mathbf{B}^{-\frac{1}{2}} \mathbf{A} (\mathbf{B}^{-\frac{1}{2}})^T)^T = \mathbf{B}^{-\frac{1}{2}} \mathbf{A}^T (\mathbf{B}^{-\frac{1}{2}})^T = \mathbf{B}^{-\frac{1}{2}} \mathbf{A} (\mathbf{B}^{-\frac{1}{2}})^T$. For this reason, the conversion in Equations (141)–(144) is referred to as *symmetric normalization* in this paper, and the symmetry of the resulting matrix provides two key insights about the starting generalized eigenvalue problem. Firstly, the eigenvalues and eigenvectors in Equation (144) are guaranteed to be real by virtue of the spectral theorem. Since the eigenvalues are not modified by the normalization process this means the same is true of the generalized eigenvalues, and since $\widetilde{\mathbf{W}} = (\mathbf{B}^{\frac{1}{2}})^T \mathbf{W}$ (with $(\mathbf{B}^{\frac{1}{2}})^T$ also being real) the same is true of the generalized eigenvectors \mathbf{W} . Secondly, the spectral theorem also says that the eigenvectors in Equation (144) can be chosen to be orthonormal w.r.t the standard Euclidean inner product, in which case $\widetilde{\mathbf{W}}^T \widetilde{\mathbf{W}} = \mathbb{1}$. Using this fact, and transforming the basis $\widetilde{\mathbf{W}}$ back into \mathbf{W} gives:

$$\widetilde{\mathbf{W}}^T \widetilde{\mathbf{W}} = \mathbf{W}^T (\mathbf{B}^{\frac{1}{2}}) (\mathbf{B}^{\frac{1}{2}})^T \mathbf{W} \quad (145)$$

$$= \mathbf{W}^T \mathbf{B} \mathbf{W} \quad (146)$$

$$= \mathbb{1} \quad (147)$$

Assuming that \mathbf{w}_i and \mathbf{w}_j denote columns of \mathbf{W} , then the rightmost part of Equation (147) can alternatively be written in an indexed form as

$$\mathbf{w}_i^T \mathbf{B} \mathbf{w}_j = (\mathbf{w}_i, \mathbf{w}_j)_{\mathbf{B}} = \delta_{ij} \quad (148)$$

where δ_{ij} is the delta Kronecker symbol. Equation (148) is particularly informative because it says that the generalized eigenvectors \mathbf{W} of the starting problem are orthogonal w.r.t. the weighted inner product $(\cdot, \cdot)_{\mathbf{B}}$.

The procedure described above is not the only way to convert Equation (140) into a regular eigenvalue problem. An alternative method makes use of the fact that since \mathbf{B} is positive definite it has a well-defined inverse \mathbf{B}^{-1} , and multiplying Equation (140) by this matrix from the left gives (Ghojogh et al., 2023)

$$\mathbf{B}^{-1} \mathbf{A} \mathbf{W} = \mathbf{W} \mathbf{\Lambda} \quad (149)$$

which is referred to as *left normalization* in this paper. Note that unlike \mathbf{A} and \mathbf{B} , the matrix $\mathbf{B}^{-1} \mathbf{A}$ on the left-hand side of Equation (149) is not necessarily symmetric. Nonetheless, since neither $\mathbf{\Lambda}$ nor \mathbf{W} are changed by this normalization, the eigenvalues and eigenvectors of $\mathbf{B}^{-1} \mathbf{A}$ are the same as the generalized counterparts in Equation (140). Thus, $\mathbf{B}^{-1} \mathbf{A}$ has real eigenvalues and the eigenvectors can be chosen to be real and orthogonal in the sense described by Equation (148).

Both normalization methods presented above can only strictly be used if \mathbf{B} is positive definite. However, if instead \mathbf{B} is positive semi-definite they can be applied by using an additional numerical hack, referred to in Ghojogh et al. (2023) as the *quick and dirty solution*. In particular, perturbing \mathbf{B} along the diagonals by a small amount ϵ changes Equation (140) to:

$$\mathbf{A} \mathbf{W} = (\mathbf{B} + \epsilon \mathbb{1}) \mathbf{W} \mathbf{\Lambda} \quad (150)$$

$$= \mathbf{B}_\epsilon \mathbf{W} \mathbf{\Lambda} \quad (151)$$

In order to understand the matrix \mathbf{B}_ϵ , note that if \mathbf{B} is positive semi-definite then it is diagonalizable and that like all matrices it commutes with the identity matrix. Therefore, \mathbf{B} and $\mathbb{1}$ share an eigenbasis and the perturbation simply increases all eigenvalues of \mathbf{B} by ϵ , so that any zero eigenvalues become positive.

Thus, \mathbf{B}_ϵ is positive definite and Equation (150) can be normalized. It is worth noting that matrices having eigenvalues numerically close to zero, known as *ill-conditioned matrices*, can be practically just as problematic as having eigenvalues equal to zero, since normalization involves computing either $\mathbf{B}^{-\frac{1}{2}}$ or \mathbf{B}^{-1} , both of which can have very large round-off errors if \mathbf{B} is ill-conditioned. Therefore, the parameter ϵ in Equation (151) needs to be large enough to avoid this issue. On the other hand, adding too much noise runs the risk erasing important information in \mathbf{B} regarding the system being studied. For these reasons, when applying this trick it is important to take care in selecting a suitable value of ϵ .

Appendix B SR

Theorem 2.2.1 *The matrix \mathbf{M} is well-defined and can alternatively be expressed as*

$$\mathbf{M} = \sum_{k=0}^{\infty} \gamma^k \mathbf{P}^k \quad (152)$$

which is known as a Neumann series.

Proof. In order to show that \mathbf{M} is well-defined, note that \mathbf{P} is a transition matrix and therefore each of its eigenvalues λ is bounded by $|\lambda| \leq 1$. Together with the fact that $\gamma \in (0, 1)$, this means that the matrix $\gamma\mathbf{P}$ has eigenvalues bounded by $|\gamma\lambda| < 1$, and therefore cannot have an eigenvalue of 1. By extension, this means that the matrix $\mathbf{1} - \gamma\mathbf{P}$ cannot have an eigenvalue of zero, and therefore must be invertible.

As a consequence of the argument above, the matrix $\gamma\mathbf{P}$ has a spectral radius $\rho(\gamma\mathbf{P}) < 1$. This is true if and only if the Neumann series

$$\sum_{k=0}^{\infty} \gamma^k \mathbf{P}^k = \mathbf{1} + \gamma\mathbf{P} + \gamma^2\mathbf{P}^2 + \gamma^3\mathbf{P}^3 + \dots \quad (153)$$

converges and is equal to $(\mathbf{1} - \gamma\mathbf{P})^{-1}$ (see Meyer (2000) p. 618). \square

Theorem 2.3.1 *If \mathbf{w} is an eigenvector of \mathbf{P} with eigenvalue $\lambda \in \mathbb{C}$, then it is also an eigenvector of \mathbf{M} with eigenvalue $\frac{1}{1-\gamma\lambda} \in \mathbb{C}$.*

Proof. Let \mathbf{w} be a right eigenvector of \mathbf{P} with eigenvalue λ . Since \mathbf{P} is a transition matrix, \mathbf{w} is also a right eigenvector of \mathbf{P}^k with eigenvalue λ^k (Seabrook and Wiskott, 2023). The action of \mathbf{M} on \mathbf{w} is then:

$$\mathbf{M}\mathbf{w} \stackrel{(9)}{=} \left(\sum_{k=0}^{\infty} \gamma^k \mathbf{P}^k \right) \mathbf{w} \quad (154)$$

$$= \sum_{k=0}^{\infty} \gamma^k \mathbf{P}^k \mathbf{w} \quad (155)$$

$$= \sum_{k=0}^{\infty} \gamma^k \lambda^k \mathbf{w} \quad (156)$$

$$= \left(\sum_{k=0}^{\infty} \gamma^k \lambda^k \right) \mathbf{w} \quad (157)$$

$$= \frac{1}{1 - \gamma\lambda} \mathbf{w} \quad (158)$$

In the last line, the geometric series is expressed in closed form. This is allowed because \mathbf{P} is a transition matrix, which means that $|\lambda| \leq 1$, and therefore $|\gamma\lambda| < 1$. Note that the eigenvalues of \mathbf{M} are related to those of \mathbf{P} in such a way that the ordering from largest to smallest is preserved. \square

Theorem 2.3.2 For an ergodic and reversible Markov chain with stationary distribution π , the matrices \mathbf{P}^k and \mathbf{M} satisfy the following properties:

- $\mathbf{\Pi P}^k$ and $\mathbf{\Pi M}$ are symmetric.
- $\mathbf{\Pi}^{\frac{1}{2}} \mathbf{P}^k \mathbf{\Pi}^{-\frac{1}{2}}$ and $\mathbf{\Pi}^{\frac{1}{2}} \mathbf{M} \mathbf{\Pi}^{-\frac{1}{2}}$ are symmetric.
- \mathbf{P}^k and \mathbf{M} are diagonalizable with real eigenvalues and eigenvectors.
- The left and right eigenvectors of \mathbf{P}^k and \mathbf{M} can be chosen to be orthogonal w.r.t to the weighted inner products $\langle \cdot, \cdot \rangle_{\mathbf{\Pi}^{-1}}$ and $\langle \cdot, \cdot \rangle_{\mathbf{\Pi}}$, respectively.

where $\mathbf{\Pi} = \text{diag}(\mathbf{\Pi})$ and $k \geq 1$.

Proof. First point: note that since the starting Markov chain is reversible, detailed balance is satisfied for the stationary distribution π (Seabrook and Wiskott, 2023). Therefore, $\mathbf{\Pi P}$ is symmetric:

$$\mathbf{\Pi P} = (\mathbf{\Pi P})^T = \mathbf{P}^T \mathbf{\Pi} \quad (159)$$

Moreover, π is guaranteed to also be the stationary distribution of the k -step Markov chain described by \mathbf{P}^k , and using Equation (159) it is possible to show that the flow matrix $\mathbf{\Pi P}^k$ corresponding to this Markov chain is also symmetric:

$$(\mathbf{\Pi P}^k)^T = (\mathbf{P}^k)^T \mathbf{\Pi} \quad (160)$$

$$= \underbrace{(\mathbf{P} \cdot \mathbf{P} \cdots \mathbf{P})^T}_{k \text{ times}} \mathbf{\Pi} \quad (161)$$

$$= \underbrace{\mathbf{P}^T \cdot \mathbf{P}^T \cdots \mathbf{P}^T}_{k \text{ times}} \mathbf{\Pi} \quad (162)$$

$$= \underbrace{\mathbf{P}^T \cdot \mathbf{P}^T \cdots \mathbf{P}^T}_{k-1 \text{ times}} \mathbf{P}^T \mathbf{\Pi} \quad (163)$$

$$\stackrel{(159)}{=} \underbrace{\mathbf{P}^T \cdot \mathbf{P}^T \cdots \mathbf{P}^T}_{k-1 \text{ times}} \mathbf{\Pi P} \quad (164)$$

Then, repeating the steps from Equation (162) to Equation (164) a further $k - 1$ times leads to

$$(\mathbf{\Pi P}^k)^T = \mathbf{\Pi P}^k \quad (165)$$

and so $\mathbf{\Pi P}^k$ is symmetric. The matrix $\mathbf{\Pi M}$ is given by:

$$\mathbf{\Pi M} \stackrel{(9)}{=} \mathbf{\Pi} \sum_{k=0}^{\infty} \gamma^k \mathbf{P}^k \quad (166)$$

$$= \sum_{k=0}^{\infty} \gamma^k \mathbf{\Pi P}^k \quad (167)$$

Note that each flow matrix $\mathbf{\Pi P}^k$ in Equation (167) is non-negative. Such matrices are subject to a well-known result formulated by Frobenius, which says that their spectral radius is less than or equal to the largest row sum (Babouklis et al., 2020; Minc, 1988). In the case of $\mathbf{\Pi P}^k$, the row sums are simply the stationary probabilities, i.e.

$$\sum_j (\mathbf{\Pi P}^k)_{ij} = \sum_j \pi_i (\mathbf{P}^k)_{ij} = \pi_i \underbrace{\sum_j (\mathbf{P}^k)_{ij}}_{=1} = \pi_i \quad (168)$$

, meaning that the spectral radius of $\mathbf{\Pi P}^k$ is no greater than the largest stationary probability, and is therefore strictly less than 1. Thus, since γ is also less than 1, the Neumann series in Equation (167) is guaranteed to converge (see Meyer (2000) p. 618), and since Equation (165) implies that each term in the sum is symmetric then so too is $\mathbf{\Pi M}$.

Second point: note that $\mathbf{\Pi}^{\frac{1}{2}} \mathbf{P} \mathbf{\Pi}^{-\frac{1}{2}}$ is guaranteed to be symmetric due to the chain being reversible (Seabrook and Wiskott, 2023). Therefore

$$\mathbf{\Pi}^{\frac{1}{2}} \mathbf{P} \mathbf{\Pi}^{-\frac{1}{2}} = \mathbf{Q} \quad (169)$$

or equivalently

$$\mathbf{P} = \mathbf{\Pi}^{-\frac{1}{2}} \mathbf{Q} \mathbf{\Pi}^{\frac{1}{2}} \quad (170)$$

for some symmetric matrix \mathbf{Q} . Exponentiating Equation (170) to the power k gives

$$\mathbf{P}^k = \underbrace{(\mathbf{\Pi}^{-\frac{1}{2}} \mathbf{Q} \mathbf{\Pi}^{\frac{1}{2}})(\mathbf{\Pi}^{-\frac{1}{2}} \mathbf{Q} \mathbf{\Pi}^{\frac{1}{2}}) \dots (\mathbf{\Pi}^{-\frac{1}{2}} \mathbf{Q} \mathbf{\Pi}^{\frac{1}{2}})}_{k \text{ times}} \quad (171)$$

$$= \mathbf{\Pi}^{-\frac{1}{2}} \mathbf{Q}^k \mathbf{\Pi}^{\frac{1}{2}} \quad (172)$$

where in Equation (171) the matrices $\mathbf{\Pi}^{\pm \frac{1}{2}}$ between each \mathbf{Q} matrix cancel out. Equation (172) is equivalent to

$$\mathbf{\Pi}^{\frac{1}{2}} \mathbf{P}^k \mathbf{\Pi}^{-\frac{1}{2}} = \mathbf{Q}^k \quad (173)$$

and since a symmetric matrix to any power is also symmetric, Equation (173) implies that $\mathbf{\Pi}^{\frac{1}{2}} \mathbf{P}^k \mathbf{\Pi}^{-\frac{1}{2}}$ is symmetric. Moreover, the matrix $\mathbf{\Pi}^{\frac{1}{2}} \mathbf{M} \mathbf{\Pi}^{-\frac{1}{2}}$ is given by:

$$\mathbf{\Pi}^{\frac{1}{2}} \mathbf{M} \mathbf{\Pi}^{-\frac{1}{2}} \stackrel{(9)}{=} \mathbf{\Pi}^{\frac{1}{2}} \left(\sum_{k=0}^{\infty} \gamma^k \mathbf{P}^k \right) \mathbf{\Pi}^{-\frac{1}{2}} \quad (174)$$

$$= \sum_{k=0}^{\infty} \gamma^k \mathbf{\Pi}^{\frac{1}{2}} \mathbf{P}^k \mathbf{\Pi}^{-\frac{1}{2}} \quad (175)$$

Note that each term $\mathbf{\Pi}^{\frac{1}{2}} \mathbf{P}^k \mathbf{\Pi}^{-\frac{1}{2}}$ is a similarity transformation on \mathbf{P}^k and therefore has the same eigenvalues and a spectral radius of 1. Thus, the sum in Equation (175) converges, and since each term $\mathbf{\Pi}^{\frac{1}{2}} \mathbf{P}^k \mathbf{\Pi}^{-\frac{1}{2}}$ then so too is $\mathbf{\Pi}^{\frac{1}{2}} \mathbf{M} \mathbf{\Pi}^{-\frac{1}{2}}$.

Third point: since $\mathbf{\Pi}^{\frac{1}{2}} \mathbf{P}^k \mathbf{\Pi}^{-\frac{1}{2}}$ is symmetric it is diagonalizable and can be expressed as

$$\mathbf{\Pi}^{\frac{1}{2}} \mathbf{P}^k \mathbf{\Pi}^{-\frac{1}{2}} = \mathbf{U} \mathbf{D} \mathbf{U}^T \quad (176)$$

where \mathbf{D} and \mathbf{U} contain the eigenvalues and eigenvectors of $\mathbf{\Pi}^{\frac{1}{2}} \mathbf{P}^k \mathbf{\Pi}^{-\frac{1}{2}}$, respectively, both of which are real and with \mathbf{U} being orthogonal (Seabrook and Wiskott, 2023). Rearranging this equation gives:

$$\mathbf{P}^k = \mathbf{\Pi}^{-\frac{1}{2}} \mathbf{U} \mathbf{D} \mathbf{U}^T \mathbf{\Pi}^{\frac{1}{2}} \quad (177)$$

$$= (\mathbf{\Pi}^{-\frac{1}{2}} \mathbf{U}) \mathbf{D} (\mathbf{\Pi}^{-\frac{1}{2}} \mathbf{U})^{-1} \quad (178)$$

$$= \tilde{\mathbf{U}} \mathbf{D} \tilde{\mathbf{U}}^{-1} \quad (179)$$

Equation (179) says that \mathbf{P}^k is diagonalizable, where \mathbf{D} are the eigenvalues and $\tilde{\mathbf{U}}^{-1}$ and $\tilde{\mathbf{U}}$ are a biorthogonal system of left and right eigenvectors, respectively (Seabrook and Wiskott, 2023). Note that in comparison to Equation (176) where the matrix on the left-hand side is symmetric and the left and right eigenvectors are the same, in Equation (179) the matrix is generally non-symmetric which is why there are distinct left and right eigenvectors (for a more in-depth discussion, see Seabrook and Wiskott (2023)). Note also that since all matrices of Equation (179) are real-valued, the eigenvalues and eigenvectors of \mathbf{P}^k are real. By an equivalent argument, all of these properties can be demonstrated for \mathbf{M} . Moreover, it is possible to pick a

single set of eigenvectors that diagonalize $\mathbf{P}^k \forall k$ (Seabrook and Wiskott, 2023), and since \mathbf{M} is a sum over different values of k it is also diagonalized by such a set of eigenvectors.

Fourth point: since $\mathbf{\Pi}^{\frac{1}{2}} \mathbf{P}^k \mathbf{\Pi}^{-\frac{1}{2}}$ is symmetric, the corresponding eigenvectors are orthogonal w.r.t the Euclidean inner product. In Equation (176), this is reflected by the fact that the matrix \mathbf{U} is orthogonal, i.e. $\mathbf{U}^T \mathbf{U} = \mathbb{1}$. By contrast, there is no guarantee that \mathbf{P}^k is symmetric or that the eigenvector matrices in Equation (179) are orthogonal. Instead, the matrix $\tilde{\mathbf{U}}^{-1}$, which contains the left eigenvectors, satisfies the following modified orthogonality property

$$(\tilde{\mathbf{U}}^{-1})^T \mathbf{\Pi}^{-1} (\tilde{\mathbf{U}}^{-1}) = (\mathbf{\Pi}^{-\frac{1}{2}} \mathbf{U})^T \mathbf{\Pi} (\mathbf{\Pi}^{-\frac{1}{2}} \mathbf{U}) \quad (180)$$

$$= \mathbf{U}^T \underbrace{\mathbf{\Pi}^{\frac{1}{2}} \mathbf{\Pi}^{-1} \mathbf{\Pi}^{\frac{1}{2}}}_{=\mathbb{1}} \mathbf{U} \quad (181)$$

$$= \mathbf{U}^T \mathbf{U} \quad (182)$$

$$= \mathbb{1} \quad (183)$$

which is equivalent to the left eigenvectors being orthogonal w.r.t $\langle \cdot, \cdot \rangle_{\mathbf{\Pi}^{-1}}$. Similarly, the matrix $\tilde{\mathbf{U}}$, which contains the right eigenvectors, satisfies

$$\tilde{\mathbf{U}}^T \mathbf{\Pi} \tilde{\mathbf{U}} = (\mathbf{\Pi}^{-\frac{1}{2}} \mathbf{U})^T \mathbf{\Pi} (\mathbf{\Pi}^{-\frac{1}{2}} \mathbf{U}) \quad (184)$$

$$= \mathbf{U}^T \underbrace{\mathbf{\Pi}^{-\frac{1}{2}} \mathbf{\Pi} \mathbf{\Pi}^{-\frac{1}{2}}}_{=\mathbb{1}} \mathbf{U} \quad (185)$$

$$= \mathbf{U}^T \mathbf{U} \quad (186)$$

$$= \mathbb{1} \quad (187)$$

which is equivalent to the right eigenvectors being orthogonal w.r.t $\langle \cdot, \cdot \rangle_{\mathbf{\Pi}}$. A similar argument can demonstrate the same properties for the left and right eigenvectors of \mathbf{M} . \square

Theorem 2.3.3 *For an ergodic Markov chain with stationary distribution $\boldsymbol{\pi}$, the matrices $(\mathbf{P}^k)_{\text{add}}$ and \mathbf{M}_{add} satisfy the following properties:*

- $\mathbf{\Pi}(\mathbf{P}^k)_{\text{add}}$ and $\mathbf{\Pi}\mathbf{M}_{\text{add}}$ are symmetric.
- $\mathbf{\Pi}^{\frac{1}{2}}(\mathbf{P}^k)_{\text{add}}\mathbf{\Pi}^{-\frac{1}{2}}$ and $\mathbf{\Pi}^{\frac{1}{2}}\mathbf{M}_{\text{add}}\mathbf{\Pi}^{-\frac{1}{2}}$ are symmetric.
- $(\mathbf{P}^k)_{\text{add}}$ and \mathbf{M}_{add} are diagonalizable with real eigenvalues and eigenvectors.
- The left and right eigenvectors of $(\mathbf{P}^k)_{\text{add}}$ and \mathbf{M}_{add} can be chosen to be orthogonal w.r.t to the weighted inner products $\langle \cdot, \cdot \rangle_{\mathbf{\Pi}^{-1}}$ and $\langle \cdot, \cdot \rangle_{\mathbf{\Pi}}$, respectively.

where $\mathbf{\Pi} = \text{diag}(\boldsymbol{\pi})$ and $k \geq 1$.

Proof. First point: note that multiplying $(\mathbf{P}^k)_{\text{add}}$ from the left by $\mathbf{\Pi}$ gives

$$\mathbf{\Pi}(\mathbf{P}^k)_{\text{add}} \stackrel{(11)}{=} \mathbf{\Pi} \left(\frac{\mathbf{P} + \mathbf{\Pi}^{-1} \mathbf{P}^T \mathbf{\Pi}}{2} \right) \quad (188)$$

$$= \frac{\mathbf{\Pi} \mathbf{P} + \mathbf{P}^T \mathbf{\Pi}}{2} \quad (189)$$

$$= \frac{\mathbf{\Pi} \mathbf{P} + (\mathbf{\Pi} \mathbf{P})^T}{2} \quad (190)$$

which is symmetric by definition. Moreover, multiplying \mathbf{M}_{add} from the left by $\mathbf{\Pi}$ gives:

$$\mathbf{\Pi} \mathbf{M}_{\text{add}} \stackrel{(15)}{=} \mathbf{\Pi} \left(\sum_{k=0}^{\infty} \gamma^k (\mathbf{P}^k)_{\text{add}} \right) \quad (191)$$

$$= \sum_{k=0}^{\infty} \gamma^k \mathbf{\Pi} (\mathbf{P}^k)_{\text{add}} \quad (192)$$

Therefore, by an equivalent argument as in the previous proof, the sum in Equation (192) converges and $\mathbf{\Pi}\mathbf{M}_{\text{add}}$ is symmetric.

Second point: note that $\mathbf{\Pi}^{\frac{1}{2}}(\mathbf{P}^k)_{\text{add}}\mathbf{\Pi}^{-\frac{1}{2}}$ can be rearranged to give

$$\mathbf{\Pi}^{\frac{1}{2}}(\mathbf{P}^k)_{\text{add}}\mathbf{\Pi}^{-\frac{1}{2}} \stackrel{(11)}{=} \mathbf{\Pi}^{\frac{1}{2}}\left(\frac{\mathbf{P} + \mathbf{\Pi}^{-1}\mathbf{P}^T\mathbf{\Pi}}{2}\right)\mathbf{\Pi}^{-\frac{1}{2}} \quad (193)$$

$$= \frac{\mathbf{\Pi}^{\frac{1}{2}}\mathbf{P}\mathbf{\Pi}^{-\frac{1}{2}} + \mathbf{\Pi}^{-\frac{1}{2}}\mathbf{P}^T\mathbf{\Pi}^{\frac{1}{2}}}{2} \quad (194)$$

$$= \frac{\mathbf{\Pi}^{\frac{1}{2}}\mathbf{P}\mathbf{\Pi}^{-\frac{1}{2}} + (\mathbf{\Pi}^{\frac{1}{2}}\mathbf{P}\mathbf{\Pi}^{-\frac{1}{2}})^T}{2} \quad (195)$$

which is true by definition. Moreover, the corresponding matrix involving \mathbf{M}_{add} is:

$$\mathbf{\Pi}^{\frac{1}{2}}\mathbf{M}_{\text{add}}\mathbf{\Pi}^{-\frac{1}{2}} \stackrel{(15)}{=} \mathbf{\Pi}^{\frac{1}{2}}\left(\sum_{k=0}^{\infty}\gamma^k(\mathbf{P}^k)_{\text{add}}\right)\mathbf{\Pi}^{-\frac{1}{2}} \quad (196)$$

$$= \sum_{k=0}^{\infty}\gamma^k\mathbf{\Pi}^{\frac{1}{2}}(\mathbf{P}^k)_{\text{add}}\mathbf{\Pi}^{-\frac{1}{2}} \quad (197)$$

Therefore, by an equivalent argument as in the previous proof, the sum in Equation (197) converges and $\mathbf{\Pi}^{\frac{1}{2}}\mathbf{M}_{\text{add}}\mathbf{\Pi}^{-\frac{1}{2}}$ is symmetric.

Third and fourth points: using the symmetry of $\mathbf{\Pi}^{\frac{1}{2}}(\mathbf{P}^k)_{\text{add}}\mathbf{\Pi}^{-\frac{1}{2}}$ and $\mathbf{\Pi}^{\frac{1}{2}}\mathbf{M}_{\text{add}}\mathbf{\Pi}^{-\frac{1}{2}}$, these two properties can be demonstrated using an equivalent argument as in the proof of Theorem 2.3.2. Note, however, that in contrast to the previous theorem $(\mathbf{P}^k)_{\text{add}}$ and \mathbf{M}_{add} do not necessarily share a basis. \square

Appendix C SFA

C.1 Addition of noise

The data covariance matrix $\mathbf{\Sigma}$ is positive semi-definite if it has one or more eigenvalues equal to zero, or equivalently if one or more variables of the data can be expressed as a linear combination of the others. One way to get rid of such dependencies is to preprocess the starting signal by adding noise along all axes, with the typical choice being centered Gaussian noise with variance σ^2 , i.e. $\mathbf{x}_{\sigma}(t) = \mathbf{x}(t) + \boldsymbol{\xi}(t)$ where $\boldsymbol{\xi}(t) \sim \mathcal{N}(\mathbf{0}, \sigma^2\mathbf{1})$ (Konen, 2009). To understand how this impacts the issue of zero eigenvalues, consider the following decomposition of the covariance matrix

$$\mathbf{\Sigma} = \langle \mathbf{c}(t)\mathbf{c}(t)^T \rangle_t \quad (198)$$

$$= \langle (\mathbf{x}(t) - \langle \mathbf{x}(t) \rangle_t)(\mathbf{x}(t) - \langle \mathbf{x}(t) \rangle_t)^T \rangle_t \quad (199)$$

$$= \langle \mathbf{x}(t)\mathbf{x}(t)^T \rangle_t - \langle \mathbf{x}(t) \rangle_t \langle \mathbf{x}(t)^T \rangle_t - \langle \mathbf{x}(t) \rangle_t \langle \mathbf{x}(t)^T \rangle_t + \langle \mathbf{x}(t) \rangle_t \langle \mathbf{x}(t)^T \rangle_t \quad (200)$$

$$= \langle \mathbf{x}(t)\mathbf{x}(t)^T \rangle_t - \langle \mathbf{x}(t) \rangle_t \langle \mathbf{x}(t)^T \rangle_t \quad (201)$$

where the first term is the 2nd moment matrix of $\mathbf{x}(t)$. In the case of the noisy signal, let $\mathbf{\Sigma}_{\sigma}$ denote the corresponding covariance matrix, in which case Equation (201) is:

$$\mathbf{\Sigma}_{\sigma} = \langle \mathbf{x}_{\sigma}(t)\mathbf{x}_{\sigma}(t)^T \rangle_t - \langle \mathbf{x}_{\sigma}(t) \rangle_t \langle \mathbf{x}_{\sigma}(t)^T \rangle_t \quad (202)$$

In the limit of large samples, it is possible to relate the eigenvalues of $\mathbf{\Sigma}_{\sigma}$ to those of $\mathbf{\Sigma}$. To see this, consider each term on the right-hand side of Equation (202) in this limit. The first term can be expanded as follows:

$$\langle \mathbf{x}_{\sigma}(t)\mathbf{x}_{\sigma}(t)^T \rangle_t = \langle (\mathbf{x}(t) + \boldsymbol{\xi}(t))(\mathbf{x}(t) + \boldsymbol{\xi}(t))^T \rangle_t \quad (203)$$

$$= \langle \mathbf{x}(t)\mathbf{x}(t)^T \rangle_t + \langle \mathbf{x}(t)\boldsymbol{\xi}(t)^T \rangle_t + \langle \boldsymbol{\xi}(t)\mathbf{x}(t)^T \rangle_t + \langle \boldsymbol{\xi}(t)\boldsymbol{\xi}(t)^T \rangle_t \quad (204)$$

For $T \rightarrow \infty$, the last term in Equation (204) is equal to $\sigma^2 \mathbf{1}$ because $\boldsymbol{\xi}(t)$ is sampled from a multivariate Gaussian with variance σ^2 , and the second and third terms are equal to zero since $\mathbf{x}(t)$ and $\boldsymbol{\xi}(t)$ are statistically independent and $\boldsymbol{\xi}(t)$ has zero mean:

$$\lim_{T \rightarrow \infty} \langle \mathbf{x}(t) \boldsymbol{\xi}(t)^T \rangle_t = \lim_{T \rightarrow \infty} \langle \mathbf{x}(t) \rangle_t \langle \boldsymbol{\xi}(t)^T \rangle_t = 0 \quad (205)$$

$$\lim_{T \rightarrow \infty} \langle \boldsymbol{\xi}(t) \mathbf{x}(t)^T \rangle_t = \lim_{T \rightarrow \infty} \langle \boldsymbol{\xi}(t)^T \rangle_t \langle \mathbf{x}(t) \rangle_t = 0 \quad (206)$$

Therefore:

$$\lim_{T \rightarrow \infty} \langle \mathbf{x}_\sigma(t) \mathbf{x}_\sigma(t)^T \rangle_t = \langle \mathbf{x}(t) \mathbf{x}(t)^T \rangle_t + \sigma^2 \mathbf{1} \quad (207)$$

The second term in Equation (202) can be expanded as follows:

$$\langle \mathbf{x}_\sigma(t) \rangle_t \langle \mathbf{x}_\sigma(t)^T \rangle_t = (\langle \mathbf{x}(t) \rangle_t + \langle \boldsymbol{\xi}(t) \rangle_t) (\langle \mathbf{x}(t) \rangle_t + \langle \boldsymbol{\xi}(t) \rangle_t)^T \quad (208)$$

$$= \langle \mathbf{x}(t) \rangle_t \langle \mathbf{x}(t)^T \rangle_t + \langle \mathbf{x}(t) \rangle_t \langle \boldsymbol{\xi}(t)^T \rangle_t + \langle \boldsymbol{\xi}(t) \rangle_t \langle \mathbf{x}(t)^T \rangle_t + \langle \boldsymbol{\xi}(t) \rangle_t \langle \boldsymbol{\xi}(t)^T \rangle_t \quad (209)$$

In the limit $T \rightarrow \infty$, all terms in Equation (209) all terms except the first are zero since $\boldsymbol{\xi}(t)$ has zero mean. Therefore:

$$\lim_{T \rightarrow \infty} \langle \mathbf{x}_\sigma(t) \rangle_t \langle \mathbf{x}_\sigma(t)^T \rangle_t = \langle \mathbf{x}(t) \rangle_t \langle \mathbf{x}(t)^T \rangle_t \quad (210)$$

Thus, combining Equations (207) and (210) leads to the following limit on $\boldsymbol{\Sigma}_\sigma$:

$$\lim_{T \rightarrow \infty} \boldsymbol{\Sigma}_\sigma = \langle \mathbf{x}(t) \mathbf{x}(t)^T \rangle_t + \sigma^2 \mathbf{1} - \langle \mathbf{x}(t) \rangle_t \langle \mathbf{x}(t)^T \rangle_t \quad (211)$$

$$= \boldsymbol{\Sigma} + \sigma^2 \mathbf{1} \quad (212)$$

Equation (212) says in the limit of large samples the the signal $\mathbf{x}_\sigma(t)$ has the same covariance matrix as $\mathbf{x}(t)$ except for a perturbation along the diagonal by σ^2 . This perturbation leaves the eigenvectors invariant and simply increases the eigenvalues by σ^2 , meaning that zero eigenvalues become positive. Thus, in this limit the relation between $\boldsymbol{\Sigma}_\sigma$ and $\boldsymbol{\Sigma}$ is the same as the relationship between \mathbf{B}_ϵ and \mathbf{B} in Equations (150) and (151), meaning that the addition of noise is one way in which the numerical hack presented in Appendix A.3 can be implemented in the context of SFA. As with the method presented in Appendix A.3, the addition of noise needs to balance two goals. On the one hand, σ needs to be large enough such that all eigenvalues equal to or close to zero are sufficiently increased and the matrices $\boldsymbol{\Sigma}^{-\frac{1}{2}}$ and $\boldsymbol{\Sigma}^{-1}$ can be approximately computed. On the other hand, σ should not be large enough that the noise masks the starting signal $\mathbf{x}(t)$. Practically, these two goals are best balanced by performing parameter tuning on σ (Konen, 2009).

It is worth noting that the addition of noise has an equivalent effect on the eigenvalues of the second moment matrix of $\mathbf{x}(t)$, which is given by:

$$\widehat{\boldsymbol{\Sigma}} = \langle \mathbf{x}(t) \mathbf{x}(t)^T \rangle_t \quad (213)$$

When $\mathbf{x}(t)$ is perturbed by noise this matrix becomes

$$\widehat{\boldsymbol{\Sigma}}_\sigma = \langle \mathbf{x}_\sigma(t) \mathbf{x}_\sigma(t)^T \rangle_t \quad (214)$$

which in the limit $T \rightarrow \infty$ is described by Equation (207). Therefore, in this limit the second moment matrix of $\mathbf{x}(t)$ is perturbed in the same way as the covariance matrix, meaning that all details outlined in the previous paragraph apply also to $\widehat{\boldsymbol{\Sigma}}$.

C.2 Symmetric normalization and whitening

In statistics, whitening refers to any linear transformation that transforms a set of starting variables with covariance matrix $\boldsymbol{\Sigma}$ into a set of new variables with unit covariance matrix (Kessy et al., 2018). Typically, whitening assumes the input data has zero mean, or equivalently that a prior centering step has been

performed. For a time series $\mathbf{x}(t)$, whitening transformations can be expressed as $\mathbf{z}(t) = \mathbf{S}\mathbf{c}(t)$ where $\mathbf{c}(t)$ is the centered signal and \mathbf{S} is some matrix, such that:

$$\langle \mathbf{z}(t)\mathbf{z}(t)^T \rangle_t = \mathbf{S}\langle \mathbf{x}(t)\mathbf{x}(t)^T \rangle_t \mathbf{S}^T \quad (215)$$

$$= \mathbf{S}\boldsymbol{\Sigma}\mathbf{S}^T \quad (216)$$

$$= \mathbb{1} \quad (217)$$

Multiplying Equations (216) and (217) by \mathbf{S}^T from the left then gives

$$(\mathbf{S}^T \mathbf{S}\boldsymbol{\Sigma})\mathbf{S}^T = \mathbf{S}^T \quad (218)$$

which in turn means that $(\mathbf{S}^T \mathbf{S}\boldsymbol{\Sigma}) = \mathbb{1}$ and therefore

$$\mathbf{S}^T \mathbf{S} = \boldsymbol{\Sigma}^{-1} \quad (219)$$

The fact that $\boldsymbol{\Sigma}^{-1}$ is on the right-hand side of Equation (219) reflects the fact that whitening transformations are only strictly defined if $\boldsymbol{\Sigma}$ is invertible, i.e. if there are no eigenvalues equal to zero or linear dependencies in the components of $\mathbf{c}(t)$. If $\boldsymbol{\Sigma}$ is not invertible, then it is still possible to find a matrix \mathbf{S} satisfying Equations (216) and (217), however the linear dependencies prohibit such a transformation being invertible which means that it is generally not possible to recover the signal $\mathbf{c}(t)$, something that is often desired in applications of whitening. Therefore, when $\boldsymbol{\Sigma}$ is non-invertible a better strategy is to first add noise such that $\boldsymbol{\Sigma}$ becomes invertible (see Appendix C.1) and then apply whitening.

Under the assumption that $\boldsymbol{\Sigma}$ is invertible, Equation (219) has the same form as Equation (137). This means that the whitening matrix \mathbf{S} satisfies the requirement for being an inverse square root of $\boldsymbol{\Sigma}$, i.e. $\mathbf{S} = \boldsymbol{\Sigma}^{-\frac{1}{2}} = \mathbf{Q}\mathbf{U}\mathbf{D}^{-\frac{1}{2}}\mathbf{U}^T$, where \mathbf{Q} is an orthogonal matrix, \mathbf{U} contains the eigenvectors of $\boldsymbol{\Sigma}$, and $\mathbf{D}^{-\frac{1}{2}}$ contains the inverse positive square roots of the eigenvalues of $\boldsymbol{\Sigma}$ (see Appendix A.2). Thus, the signal $\mathbf{z}(t)$ and its time derivative $\dot{\mathbf{z}}(t)$ can be expressed as $\mathbf{z}(t) = \boldsymbol{\Sigma}^{-\frac{1}{2}}\mathbf{c}(t)$ and $\dot{\mathbf{z}}(t) = \boldsymbol{\Sigma}^{-\frac{1}{2}}\dot{\mathbf{c}}(t)$, respectively, which means that the covariance matrix of $\dot{\mathbf{z}}(t)$ is given by

$$\langle \dot{\mathbf{z}}(t)\dot{\mathbf{z}}(t)^T \rangle_t = \boldsymbol{\Sigma}^{-\frac{1}{2}}\langle \dot{\mathbf{c}}(t)\dot{\mathbf{c}}(t)^T \rangle_t (\boldsymbol{\Sigma}^{-\frac{1}{2}})^T \quad (220)$$

$$= \boldsymbol{\Sigma}^{-\frac{1}{2}}\dot{\boldsymbol{\Sigma}}(\boldsymbol{\Sigma}^{-\frac{1}{2}})^T \quad (221)$$

the STC matrix with time-lag τ of $\mathbf{z}(t)$ by

$$\frac{1}{2}(\langle \mathbf{z}(t)\mathbf{z}(t+\tau)^T \rangle_t + \langle \mathbf{z}(t+\tau)\mathbf{z}(t)^T \rangle_t) = \frac{1}{2}(\boldsymbol{\Sigma}^{-\frac{1}{2}}\langle \mathbf{c}(t)\mathbf{c}(t+\tau)^T \rangle_t (\boldsymbol{\Sigma}^{-\frac{1}{2}})^T + \boldsymbol{\Sigma}^{-\frac{1}{2}}\langle \mathbf{c}(t+\tau)\mathbf{c}(t)^T \rangle_t (\boldsymbol{\Sigma}^{-\frac{1}{2}})^T) \quad (222)$$

$$= \boldsymbol{\Sigma}^{-\frac{1}{2}}\left(\frac{1}{2}(\langle \mathbf{c}(t)\mathbf{c}(t+\tau)^T \rangle_t + \langle \mathbf{c}(t+\tau)\mathbf{c}(t)^T \rangle_t)\right) (\boldsymbol{\Sigma}^{-\frac{1}{2}})^T \quad (223)$$

$$= \boldsymbol{\Sigma}^{-\frac{1}{2}}\boldsymbol{\Omega}_\tau (\boldsymbol{\Sigma}^{-\frac{1}{2}})^T \quad (224)$$

and the LF matrix of $\mathbf{z}(t)$ by

$$\sum_{\tau=0}^{\tau_{\max}} \frac{\gamma^\tau}{2} (\langle \mathbf{z}(t)\mathbf{z}(t+\tau)^T \rangle_t + \langle \mathbf{z}(t+\tau)\mathbf{z}(t)^T \rangle_t) \stackrel{(224)}{=} \sum_{\tau=0}^{\tau_{\max}} \gamma^\tau \boldsymbol{\Sigma}^{-\frac{1}{2}}\boldsymbol{\Omega}_\tau (\boldsymbol{\Sigma}^{-\frac{1}{2}})^T \quad (225)$$

$$= \boldsymbol{\Sigma}^{-\frac{1}{2}}\left(\sum_{\tau=0}^{\tau_{\max}} \gamma^\tau \boldsymbol{\Omega}_\tau\right) (\boldsymbol{\Sigma}^{-\frac{1}{2}})^T \quad (226)$$

$$= \boldsymbol{\Sigma}^{-\frac{1}{2}}\boldsymbol{\Psi}_\gamma (\boldsymbol{\Sigma}^{-\frac{1}{2}})^T \quad (227)$$

Therefore, together with the fact that $\mathbf{z}(t)$ has unit covariance, performing SFA, τ SFA, or LFSFA on a whitened time series is equivalent to solving the regular eigenvalue problem for $\boldsymbol{\Sigma}^{-\frac{1}{2}}\dot{\boldsymbol{\Sigma}}(\boldsymbol{\Sigma}^{-\frac{1}{2}})^T$, $\boldsymbol{\Sigma}^{-\frac{1}{2}}(\boldsymbol{\Omega}_\tau \boldsymbol{\Sigma}^{-\frac{1}{2}})^T$,

or $\Sigma^{-\frac{1}{2}}\Psi_\gamma(\Sigma^{-\frac{1}{2}})^T$, respectively, which are precisely the problems that emerge when applying symmetric normalization to Type I SFA, τ SFA, or LFSFA, respectively.

Something worth pointing out about the whitening transformation $\Sigma^{-\frac{1}{2}} = \mathbf{Q}\mathbf{U}\mathbf{D}^{-\frac{1}{2}}\mathbf{U}^T$ is that due to the matrix \mathbf{Q} it is only defined up to a rotation, and because of this there exist a variety of different techniques for whitening a given dataset (Kessy et al., 2018). The two most common variants in the context of SFA are ZCA- and PCA-whitening, with the former corresponding to $\mathbf{Q} = \mathbb{1}$ and $\Sigma^{-\frac{1}{2}} = \mathbf{U}\mathbf{D}^{-\frac{1}{2}}\mathbf{U}^T$ and the latter to $\mathbf{Q} = \mathbf{U}^T$ and $\Sigma^{-\frac{1}{2}} = \mathbf{D}^{-\frac{1}{2}}\mathbf{U}^T$. In words, these transformations can be described sequentially from right to left in the following two/three steps: (i) rotate the coordinate system into the eigenbasis \mathbf{U}^T of Σ , (ii) scale the components along each axis by $D_{ii}^{-\frac{1}{2}} = \lambda_i^{-\frac{1}{2}}$, where λ_i is the eigenvalue associated to each eigenvector, (iii) in the case of ZCA, rotate back into the original coordinate system using the transformation \mathbf{U} . It is worth noting that there are two ways in which ZCA is special in comparison to other whitening methods. Firstly, the corresponding matrix is guaranteed to be symmetric since $(\mathbf{U}\mathbf{D}^{-\frac{1}{2}}\mathbf{U}^T)^T = \mathbf{U}\mathbf{D}^{-\frac{1}{2}}\mathbf{U}^T$, while for $\mathbf{Q}^T \neq \mathbb{1}$ this is generally not the case. Secondly, due to step (iii) in ZCA, this version of whitening is the one that preserves the original orientation of data points as much as possible.

Appendix D Convergence Theorems

D.1 Type I SFA Problems

Theorem 4.2.1 *For a Markovian one-hot trajectory $\mathbf{x}(t)$, the matrix Σ associated to the Type I constraints obeys the following limit:*

$$\lim_{T \rightarrow \infty} \Sigma = \mathbf{\Pi} - \boldsymbol{\pi}\boldsymbol{\pi}^T \quad (228)$$

where $\boldsymbol{\pi}$ is the unique stationary distribution of the underlying Markov chain and $\mathbf{\Pi} = \text{diag}(\boldsymbol{\pi})$. Moreover, the limiting matrix $\mathbf{\Pi} - \boldsymbol{\pi}\boldsymbol{\pi}^T$ is guaranteed to have a single eigenvalue of 0.

Proof. The covariance matrix Σ of $\mathbf{x}(t)$ can be written as (see Equations (198)–(201))

$$\Sigma = \langle \mathbf{x}(t)\mathbf{x}(t)^T \rangle_t - \langle \mathbf{x}(t) \rangle_t \langle \mathbf{x}(t)^T \rangle_t \quad (229)$$

or in elementwise notation as

$$\Sigma_{ij} = \langle x_i(t)x_j(t) \rangle_t - \langle x_i(t) \rangle_t \langle x_j(t) \rangle_t \quad (230)$$

In the second term of Equation (230), $\langle x_i(t) \rangle_t$ is the average value of $x_i(t)$. Since $x_i(t) = 1$ when state s_i is occupied and 0 otherwise, this average is equivalent to the proportion of times that s_i is occupied in the entire trajectory. Since the Markov chain is ergodic by assumption, this proportion converges as $T \rightarrow \infty$ to a unique stationary probability π_i (Seabrook and Wiskott, 2023). Therefore, in this limit the second term of Equation (230) is $\pi_i\pi_j$. For the first term of Equation (230), note that due to the properties of the one-hot encoding the product $x_i(t)x_j(t)$ is non-zero only if $i = j$, in which case it is equal to $x_i^2(t)$. Since $x_i^2(t)$ is equivalent to $x_i(t)$ for a one-hot encoding, its average is also equal to the stationary probability π_i . Therefore

$$\lim_{T \rightarrow \infty} \Sigma_{ij} = \begin{cases} \pi_i - \pi_i^2 & \text{if } i = j \\ -\pi_i\pi_j & \text{otherwise} \end{cases} \quad (231)$$

or in matrix notation

$$\lim_{T \rightarrow \infty} \Sigma = \mathbf{\Pi} - \boldsymbol{\pi}\boldsymbol{\pi}^T \quad (232)$$

Note that the matrix $\boldsymbol{\pi}\boldsymbol{\pi}^T$ in Equation (232) is an outer product of the stationary distribution $\boldsymbol{\pi}$ with itself. Therefore, this matrix is symmetric and non-negative. Thus, $\boldsymbol{\pi}\boldsymbol{\pi}^T$ can be thought of as a weight matrix corresponding to an undirected graph \mathcal{G} with edge weights $\pi_i\pi_j$ (Seabrook and Wiskott, 2023). From this perspective, the degrees of this graph are given by

$$\sum_j \pi_i\pi_j = \pi_i \sum_j \pi_j = \pi_i \quad (233)$$

which are precisely the entries of the diagonal matrix $\mathbf{\Pi}$. Therefore, $\mathbf{\Pi} - \boldsymbol{\pi}\boldsymbol{\pi}^T$ describes the graph Laplacian of \mathcal{G} . Moreover, since the chain is ergodic, this graph is fully connected meaning that this matrix is guaranteed to have a single eigenvalue of zero (Seabrook and Wiskott, 2023). \square

Theorem 4.2.2 *For a Markovian one-hot trajectory $\mathbf{x}(t)$, the matrices $\dot{\mathbf{\Sigma}}$, $\mathbf{\Omega}_\tau$, and $\mathbf{\Psi}_\gamma$ associated to the Type I objectives obey the following limits:*

$$\lim_{T \rightarrow \infty} \dot{\mathbf{\Sigma}} = \mathbf{L}_{\text{dir}} + \boldsymbol{\pi}\boldsymbol{\pi}^T \quad (234)$$

$$\lim_{T \rightarrow \infty} \mathbf{\Omega}_\tau = \mathbf{\Pi}(\mathbf{P}^\tau)_{\text{add}} - \boldsymbol{\pi}\boldsymbol{\pi}^T \quad (235)$$

$$\lim_{T \rightarrow \infty} \mathbf{\Psi}_\gamma = \mathbf{\Pi}\mathbf{M}_{\text{add}} - \alpha\boldsymbol{\pi}\boldsymbol{\pi}^T \quad (236)$$

where \mathbf{L}_{dir} is the combinatorial directed Laplacian matrix associated to the underlying Markov chain, \mathbf{P} is the transition matrix, \mathbf{M} is the SR matrix with discount factor γ , and $\alpha = \frac{1 - \gamma^{\tau_{\text{max}} + 1}}{1 - \gamma} \in [1, \frac{1}{1 - \gamma})$ is a scalar constant.

Proof. Consider first the STC matrix at time-lag τ , which is given by

$$\mathbf{\Omega}_\tau = \frac{1}{2} (\langle \mathbf{c}(t)\mathbf{c}(t + \tau)^T \rangle_t + \langle \mathbf{c}(t + \tau)\mathbf{c}(t)^T \rangle_t) \quad (237)$$

or in elementwise notation

$$(\mathbf{\Omega}_\tau)_{ij} = \frac{1}{2} (\langle c_i(t)c_j(t + \tau) \rangle_t + \langle c_i(t + \tau)c_j(t) \rangle_t) \quad (238)$$

The first bracketed term in Equation (238) can be rearranged to give:

$$\langle c_i(t)c_j(t + \tau) \rangle_t = \langle (x_i(t) - \langle x_i(t) \rangle_t)(x_j(t + \tau) - \langle x_j(t) \rangle_t) \rangle_t \quad (239)$$

$$= \langle x_i(t)x_j(t + \tau) \rangle_t - \langle x_i(t) \rangle_t \langle x_j(t) \rangle_t - \langle x_i(t) \rangle_t \langle x_j(t + \tau) \rangle_t + \langle x_i(t) \rangle_t \langle x_j(t) \rangle_t \quad (240)$$

In the first term of Equation (240), the product $x_i(t)x_j(t + \tau)$ is equal to 1 if state s_i is occupied at time t and state s_j is occupied τ steps later, and is zero otherwise. Therefore, this first term is equivalent to the frequency with which this τ -step transition happens. For an ergodic Markov chain this converges as $T \rightarrow \infty$ to the flow probability from s_i to s_j of the τ -step Markov chain, i.e. $\pi_i(\mathbf{P}^\tau)_{ij}$ (Seabrook and Wiskott, 2023). The other terms in Equation (240) all converge to $\pi_i\pi_j$ as $T \rightarrow \infty$, meaning that:

$$\lim_{T \rightarrow \infty} \langle c_i(t)c_j(t + \tau) \rangle_t = \pi_i(\mathbf{P}^\tau)_{ij} - \pi_i\pi_j - \pi_i\pi_j + \pi_i\pi_j \quad (241)$$

$$= \pi_i(\mathbf{P}^\tau)_{ij} - \pi_i\pi_j \quad (242)$$

By an equivalent argument, it is possible to show a similar result for the second bracketed term in Equation (238):

$$\lim_{T \rightarrow \infty} \langle c_i(t + \tau)c_j(t) \rangle_t = \pi_j(\mathbf{P}^\tau)_{ji} - \pi_i\pi_j \quad (243)$$

Therefore, in this limit Equation (238) becomes

$$\lim_{T \rightarrow \infty} (\mathbf{\Omega}_\tau)_{ij} = \frac{1}{2} (\pi_i(\mathbf{P}^\tau)_{ij} - \pi_i\pi_j + \pi_j(\mathbf{P}^\tau)_{ji} - \pi_i\pi_j) \quad (244)$$

$$= \frac{\pi_i(\mathbf{P}^\tau)_{ij} + \pi_j(\mathbf{P}^\tau)_{ji}}{2} - \pi_i\pi_j \quad (245)$$

or in matrix notation

$$\lim_{T \rightarrow \infty} \Omega_\tau = \frac{\mathbf{\Pi} \mathbf{P}^\tau + (\mathbf{\Pi} \mathbf{P}^\tau)^T}{2} - \boldsymbol{\pi} \boldsymbol{\pi}^T \quad (246)$$

$$= \frac{\mathbf{\Pi} \mathbf{P}^\tau + (\mathbf{P}^\tau)^T \mathbf{\Pi}^T}{2} - \boldsymbol{\pi} \boldsymbol{\pi}^T \quad (247)$$

$$= \frac{\mathbf{\Pi} \mathbf{P}^\tau + (\mathbf{P}^\tau)^T \mathbf{\Pi}^T}{2} - \boldsymbol{\pi} \boldsymbol{\pi} \quad (248)$$

$$= \mathbf{\Pi} \left(\frac{\mathbf{P}^\tau + \mathbf{\Pi}^{-1} (\mathbf{P}^\tau)^T \mathbf{\Pi}}{2} \right) - \boldsymbol{\pi} \boldsymbol{\pi}^T \quad (249)$$

$$= \mathbf{\Pi} (\mathbf{P}^\tau)_{\text{add}} - \boldsymbol{\pi} \boldsymbol{\pi}^T \quad (250)$$

where the subscript in Equation (250) denotes the process of additive reversibilization (see Section 2.3).

The LF matrix is related to Ω_τ by:

$$\Psi_\gamma = \sum_{\tau=0}^{\tau_{\max}} \gamma^\tau \Omega_\tau \quad (251)$$

Therefore, in the limit $T \rightarrow \infty$ this matrix evaluates to

$$\lim_{T \rightarrow \infty} \Psi_\gamma = \lim_{T \rightarrow \infty} \left(\sum_{\tau=0}^{\tau_{\max}} \gamma^\tau \Omega_\tau \right) \quad (252)$$

$$= \sum_{\tau=0}^{\tau_{\max}} \gamma^\tau \left(\lim_{T \rightarrow \infty} \Omega_\tau \right) \quad (253)$$

$$\stackrel{(250)}{=} \sum_{\tau=0}^{\tau_{\max}} \gamma^\tau \left(\mathbf{\Pi} (\mathbf{P}^\tau)_{\text{add}} - \boldsymbol{\pi} \boldsymbol{\pi}^T \right) \quad (254)$$

$$= \mathbf{\Pi} \left(\sum_{\tau=0}^{\tau_{\max}} \gamma^\tau (\mathbf{P}^\tau)_{\text{add}} \right) - \boldsymbol{\pi} \boldsymbol{\pi}^T \sum_{\tau=0}^{\tau_{\max}} \gamma^\tau \quad (255)$$

$$\stackrel{(15)}{=} \mathbf{\Pi} \mathbf{M}_{\text{add}} - \boldsymbol{\pi} \boldsymbol{\pi}^T \underbrace{\left(\frac{1 - \gamma^{\tau_{\max} + 1}}{1 - \gamma} \right)}_{=\alpha} \quad (256)$$

$$= \mathbf{\Pi} \mathbf{M}_{\text{add}} - \alpha \boldsymbol{\pi} \boldsymbol{\pi}^T \quad (257)$$

Note that the only difference between \mathbf{M}_{add} in the equations above and the definition in Equation (15) is that the former has a finite horizon while the latter has an infinite horizon (see Section 2.4). Moreover, the second term in Equation (255) is evaluated using the formula for a geometric series with a finite number of terms, and is equal to a constant α that depends on γ and τ_{\max} . For the minimum value $\tau_{\max} = 1$, this constant is 1, and while there is no maximum value of τ_{\max} the limiting value of $\tau_{\max} = \infty$ yields $\frac{1}{1-\gamma}$. Therefore, $\alpha \in [1, \frac{1}{1-\gamma})$.

The matrix $\dot{\Sigma}$ is related to Ω_1 and Σ by

$$\dot{\Sigma} = 2(\Sigma - \Omega_1) \quad (258)$$

Therefore, in the limit $T \rightarrow \infty$ this matrix evaluates to

$$\lim_{T \rightarrow \infty} \dot{\Sigma} = \lim_{T \rightarrow \infty} 2(\Sigma - \Omega_1) \quad (259)$$

$$\stackrel{(250,232)}{=} 2\Pi - 2\Pi P_{\text{add}} + \pi \pi^T \quad (260)$$

$$\stackrel{(11)}{=} 2\left(\Pi - \frac{\Pi P + P^T \Pi}{2}\right) + \pi \pi^T \quad (261)$$

$$= 2\left(\underbrace{\Pi - \frac{\Pi P + (\Pi P)^T}{2}}_{=\mathbf{L}_{\text{dir}}}\right) + \pi \pi^T \quad (262)$$

$$= 2\mathbf{L}_{\text{dir}} + \pi \pi^T \quad (263)$$

where \mathbf{L}_{dir} is the *combinatorial directed Laplacian* defined in Chung (2005). This object can be understood using concepts from Markov chain theory (Seabrook and Wiskott, 2023). In particular, ΠP contains the stationary flow probabilities of the underlying Markov chain, which are all non-negative. Therefore, this matrix can be interpreted as the weight matrix of a graph G connecting all pairs of states $s_i, s_j \in \mathcal{S}$. Note that ΠP is related to P by a scaling of the rows by the stationary probabilities. Therefore, in the terminology of Seabrook and Wiskott (2023), G belongs to the random walk set of the underlying Markov chain, and so performing a random walk on G produces this Markov chain. Moreover, since the chain is not assumed to be reversible ΠP is generally be non-symmetric, in which case G is a directed graph. While graph Laplacians are typically defined for undirected graphs, various methods have been proposed for the extension to the directed case (Seabrook and Wiskott, 2023). The quantity \mathbf{L}_{dir} does this by symmetrizing the edges in G to produce a new undirected graph G' for which the weight matrix is $\frac{\Pi P + (\Pi P)^T}{2}$ and the degree of each vertex is given by:

$$d_i = \frac{1}{2} \sum_j \pi_i P_{ij} + \frac{1}{2} \sum_j \pi_j P_{ji} \quad (264)$$

$$= \frac{\pi_i}{2} \underbrace{\sum_j P_{ij}}_{=1} + \frac{\pi_i}{2} \quad (265)$$

$$= \pi_i \quad (266)$$

Therefore, \mathbf{L}_{dir} is like the combinatorial graph Laplacian for undirected graphs, i.e. $\mathbf{L} = \mathbf{D} - \mathbf{W}$, but defined on the symmetrized graph G' . □

D.2 Type II SFA Problems

Theorem 4.2.3 *For a Markovian one-hot trajectory $\mathbf{x}(t)$, the matrix $\widehat{\Sigma}$ associated to the Type II constraints obeys the following limit:*

$$\lim_{T \rightarrow \infty} \widehat{\Sigma} = \Pi \quad (267)$$

where π is the unique stationary distribution of the underlying Markov chain and $\Pi = \text{diag}(\pi)$. Moreover, the limiting matrix Π is guaranteed to have no eigenvalues of 0.

Proof. The 2nd moment matrix $\widehat{\Sigma}$ of $\mathbf{x}(t)$ is given by

$$\Sigma = \langle \mathbf{x}(t) \mathbf{x}(t)^T \rangle_t \quad (268)$$

or in elementwise notation as

$$\widehat{\Sigma}_{ij} = \langle x_i(t) x_j(t) \rangle_t \quad (269)$$

Equation (269) is simply the first term of Equation (230), and therefore applying the same logic as in the previous proof leads to:

$$\lim_{T \rightarrow \infty} \widehat{\Sigma}_{ij} = \begin{cases} \pi_i & \text{if } i = j \\ 0 & \text{otherwise} \end{cases} \quad (270)$$

or in matrix notation

$$\lim_{T \rightarrow \infty} \widehat{\Sigma} = \mathbf{\Pi} \quad (271)$$

Note that the matrix $\mathbf{\Pi}$ is a diagonal matrix containing the stationary probabilities of the Markov chain, which are also the eigenvalues of this matrix. Moreover, since the chain is ergodic by assumption, all stationary probabilities, or equivalently all eigenvalues, are strictly positive. \square

Theorem 4.2.4 *For a Markovian one-hot trajectory $\mathbf{x}(t)$, the matrices $\widehat{\Sigma}$, $\widehat{\Omega}_\tau$, and $\widehat{\Psi}_\gamma$ associated to the Type II objectives obey the following limits:*

$$\lim_{T \rightarrow \infty} \widehat{\Sigma} = \mathbf{L}_{\text{dir}} \quad (272)$$

$$\lim_{T \rightarrow \infty} \widehat{\Omega}_\tau = \mathbf{\Pi}(\mathbf{P}^\tau)_{\text{add}} \quad (273)$$

$$\lim_{T \rightarrow \infty} \widehat{\Psi}_\gamma = \mathbf{\Pi} \mathbf{M}_{\text{add}} \quad (274)$$

where \mathbf{L}_{dir} is the combinatorial directed Laplacian matrix associated to the underlying Markov chain, \mathbf{P} is the transition matrix, and \mathbf{M} is the SR matrix with discount factor γ .

Proof. The matrix $\widehat{\Omega}_\tau$ is the same as $\mathbf{\Omega}_\tau$ except that no centering transformation is assumed and $\mathbf{c}(t)$ is exchanged for $\mathbf{x}(t)$, i.e.

$$\widehat{\Omega}_\tau = \frac{1}{2} (\langle \mathbf{x}(t) \mathbf{x}(t + \tau)^T \rangle_t + \langle \mathbf{x}(t + \tau) \mathbf{x}(t)^T \rangle_t) \quad (275)$$

or in elementwise notation

$$(\widehat{\Omega}_\tau)_{ij} = \frac{1}{2} (\langle x_i(t) x_j(t + \tau) \rangle_t + \langle x_i(t + \tau) x_j(t) \rangle_t) \quad (276)$$

By the same reasoning as in the proof of Theorem 4.2.4, in the limit $T \rightarrow \infty$ the first and second bracketed terms in Equation (276) converge to $\pi_i(\mathbf{P}^\tau)_{ij}$ and $\pi_j(\mathbf{P}^\tau)_{ji}$, respectively. Therefore

$$\lim_{T \rightarrow \infty} (\widehat{\Omega}_\tau)_{ij} = \frac{\pi_i(\mathbf{P}^\tau)_{ij} + \pi_j(\mathbf{P}^\tau)_{ji}}{2} \quad (277)$$

or in matrix notation

$$\lim_{T \rightarrow \infty} \widehat{\Omega}_\tau = \frac{\mathbf{\Pi} \mathbf{P}^\tau + (\mathbf{\Pi} \mathbf{P}^\tau)^T}{2} \quad (278)$$

$$= \mathbf{\Pi}(\mathbf{P}^\tau)_{\text{add}} \quad (279)$$

where the first line reduces to the second line following the same steps as in Equations (246)–(250).

The matrix $\widehat{\Psi}_\gamma$ is related to $\widehat{\Omega}_\tau$ by

$$\widehat{\Psi}_\gamma = \sum_{\tau=0}^{\tau_{\text{max}}} \gamma^\tau \widehat{\Omega}_\tau \quad (280)$$

and can be evaluated in the limit $T \rightarrow \infty$ by using Equation (279) and applying a similar set of steps as in Equations (252)–(257), i.e.

$$\lim_{T \rightarrow \infty} \widehat{\Psi}_\gamma = \lim_{T \rightarrow \infty} \left(\sum_{\tau=0}^{\tau_{\max}} \gamma^\tau \widehat{\Omega}_\tau \right) \quad (281)$$

$$= \sum_{\tau=0}^{\tau_{\max}} \gamma^\tau \left(\lim_{T \rightarrow \infty} \widehat{\Omega}_\tau \right) \quad (282)$$

$$= \sum_{\tau=0}^{\tau_{\max}} \gamma^\tau \left(\mathbf{\Pi}(\mathbf{P}^\tau)_{\text{add}} \right) \quad (283)$$

$$= \mathbf{\Pi} \left(\sum_{\tau=0}^{\tau_{\max}} \gamma^\tau (\mathbf{P}^\tau)_{\text{add}} \right) \quad (284)$$

$$= \mathbf{\Pi} \mathbf{M}_{\text{add}} \quad (285)$$

Following the same argument as in Equations (45)–(49), it is possible to show that the matrices $\widehat{\Sigma}$, $\widehat{\Sigma}$, and $\widehat{\Omega}_1$ are related in the same way as $\dot{\Sigma}$, Σ , and Ω_1 , i.e.

$$\widehat{\Sigma} = 2(\widehat{\Sigma} - \widehat{\Omega}_1) \quad (286)$$

Equation (286) evaluates in the limit $T \rightarrow \infty$ to:

$$\lim_{T \rightarrow \infty} \widehat{\Sigma} = \lim_{T \rightarrow \infty} 2(\widehat{\Sigma} - \widehat{\Omega}_1) \quad (287)$$

$$\stackrel{(279,271)}{=} 2\mathbf{\Pi} - 2\mathbf{\Pi} \mathbf{P}_{\text{add}} \quad (288)$$

$$\stackrel{(262)}{=} \mathbf{L}_{\text{dir}} \quad (289)$$

□

References

- Babouklis, F., Adam, M., and Assimakis, N. (2020). Bounds on the Spectral Radius of Nonnegative Matrices. In *2020 International Conference on Mathematics and Computers in Science and Engineering (MACISE)*, pages 51–55, Madrid, Spain. IEEE.
- Banerjee, S. and Roy, A. (2014). *Linear Algebra and Matrix Analysis for Statistics*. Chapman & Hall/CRC Texts in Statistical Science Series. CRC Press, Taylor & Francis Group, Boca Raton.
- Belouchrani, A., Abed-Meraim, K., Cardoso, J.-F., and Moulines, E. (Feb./1997). A blind source separation technique using second-order statistics. *IEEE Transactions on Signal Processing*, 45(2):434–444.
- Berkes, P. and Wiskott, L. (2005). Slow feature analysis yields a rich repertoire of complex cell properties. *Journal of Vision*, 5(6):9–9.
- Blaschke, T., Berkes, P., and Wiskott, L. (2006). What Is the Relation Between Slow Feature Analysis and Independent Component Analysis? *Neural Computation*, 18(10):2495–2508.
- Carvalho, W., Tomov, M. S., de Cothi, W., Barry, C., and Gershman, S. J. (2024). Predictive representations: Building blocks of intelligence.
- Chung, F. (2005). Laplacians and the Cheeger Inequality for Directed Graphs. *Annals of Combinatorics*, 9(1):1–19.

- Creutzig, F. and Sprekeler, H. (2008). Predictive Coding and the Slowness Principle: An Information-Theoretic Approach. *Neural Computation*, 20(4):1026–1041.
- Dayan, P. (1993). Improving Generalization for Temporal Difference Learning: The Successor Representation. *Neural Computation*, 5(4):613–624.
- Ducarouge, A. and Sigaud, O. (2017). The Successor Representation as a model of behavioural flexibility.
- Escalante-B., A. N. and Wiskott, L. (2020). Improved graph-based SFA: Information preservation complements the slowness principle. *Machine Learning*, 109(5):999–1037.
- Földiák, P. (1991). Learning Invariance from Transformation Sequences. *Neural Computation*, 3(2):194–200.
- Franzius, M., Sprekeler, H., and Wiskott, L. (2007). Slowness and Sparseness Lead to Place, Head-Direction, and Spatial-View Cells. *PLoS Computational Biology*, 3(8):e166.
- Franzius, M., Wilbert, N., and Wiskott, L. (2008). Invariant Object Recognition with Slow Feature Analysis. In Kůrková, V., Neruda, R., and Koutník, J., editors, *Artificial Neural Networks - ICANN 2008*, volume 5163, pages 961–970. Springer Berlin Heidelberg, Berlin, Heidelberg.
- Gershman, S. J. (2017). Predicting the past, remembering the future. *Current Opinion in Behavioral Sciences*, 17:7–13.
- Gershman, S. J. (2018). The Successor Representation: Its Computational Logic and Neural Substrates. *The Journal of Neuroscience*, 38(33):7193–7200.
- Ghojogh, B., Karray, F., and Crowley, M. (2023). Eigenvalue and generalized eigenvalue problems: Tutorial.
- Ikramov, Kh. D. (1993). Matrix pencils: Theory, applications, and numerical methods. *Journal of Soviet Mathematics*, 64(2):783–853.
- Keck, J. S., Barry, C., Doeller, C. F., and Jost, J. (2024). Symmetry and Generalization in Local Learning of Predictive Representations.
- Kessy, A., Lewin, A., and Strimmer, K. (2018). Optimal Whitening and Decorrelation. *The American Statistician*, 72(4):309–314.
- Klus, S., Nüske, F., Koltai, P., Wu, H., Kevrekidis, I., Schütte, C., and Noé, F. (2018). Data-Driven Model Reduction and Transfer Operator Approximation. *Journal of Nonlinear Science*, 28(3):985–1010.
- Konen, W. (2009). On the numeric stability of the SFA implementation sfa-tk.
- Legenstein, R., Wilbert, N., and Wiskott, L. (2010). Reinforcement Learning on Slow Features of High-Dimensional Input Streams. *PLoS Computational Biology*, 6(8):e1000894.
- Meyer, C. D. (2000). *Matrix Analysis and Applied Linear Algebra*. Society for Industrial and Applied Mathematics, Philadelphia.
- Minc, H. (1988). *Nonnegative Matrices*. Wiley-Interscience Series in Discrete Mathematics and Optimization. Wiley, New York.
- Moffett, A. S. and Shukla, D. (2017). On the transferability of time-lagged independent components between similar molecular dynamics systems.
- Molgedey, L. and Schuster, H. G. (1994). Separation of a mixture of independent signals using time delayed correlations. *Physical Review Letters*, 72(23):3634–3637.

- Naritomi, Y. and Fuchigami, S. (2011). Slow dynamics in protein fluctuations revealed by time-structure based independent component analysis: The case of domain motions. *The Journal of Chemical Physics*, 134(6):065101.
- Oppenheim, A. V., Willsky, A. S., and Nawab, S. H. (2016). *Signals & Systems*. Pearson, Noida, 3rd ed. impression edition.
- Pérez-Hernández, G., Paul, F., Giorgino, T., De Fabritiis, G., and Noé, F. (2013). Identification of slow molecular order parameters for Markov model construction. *The Journal of Chemical Physics*, 139(1):015102.
- Piray, P. and Daw, N. D. (2021). Linear reinforcement learning in planning, grid fields, and cognitive control. *Nature Communications*, 12(1):4942.
- Potters, M. and Bouchaud, J.-P. (2020). *A First Course in Random Matrix Theory: For Physicists, Engineers and Data Scientists*. Cambridge University Press, 1 edition.
- Russek, E. M., Momennejad, I., Botvinick, M. M., Gershman, S. J., and Daw, N. D. (2017). Predictive representations can link model-based reinforcement learning to model-free mechanisms. *PLOS Computational Biology*, 13(9):e1005768.
- Schönfeld, F. and Wiskott, L. (2015). Modeling place field activity with hierarchical slow feature analysis. *Frontiers in Computational Neuroscience*, 9.
- Schüler, M. and Wiskott, L. (2024). Slow features of directed behavior in spatial environments and the effect on value function approximation (work in progress).
- Schultze, S. and Grubmüller, H. (2021). Time-Lagged Independent Component Analysis of Random Walks and Protein Dynamics. *Journal of Chemical Theory and Computation*, 17(9):5766–5776.
- Seabrook, E. and Wiskott, L. (2023). A Tutorial on the Spectral Theory of Markov Chains. *Neural Computation*, 35(11):1713–1796.
- Sprekeler, H. (2011). On the Relation of Slow Feature Analysis and Laplacian Eigenmaps. *Neural Computation*, 23(12):3287–3302.
- Sprekeler, H. and Wiskott, L. (2008). Understanding Slow Feature Analysis: A Mathematical Framework. *SSRN Electronic Journal*.
- Sprekeler, H., Zito, T., and Wiskott, L. (2014). An extension of slow feature analysis for nonlinear blind source separation. *Journal of Machine Learning Research*, 15(26):921–947.
- Sprekeler, Henning Wiskott, L., Universität Berlin, H.-U., and Fakultät, M.-N. (2009). Slowness learning : Mathematical approaches and synaptic mechanisms.
- Stachenfeld, K. L., Botvinick, M., and Gershman, S. J. (2014). Design principles of the hippocampal cognitive map. In *Advances in Neural Information Processing Systems*, volume 27. Curran Associates, Inc.
- Stachenfeld, K. L., Botvinick, M. M., and Gershman, S. J. (2017). The hippocampus as a predictive map. *Nature Neuroscience*, 20(11):1643–1653.
- Sutton, R. S. and Barto, A. G. (2018). *Reinforcement Learning: An Introduction*. Adaptive Computation and Machine Learning Series. The MIT Press, Cambridge, Massachusetts, second edition edition.
- Wang, J. and Zhao, C. (2020). Variants of slow feature analysis framework for automatic detection and isolation of multiple oscillations in coupled control loops. *Computers & Chemical Engineering*, 141:107029.
- Wiskott, L. (2003). Slow Feature Analysis: A Theoretical Analysis of Optimal Free Responses. *Neural Computation*, 15(9):2147–2177.

- Wiskott, L. and Schönfeld, F. (2019). Laplacian Matrix for Dimensionality Reduction and Clustering.
- Wiskott, L. and Sejnowski, T. J. (2002). Slow Feature Analysis: Unsupervised Learning of Invariances. *Neural Computation*, 14(4):715–770.
- Ziehe, A. and Müller, K.-R. (1998). TDSEP — an efficient algorithm for blind separation using time structure. In Niklasson, L., Bodén, M., and Ziemke, T., editors, *ICANN 98*, pages 675–680. Springer London, London.